UNIVERSITEIT VAN PRETORIA
UNIVERSITY OF PRETORIA
YUNIBESITHI YA PRETORIA

A COMPUTATIONAL MODELLING STUDY OF CHLORINE DIOXIDE AND ITS ROLE IN WATER PURIFICATION CYCLES

by

Natasha Misheer

Submitted in partial fulfilment for the degree of

Doctor of Philosophy of Science (PhD)

Faculty of Natural and Agricultural Sciences

University of Pretoria

South Africa

(2023)

Supervisor: Dr Jan A Pretorius

Centre for the Advancement of Scholarship & Department of Chemistry

University of Pretoria

DECLARATION

I, *Natasha Misheer* declares that this dissertation, which I hereby submit for the degree of Doctor of Philosophy of Science (PhD), in Chemistry at the University of Pretoria, is my own work and has not previously been submitted by me for a degree at this or any other tertiary institution.

Signature: 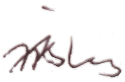 Date: 16 November 2023

Published output of this work:

Submitted to: *Heliyon Journal of Science* (Chemistry)

"Semi-empirical supported, *Ab Initio* derived Thermodynamic properties for $C\ell O_2$ and its sub- and extended- species, applied in water treatment cycles", by: Natasha Misheer, Jan A Pretorius and Patrick Ndungu

DEDICATION

I dedicate this achievement to my parents Rabichund and Bindu Misheer and my late brother Nitesh Misheer. A special mention to my mum Bindu Misheer, my heartfelt gratitude to you mum for your support. I appreciated your efforts to sometimes “burn the midnight oil with me”. My parents unwavering belief in my abilities helped me to push through the innumerable difficulties and achieve what seemed like an unattainable feat.

ACKNOWLEDGEMENTS

- I would like to thank my parents for their constant encouragement and motivation. You both encouraged me to persevere against all odds.
- My heartfelt gratitude to my brother Ajay Misheer. for your steadfast support and lending a sympathetic ear to my issues.
- My sincere gratitude to my nieces Kajal and Keasha Misheer for their motivation to achieve this accomplishment. The mere fact that you both look to me for inspiration to achieve success in your own lives impelled me to refuse to accept defeat.
- I would like to acknowledge my supervisor Dr Jannie Pretorius
- My heartfelt gratitude to Prof Vinesh Maharaj, Prof Patrick Ndungu and Prof Barend Eramus. Your support motivated me to endure tremendous difficulties and to achieve my ultimate goal.
- I take this opportunity to convey my sincerest appreciation to Prof Patrick Ndungu and Prof Vinesh Maharaj for your guidance.
- I would like to thank my friends for supporting me throughout the duration of my studies. Your encouragement helped me succeed at a task that seemed impossible at times.
- I thank God for always giving me the strength to achieve my goals. Nothing is ever possible without your presence.

ABSTRACT

This study involves the computational investigation into the perceived reactivity of a group of sixty (60) sub- and extended- chlorine oxide species with the general formulae of $C\ell_xO_y$ applied to water purification. In order to achieve the ultimate objective of elucidating their chemical role in aqueous media, acting as oxidative agents, an intensive computational approach has been followed to determine their thermochemical properties. The extended species of $C\ell O_2$ display a complex sequence of bonding character with an appreciable charge dissipation (extracted as partial charges), which complicates the effective selection of basis sets and electronic structural optimization, during *Ab Initio* analyses. Besides a single molecular computational analysis, an alternative grand canonical ensemble approach was introduced, applying *Gibbs* ensemble *Monte Carlo* simulations, supported by revised force field parameters to derive at optimum model sizes. In this context, this approach proved highly efficient, resulting in consistent thermochemical properties for all species, through optimum selection of Hamiltonians and appropriate basis sets, during quantum chemical analyses.

Excellent correlations with published Heat of Formation energies were obtained for almost all the ensemble derived species. A few energy discrepancies identified during *Ab Initio* (*VASP* and *Gaussian* software) calculations will need to be investigated more thoroughly in a further study. Chemical structure geometries were typically maintained for all models and self-consistency reached in all the quantum chemical refinement cycles.

Some of these species are presented as radical and ionic entities, which complicates their quantum atom potential representations. This observation specifically applies to species exhibiting variable spin conditions. This spin variability can further promote spin contamination, through extensive polarization contributions. Charged species were unfortunately not exposed to empirical ensemble simulations (reasons given) and had to be considered as single molecular entities.

MAIN INDEX

LIST OF ABBREVIATIONS

ΔH_f	Heat of Formation
ΔG_f	Free Energy of Formation
Å	Angstroms
AM1	Austin Model 1 (MOPAC)
ATcT	Active Thermochemical Tables
BFGS	Broyden-Fletcher-Goldfarb-Shanno
B3LYP	Becke's three-parameter nonlocal exchange functional with the correlation functional of Lee, Yang, and Parr
CCSD(T)	Coupled Cluster Single-Double Excitation (with Triples)
CG	Conjugate Gradient (*VASP*) minimization method
$C\ell^-$	Chloride
$C\ell O_2^-$	Chlorite
$C\ell O_2$	Chlorine dioxide
$C\ell O_3^-$	Chlorate
cvff	Consistent-Valence force field
DBPs	Disinfection byproducts
DFT	Density Functional Theory
DOS	Density of states (*VASP*)
DPD	N, N-diethyl-p-phenylenediamine
$\bar{e}$	electron
EF	Eigenvector Following
FACT	The Facility for the Analysis of Chemical Thermodynamics (*FactSage software*)
FFT	Fast Fourier Transform
GAC	Granular activated carbon
GEMC	Gibbs ensemble Monte Carlo (*GIBBS*)
GGA	Generalized Gradient Approximation
HAAs	Haloacetic acids
HANs	Haloacetonitriles
$HC\ell O_2$	Chlorous acid
HF	Hartee Fock theory
HLC	Higher-level correction
$KC\ell O_3$	Potassium chlorate
LBFGS	Limited memory Broyden-Fletcher-Goldfarb-Shanno
MBJLDA	Modified Becke Johnson Local Density Approximation *(VASP)*
MCL	Maximum contaminant level (MCL)

MedeA	Materials Exploration and Design Analysis (Software from Materials Design Inc.)
MNDO	Modified Neglect of Diatomic Overlap *(MOPAC)*
MINDO	Modified Intermediate Neglect of Diatomic Overlap (*MOPAC)*
MNDOD	Modified Neglect of Diatomic Overlap with d Atomic Orbitals (*MOPAC*)
MO	Molecular orbital
MOPAC	Molecular Orbital Package
MRDL	Maximum residual disinfectant limit
MS0	Made Simple 0 *(Gaussian)*
MS1	Made Simple 1 *(Gaussian)*
MS2	Made Simple 2 *(Gaussian)*
mw	Molecular weight
NDC	Severe nondynamical correlation
NDDO	Neglect of diatomic differential overlap
NLLSQ	Non-Linear Least Squares gradient minimisation method
NOM	Natural Organic Matter
NTP	Normal Temperature and Pressure
pcff	Polymer Consistent force field
PM6	Parametric Method 6 (MOPAC)
PM3	Parametric Method 3 (MOPAC)
PM7	Parametric Method 7 (MOPAC)
QCISD(T)	Quadratic configuration interaction single-double excitation (with triples)
revTPSS	Revised Tao-Perdew-Staroverov-Scuseria
RHF	Restricted Hartee Fock
UHF	Unrestricted Hartee Fock
RM1	Recife model 1 (MOPAC)
ROHF	Restricted Open Shell Hartree Fock
SCAN	Strongly Constrained and Appropriately Normed *(Gaussian)*
THMs	Trihalomethanes
TOX	Total organic halogen
TPPS	Tao-Perdew-Staroverov-Scuseria
TS	Transition energies (*VASP*)
VASP	Vienna Ab Initio Simulation Package

CHAPTER-1: INTRODUCTION

1.1 Problem Statement

Natural Organic Matter (NOM) removal from water has become increasingly difficult, due to the wide variety of organic compounds found in an aquatic environment [1]. NOM has the ability to disrupt or interfere in many processes in the water treatment cycle [2]. It is well known that the enhanced coagulation process which comprises flocculation and coagulation, alters the chemical/physical nature of dissolved and suspended solids, allowing for removal in a clarifier. However, coagulation can only efficiently remove hydrophobic and high molecular fractions of NOM [3]. The remaining NOM species persists in the aquatic environment and interfere with the rest of the process treatment steps.

Application and the online chemical production of $C\ell O_2$ in the presence of a water treatment plant, will demand strict compliance to *Occupation Health and Safety* conditions and can be considered to be the main inhibiting factor, in favor of purging chlorine from pressurized cylinders.

1.2 Objective of this Study

The objective of the investigation focuses on a computational construction of $C\ell O_2$ extended- and sub- species, to elucidate their thermochemical reaction schemes, in an attempt to identify the main species persisting in an aqueous medium.

The ultimate objective is to demonstrate the exceptional behaviour of $C\ell O_2$ as a water pre-treatment agent, but also to derive at optimum conditions for these species to survive sufficiently long, to act as pathogen controlling agent, a topic of a further study.

This study aims to understand if the added oxidant ($C\ell O_2$), can alter the remaining NOM species' chemical properties, such that they can further aid the enhanced coagulation process resulting in higher organic removal.

1.3 Background and Study Step

The study involves a selection of a significant group of chemically extended- and sub-species of $C\ell O_2$, including a series of hydrogen derived $HC\ell_xO_y$ species. These chemical species are mostly unstable and therefore difficult to sustain an environment to measure their properties through spectroscopic or other chemical instrumental techniques [4]. An extended sub-set of species (some as radical and ionic in nature) can be constructed from their common denominating radical compound $C\ell O_2$. This 'synthetic' step is applied, mainly due to their short life span and extreme kinetics in aqueous based chemical reaction cycles [5].

a) An electronic and dynamic structural optimization step was first undertaken to derive effective model geometries, validated against published Heats of Formation. Both *Ab Initio* (***VASP***) and

s*emi-empirical* (***MOPAC***) quantum chemistry software systems have been used for this step and acted as prelude to Monte Carlo Simulations at the *Grand Canonical* ensemble model scale

b) A *Grand Canonical* ensemble (GEMC) step was introduced to formulate larger (bulk) models, in an attempt to correlate associated Heats of Formations against single molecular properties. As a result of the restriction of force field definitions, only neutral and radical species were exposed to Monte Carlo, *Grand Canonical* ensemble simulations, to derive at their respective optimum model sizes (based on their optimum bulk model Internal Energies U_i).

c) An extensive set of empirical force field parameters for the radical species of $C\ell O_2$ have had to be derived, in order to perform the GEMC empirical simulations. The *pcff+* set of force field parameters were employed and adjusted for this study. The materials based ***MedeA/GIBBS*** software was employed for the GEMC simulations.

d) These extended optimum GEMC model presentations were then exposed to semi-empirical quantum chemistry vibrational analysis (***MOPAC-2016*** software) to derive an active set of thermochemical properties.

e) Single species were exposed to the *Ab Initio* derivation of internal electronic energies (including the zero-point energy) for all species, using the ***Gaussian-16*** and ***MOPAC-2016*** software, to derive at a complementary set of thermochemical properties.

f) A *Density Functional* (DFT) approach was then followed, applying the ***VASP*** software system in periodic environments, for all single species (initially to derive at optimum geometries, but also to obtain thermochemical properties)

g) The final phase of this study involved a species-based thermodynamic analysis, applying the PC-based ***FactSage*** software program, to predict the most relevant chemical reaction phenomena in an aqueous medium.

1.4 Limitation of the study

The investigation into the effects that the $C\ell O_2$ species (oxidant) have on NOM species characteristics, are extremely vast and requires multiple studies which are time consuming. The simulation of the interaction of various NOM species with the known persistent $C\ell O_2$ species, could not be examined in this study. Furthermore, the ability of $C\ell O_2$ to act as a pathogen controlling agent must also be undertaken as further investigations.

1.5 References

[1] H. Feng, Y. N. Liang and X. Hu, "Natural Organic Matter (NOM). An Underexplored Resource for Environmental Conservation and Remediation," Materials Today Sustainability, vol. 19, p. 100159, 2022.

[2] N. Abdullah, N. Yusof, W. Lau, J. Jaafar and A. Ismail, "Recent Trends of Heavy Metal Removal from Water/Wastewater by Membrane Technologies," Journal of Industrial and Engineering Chemistry, vol. 76, pp. 17-38, 2019.

[3] R. D. Letterman and S. Yiacoumi, "Water Quality and Treatment, A Handbook on Drinking Water," in Chapter 8: Coagulation and Flocculation, Denver, Colorado, American Water Works Association, 2010.

[4] E. G. Alvarez, N. Carslaw, S. Dusanter, P. Edwards, V. G. Mihucz, D. Heard, J. Kleffmann, S. Nehr, C. Schoemacker and D. Venables, "Techniques for Measuring Indoor Radicals and Radical Precursors," Applied Spectroscopy Reviews, vol. 57, no. 7, pp. 580-624, 2022.

[5] M. Hayyan, M. A. Hashim and I. M. Alnashef, "Superoxide Ion: Generation and Chemical Implications," Chemical Reviews, vol. 116, no. 5, p. 3029–3085, 2016.

CHAPTER-2: LITERATURE REVIEW

2.1 Background

This chapter offers a detailed summary of the extensive chemical applications, chemical and physical properties and vast array of wider phenomena (e.g. medical applications, paper and pulp, pathogen control) already recorded for $C\ell O_2$ and its extended and sub species. This also demonstrates the complexity contained in such a "small" chemical compound, having electronic properties of a radical, reduced or oxidized into ions as well. It is furthermore important to realise the related complexity, to undertake electronic level computations on these species. Their geometries and stereo-chemical presentations are generally known to be insufficiently 'described' by the quantum chemical software systems of today.

2.2 Historic Statement

Chlorine dioxide ($C\ell O_2$) was discovered in 1814 by Sir Humphrey Davy whose likeness is illustrated in Figure-2.1 [1]. He produced $C\ell O_2$ in the gaseous phase by reacting sulphuric acid (H_2SO_4) with potassium chlorate ($KC\ell O_3$) [2]. Later he replaced H_2SO_4 with hypochlorous acid ($HOC\ell$) [1]. Equation (1) highlighted below has recently gained popularity as the typical method used to yield huge quantities of $C\ell O_2$ [2]. Sodium chlorate ($NaC\ell O_3$) replaced potassium chlorate in the reaction [3]:

$$2NaC\ell O_3 + 4HC\ell \rightarrow 2C\ell O_2 + C\ell_2 + 2NaC\ell + 2H_2O \qquad (1)$$

*Figure-**2.1**:* Sir Humphrey Davy [4]

The $C\ell O_2$ molecule contains an odd number of valence electrons, and is classified as a paramagnetic radical in the triplet spin state. L.O. Brockway [5] presented a three-electron bond electronic structure for $C\ell O_2$. Chemist Linus Pauling carried out investigations which led to the discovery of two resonance structures encompassing a double bond on one side and a single bond which comprised of a $3\bar{e}$ bond on the other [6]. It is an extremely energetic and volatile molecule considering its size and is the only substance that can still persist as a monomeric free radical even in diluted aqueous solutions. [7].

2.3 Properties, Applications and Chemical Character

2.3.1 *$C\ell O_2$ generation*

Three methods of $C\ell O_2$ generation have been identified in open literature. It can be generated by reacting sodium chlorite with reacting with gaseous chlorine.

$$2NaC\ell O_2 + C\ell_2(g) \rightarrow 2C\ell O_2(g) + 2NaC\ell \quad (2)$$

Secondly, sodium chlorite can be reacted with hypochlorous acid ($HOC\ell$) to produce $C\ell O_2$.

$$2NaC\ell O_2 + HOC\ell \rightarrow 2C\ell O_2(g) + NaC\ell + NaOH \quad (3)$$

And the reaction of sodium chlorite with hydrochloric acid ($HC\ell$) also produces $C\ell O_2$.

$$5NaC\ell O_2 + 4HC\ell \rightarrow 4C\ell O_2(g) + 5NaC\ell + 2H_2O \quad (4)$$

Reactions (2), (3), and (4) demonstrate how generation steps can differ [8], [9]. The most efficient conversion of sodium chlorite to $C\ell O_2$ (80%) when using hydrochloric acid is achieved through reaction (4) above. This method is currently widely used in industry in most water process applications [10].

Chlorite ($NaC\ell O_2$) is a stable precursor of $C\ell O_2$ that is safely transported and utilised to generate $C\ell O_2$ as per the process reflected in Equation (4) [11]. This stable precursor is produced commercially by reacting $C\ell O_2$ with the reducing agent hydrogen peroxide [12].

$$2C\ell O_2 + H_2O_2 + 2NaOH \rightarrow 2NaC\ell O_2 + 2H_2O + O_2 \quad (5)$$

2.3.2 $C\ell O_2$ Physico-chemical properties

The gas phase of $C\ell O_2$ has the following thermochemical properties [13] at Normal Temperature and Pressure (NTP):

1. Enthalpy of formation: 102.5 kJ/mol [13]
2. Gibbs energy of formation: 120.5 kJ/mol [13]
3. Entropy: 256.8 J/mol K [13]
4. Heat capacity: 42.0 J/mol K [13]
5. The dipole moment of $C\ell O_2$ is 1.69 Debye units [14], [15]

The reactivity of $C\ell O_2$ and its physical chemical properties have been studied extensively. Some key physical-chemical parameters are listed below:

1. $C\ell O_2$ is reduced to chlorite ($C\ell O_2^-$) for it to react predominantly as a highly selective oxidant [16], [8], [17]. The equivalent electron transfer reactions are similar to those occurring when singlet oxygen acts as an oxidant [18], [19].
2. The chlorine-oxygen bonds have been described as double bond comprising an angle of about 117.5° [14], [20] and a chlorine oxygen bond length of 1.47 Å.

3. $C\ell O_2$ has a maximum absorption response at 359 nm and a molar absorptivity of 1250 litres/mol
4. cm [14], [20].
5. When $C\ell O_2$ comes in contact with aqueous pollutants, it typically reduces to chlorite ion ($C\ell O_2$+NOM → Products + $C\ell O_2^-$) [21], [22].
6. A significant difference between $C\ell O_2$ and chlorine is the ability of $C\ell O_2$ to exist as a dissolved true gas in solution and has superior solubility in water, ten times greater than the solubility of chlorine in water [7]. This ability supports $C\ell O_2$ in maintaining its biocidal effectiveness over a wide pH range [23], [24]. Hence, the use of $C\ell O_2$ is favoured for the operation of cooling systems that have poor pH control.
7. $C\ell O_2$ is an oxidizing agent, not a chlorinating agent [7].
8. Its application in water treatment, containing high organic content, has the benefit of hardly forming trihalomethanes (THMs) [15].
9. It has a "lower oxidation strength than ozone but is more powerful than chlorine" [25].

2.3.3 *$C\ell O_2$ Structure*

According to Pauling's theory, the molecular geometry (shape) of $C\ell O_2$ is considered angular whilst the electronic shape is tetrahedral due to the presence of five valence electrons [26]. The five valence shell π-electrons are oriented in the $(1b_l)^2(1a_2)^2(2b)^1$ molecular orbital (MO) configuration [27], [28]. The removal of the 3d-atomic orbitals from the chlorine atom results in the modification of $(1b_l)^2$ $(1a_2)^2(2b)^1$ configuration whereby the five electrons become distributed across three overlapping $p-\pi$ atomic orbitals (AOs) [27], [28].

2.3.4 *$C\ell O_2$ as a Disinfectant*

$C\ell O_2$ is being applied progressively to control microbiological growth in various industries. $C\ell O_2$ has a stronger oxidizing power, hence small doses produce effective pathogen control. This property makes $C\ell O_2$ an economical dosing option which also highlights its safety aspects in terms of storage and deployment. In terms of microbiological control or disinfection, $C\ell O_2$ finds use in the following:

- Pulp and paper industries for paper pulp bleaching [29], [30]
- Fruit and vegetable process industries where it is used to clean and preserve fruit and vegetables, extending the shelf life of the produce [31].
- Various canning plants for meat and poultry add $C\ell O_2$ as a process aid to reduce the microbial plate counts [32].

$C\ell O_2$ is utilised as a primary or secondary disinfectant in water treatment, for the production of potable water. The key factors that favour its use include [33]:

- Taste and odor control

- THM/halo-acetic acids (HAA) reduction
- Iron (Fe) and manganese (Mn) control
- Colour removal
- Sulphide and phenol degradation.

2.4 Microbiological Properties of $C\ell O_2$

$C\ell O_2$ has a more efficient antimicrobial activity than chlorine [34]. $C\ell O_2$ has been documented to have the ability of eliminating *Cryptosporidium*, *Giardia and Legionella sp.* effectively [35]**,** [36]**.** It is very efficient in killing bacteria and especially successful in deactivating viruses [37]. Organic components in bacterial cells interact with $C\ell O_2$ which results in the inhibition and destruction of cellular processes. $C\ell O_2$ penetrates the cell walls of bacteria and inactivates amino acids and the RNA present in the cell [38]. $C\ell O_2$ adsorbs into the surface area of bacterial cells and concentrates around the bacterial cell, where it can act effectively due to the physical adsorption process. $C\ell O_2$ hence, infiltrates the bacterial cell thereby destroying enzymes [39], [40], [41].

An example of the action $C\ell O_2$ on bacterial cells is demonstrated by the reaction of $C\ell O_2$ on *E. coli.* $C\ell O_2$ interferes with the external membrane of *E. coli by* promoting substantial leakage of K^+ ions out of the specimen via inhibition of enzyme β-D-galactosidase [42]. This point again suggests that $C\ell O_2$ acts by targeting the cell wall of micro-organisms.

Virus elimination differs from bacterial elimination, by directly reacting with water soluble peptone which in turns prevents the formation of amino acids that is required for protein synthesis. Hence, protein formation is prevented which leads to death of the viruses. [43]. It inactivates microorganisms by directly oxidizing tyrosine-, methionyl- or cysteine-containing proteins that disrupt important structural functions in the enzyme metabolic processes [44], [43].

2.4.1 *Microbial action of $C\ell O_2$ in alkaline medium*

In the presence of an alkaline solutions, $C\ell O_2$ disproportionate to chlorite ($C\ell O_2^-$) and chlorate ($C\ell O_3^-$) via the following reaction [24]:

$$2C\ell O_2 + 2OH^- \rightarrow H_2O + C\ell O_2^- + C\ell O_3^- \qquad (6)$$

This reaction is catalysed by hydrogen (H^+) ions. The half-life of aqueous mixtures of $C\ell O_2$ decreases with increasing pH.

Since the “organic matter” is oxidised by undissociated chlorine dioxide as the $C\ell O_2^-$ ion [45], it is possible that $C\ell O_3^-$ is the most reactive species that is responsible for the inactivation of the poliovirus in an alkaline environment. Alvarez *et al.*, [46], [47], studied the mechanism of inactivation of the polio virus by $C\ell O_2$ and reported that addition of $C\ell O_2$ in an alkaline medium, resulted in the separation of the RNA from the capsids. $C\ell O_2$ penetrates into HeLa cells of the virus and initiates the protein uncoating process [46], [47] . The inactivation process takes place at pH 6.0 where $C\ell O_2$

penetrates the protein coat and changes the pH thereby altering the viral RNA reducing its ability of producing templates for RNA replication [46], [47].

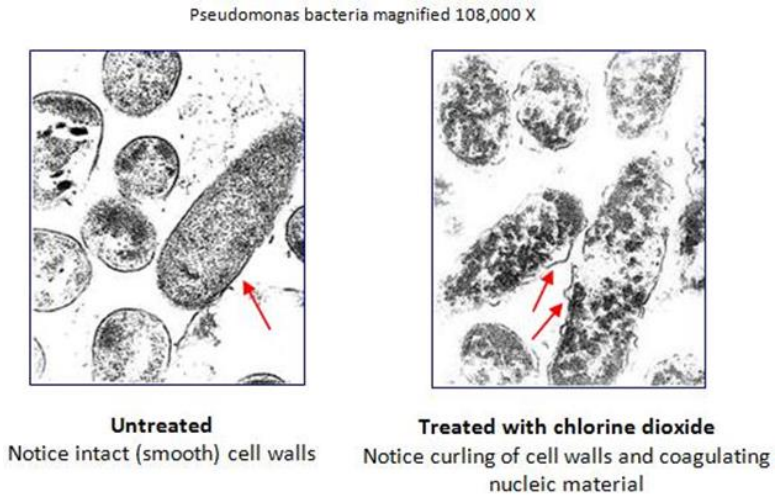

Figure- **2.2:** Impact of ClO_2 on micro-organism cell depletion [33]

High pH also increases the susceptibility of the virus to $C\ell O_2$ attack [46], [47] . The reaction is not time dependent nor concentration dependent [38]. In contrast to non-oxidising disinfectants, $C\ell O_2$ kills micro-organisms regardless of it being in an active or passive state. Therefore, a lower concentration of $C\ell O_2$ is required to effectively kill micro-organisms, which cannot build up any resistance against $C\ell O_2$.

$C\ell O_2$ has a higher 'oxidative capacity' than all disinfectants [48]. The capacity of chemicals denotes the number of electrons one molecule can accept from its surrounding molecules. In the case $C\ell O_2$, this means that it can gain five electrons from microbial species per molecule, making it a superior biocide to alternative oxidisers, which typically are only able to gain two electrons. The oxidative capacity of $C\ell O_2$ compared to other disinfectants is presented in Table 2.1.

*Table-**2.1:*** Chlorine Dioxide Oxidation Capacity compared with other Disinfectants [48]

Oxidant	$C\ell O_2$	H_2O_2	$NaC\ell O_2$	$KMnO_4$	$C\ell_2$	$NaC\ell O$
Capacity Oxidation	263%	209%	157%	111%	100%	93%

- Oxidation capacities tabulated in table 2.1 indicate that $C\ell O_2$ has the highest oxidation capacity compared to other disinfectants.
- This oxidizing capacity substantiates why $C\ell O_2$ is considered to be the most effective disinfectant agent.

- $C\ell O_2$ is highly soluble in water and, unlike ozone, does not react with the extracellular polysaccharides of biofilms, hence it can rapidly eliminate biofilms [49], [50].
- $C\ell O_2$ penetrates into biofilms swiftly, to destroy the microbes present inside the film and oxidises the polysaccharide matrix that retains the bio-film structure [51], [52]. As a result, the biofilm dissociates into pieces that remain steady. An acidic environment forms as the biofilm begins to grow again, and the chlorite ions are transformed into $C\ell O_2$ in this environment. Hence, the remaining biofilm is eliminated [50]. Many researchers have described exceptional results whilst using $C\ell O_2$ as a biocide [49], [53], [54], [50].

2.5 Radicals and Other Reactive by-products of $C\ell O_2$

There are various chlorine oxide species that are either classified as radicals or highly reactive species i.e., $C\ell O$, $C\ell O_2$, $C\ell O_3$, $C\ell O_4$, $HOC\ell$, $HC\ell O_2$ $C\ell_2O$, $C\ell_2O_3$, $C\ell_2O_4$ and $C\ell_2O_6$. The mono-chlorine oxides are highly reactive *radicals* which are challenging to detect since they are fairly short-lived species [55]. The di-chlorine oxides are highly unstable [55].

$C\ell O_2$ undergoes a decomposition reaction in aqueous medium that produces chlorite and chlorate ions:

$$2C\ell O_2 + H_2O \rightarrow C\ell O_2^- + C\ell O_3^- + 2H^+ \quad (7)$$

A solution of $C\ell O_2$ in water will degrade upon exposure to light, through a complicated reaction mechanism. Chloride ($C\ell^-$), chlorite ($C\ell O_2^-$) and chlorate ($C\ell O_3^-$) are the products that form, from the disproportionation reaction of $C\ell O_2$. Other radical formation products observed are: $HC\ell O_2$, $C\ell O_2^-$, $HOC\ell$, and $C\ell_2$ [56]. "Approximately 70% of applied $C\ell O_2$ forms chlorite, while about 10% forms chlorate [57]". The free radical is found in gaseous form above 11 to 12°C [58], [8], [20].

2.6 Decomposition and Dissociation of CℓO2

Chlorate ($C\ell O_3^-$) and chlorite ($C\ell O_2^-$) concentrations are both present in the pH range between 1 and 4. Chlorite ($C\ell O_2^-$) is the main species above pH 4. Although chlorite is also a byproduct of a complicated mechanism involving the decomposition of $C\ell O_2$ in water, it is predominantly produced during NOM oxidation [59], [52]. The reactions that follow (equations (8) – (9)), describe what potentially can happen when $C\ell O_2$ dissociates spontaneously:

First, $C\ell O_2$ abstracts an electron via the reduction process resulting in chlorite:

$$C\ell O_2 + e^- \rightarrow C\ell O_2^- \quad (8)$$

The chlorite ion is reduced to form a chloride ion:

$$C\ell O_2^- + 4H^+ + 4e^- \rightarrow C\ell^- + 2H_2O \quad (9)$$

These reactions suggest that $C\ell O_2$ accepts five electrons and is reduced to chloride ($C\ell^-$). The chlorine atom does not change until stable chloride is formed. Hence formation of chlorinated substances is prevented. Chlorine gas reactions on the other hand are driven by addition and substitution reactions whereby, chlorine atoms incorporate into organic material. The chlorous acid equilibrium reaction produces a fairly low pKa of 1.8 for the chlorite ion ($C\ell O_2^-$). However, base ion pair equilibrium reaction pH for hypochlorous acid/hyopochlorite has been recorded to fall near pH 7. "This suggests that the chlorite ion ($C\ell O_2^-$) exists as the dominant species in drinking water and in the human body [12], [60].

2.7 Decomposition of Alkaline $NaC\ell O_2$ Solutions

Since $NaC\ell O_2$ is used to generate $C\ell O_2$ (**refer to section 2.3.1**), its decomposition products in aqueous medium are also emphasized below. $C\ell O_2$ does not result from the decomposition reaction of $NaC\ell O_2$ in hot, highly alkaline solution; instead, $C\ell O_3^-$ is the main by-product of the breakdown reaction [61].

$$3NaC\ell O_2 \rightarrow 2NaC\ell O_3 + NaC\ell \qquad (10)$$

2.7.1 *Decomposition of $NaC\ell O_2$ in Neutral Solutions*

Neutral solutions of sodium chlorite are stable. The solution will decompose slowly upon exposure to light and heat [62], [61]. A chlorite ion solution becomes less stable as the pH decreases. The disintegration of a neutral sodium chlorite mixture does not produce $C\ell O_2$, only chlorite ($C\ell O_2^-$) and chlorate ($C\ell O_3^-$) ions are formed [63].

2.7.2 *Dissociation of chlorous acid ($HC\ell O_2$)*

Chlorous acid is the least stable of all the chlorine oxyacids and is also occasionally used in the generation of $C\ell O_2$ [11]. Its behaviour in aqueous medium is highlighted in equations (11-14). In relation to chlorous acid, the decomposition reaction of chlorous acid is second order.

Bohmlander [64] found that the initial reaction is second order with a delayed transition to a first order reaction [64]. He then proposed the dissociation reaction for chlorous acid. The initial reaction follows the path between pH 0.5 to pH 2 (below):

$$2HC\ell O_2 \rightarrow C\ell O_3^- + H^+ + HOC\ell\bullet \qquad (11)$$

And:

$$2HC\ell O_2 + C\ell^- \rightarrow C\ell O_2 + HOC\ell\bullet + OH^- + C\ell\bullet \qquad (12)$$

Followed by:

$$2HC\ell O_2 + C\ell\bullet \rightarrow C\ell O_2 + 2HOC\ell\bullet \qquad (13)$$

After 10 minutes, the reaction is no longer rate limiting and is written as:

$$2HC\ell O_2 + HOC\ell \rightarrow C\ell O_2 + C\ell^- + H_2O + H^+ \qquad [64] \qquad (14)$$

In water, $C\ell O_2$ forms a solid polyhydrate [65]. Above about 18.2 °C, the hydrates lose some of their solubility and transform back into their unhydrated form [66]. $C\ell O_2$ hydrolyzes relatively slowly, although light and heat speed up the decomposition process. $C\ell O_2$ decomposes at 0 and 60˚C according to:

$$6C\ell O_2 + 3H_2O \rightarrow 5HC\ell O_3 + HC\ell \qquad [8] \qquad (15)$$

The reaction is accelerated by the hydrogen and chloride ion. There is some evidence that $C\ell O_2$ breaks down into chlorine and oxygen [11].

Various reaction schemes have been published for chlorine oxide molecule. "It is commonly assumed that terminal oxygens form dative bonds with chlorine whereas bridging-oxygen-chlorine bonds are covalent [55]. Most studies have focused on photo excitation processes in the stratosphere and not in liquid meduim. These reaction schemes are nevertheless represented below to give an idea of possible species formation.

With: M= Molecule (**non-reactive molecule**)

$$HC\ell O_4\,(+M) \rightarrow OH + C\ell O_3\,(+M) \qquad (16)$$

$$OH + C\ell O_3\,(+M) \rightarrow HC\ell O_4{*} \rightarrow HC\ell O_4\,(+M) \qquad (17)$$

$$\rightarrow HOOC\ell O_2{*} \rightarrow HO_2 + C\ell O_2 \qquad [19] \qquad (18)$$

$$OC\ell O + h\nu \rightarrow C\ell O + O \qquad (19)$$

$$C\ell O + O \rightarrow C\ell OO \qquad [67] \qquad (20)$$

$$OC\ell O + O \rightarrow C\ell O_3 \qquad (21)$$

$$C\ell O_3 + C\ell O \rightarrow C\ell_2O_4 \qquad [67] \qquad (22)$$

$$C\ell O + C\ell O + M \rightarrow C\ell_2O_2 + M \qquad (23)$$

$$C\ell O.H_2O + C\ell O \rightarrow C\ell_2O_2 + H_2O \qquad [68] \qquad (24)$$

Francisco and Sanders [68] confirmed the existence of a $C\ell O.H_2O$ radical complex that enhances the formation of a dimer as seen in Equation 24.

$$OH + C\ell O \rightarrow HO_2 + C\ell \qquad (25)$$

$$HO_2 + C\ell \rightarrow HC\ell + O_2 \qquad [69] \qquad (26)$$

$$C\ell O_2 + hv \rightarrow C\ell O + O \qquad (27)$$

$$C\ell O_2 + O \rightarrow C\ell O + O_2 \qquad (28)$$

$$C\ell O + O \rightarrow C\ell + O_2 \qquad [70], [71] \qquad (29)$$

$$SO_4^- + C\ell^- \rightleftharpoons SO_4^{2-} + \bullet C\ell \qquad (30)$$

$$C\ell + C\ell^- \rightleftharpoons \bullet C\ell_2^- \qquad [72] \qquad (31)$$

$$OH + C\ell \rightleftharpoons HO\bullet C\ell^- \qquad (32)$$

$$HO\bullet C\ell^- + H^+ \rightarrow H_2O + C\ell \qquad (33)$$

The oxidation of chloride ions in aqueous solutions is known to produce the $\bullet C\ell_2^-$ radical as an intermediate [73], [74].

2.8 Chlorine Dioxide Reaction/Reactivity Properties

$C\ell O_2$ will likely react with any inorganic species present in water being treated for potable use. Based on the following selected example reactions (reaction 34 - 38), $C\ell O_2$ may likely form insoluble or aqueous species that may be removed by flocculation processes, although beyond the scope of this thesis, these are areas of study that should be looked into when utilising $C\ell O_2$ for potable water treatment.

2.8.1 *Oxidation of iron*

$$C\ell O_2 + FeO + NaOH + H_2O \rightarrow Fe(OH)_3 + NaC\ell O_2 \quad [12] \qquad (34)$$

FeO is responsible for influencing the aesthetic property of water as it is capable of imparting undesirable colour to potable water [75]. It can be removed during the flocculation (clarification) process.

2.8.2 *Oxidation of manganese*

$$2C\ell O_2 + MnSO_4 + 4NaOH \rightarrow MnO_2 + 2NaC\ell O_2 + Na_2SO_4 + 2H_2O \quad [12] \qquad (35)$$

The formation of MnO_2 is noted for its use in water softening process, hence its presence can assist the water purification process substantially [76].

2.8.3 *Oxidation of sodium sulphide*

$$2C\ell O_2 + 2Na_2S \rightarrow 2NaC\ell + Na_2SO_4 + S \quad [12] \qquad (36)$$

Ingestion of potable water with excessive levels of Na_2SO_4 can cause intestinal discomfort leading to diarrhea [77].

2.8.4 *Oxidation of nitrogen oxide pollutant*

$$C\ell O_2 + 2NO + H_2O \rightarrow NO_2 + HNO_3 + HC\ell \quad [12] \qquad (37)$$

Nitrogen oxide is considered to be flue gas pollutant. $C\ell O_2$ can be used to remove this pollutant from flue gas.

2.8.5 *Aluminum, magnesium, zinc & cadmium (M) react with $C\ell O_2$*

$$M + xC\ell O_2 \rightarrow M(C\ell O_2)x \quad [12] \qquad (38)$$

$C\ell O_2$ bleaches aluminum, magnesium, zinc & cadmium by oxidizing them

2.8.6 *Organic Reactions with $C\ell O_2$*

When reacting with organic compounds in water, $C\ell O_2$ has converted such compounds to aldehydes, carboxylic acids, ketones and quinones [12]. Hydrocarbons chain lengths that exceed eight carbons are easily oxidised by $C\ell O_2$ [39].

$C\ell O_2$ oxidizes triethylamine in aqueous solution with the production of diethylamine, acetaldehyde, hydrogen ion, and chlorite ion [12].

$$2C\ell O_2 + H_2O + (C_2H_5)_3N \rightarrow (C_2H_5)_2NH + 2C\ell O_2^- + CH_3CHO + 2H^+ \qquad (39)$$

$C\ell O_2$ changes large aromatic and long aliphatic chain organic compounds into tiny and hydrophilic organics, largely destroying the aromatic bond structure of NOM [78].

The interactions between various organic compounds and $C\ell O_2$ in water has been tabulated in Table 2.2.

*Table-**2.2**:* Interactions of organic compounds with $C\ell O_2$ in water

Reactants	Products/ Description of reaction	Reference
H_2O + $C\ell O_2$ + olefins	aldehydes, epoxides, chlorohydrins, dichloro-derivatives and chloro-unsaturated ketones	[12], [79]
H_2O + $C\ell O_2$ + ethylenic double bonds	ketones, epoxides, alcohols	[12]
H_2O + $C\ell O_2$ + toluene	CH_3, $CH_2C\ell$, CH_2OH	[12]
H_2O + $C\ell O_2$ + anthracene at 45˚C	anthraquinone and l,4-dichloroanthracene	[12]
H_2O + $C\ell O_2$ + phenanthrene	diphenic acid and 9-chlorophenanthrene	[12]
H_2O + $C\ell O_2$ + 3,4-benzopyrene	quinones, traces of chlorinated benzopyrene (no longer considered carcinogenic)	[12]
H_2O + $C\ell O_2$ + aldehydes	carboxylic acids	[12]
H_2O + $C\ell O_2$ + ketones	alcohols	[12]
H_2O + $C\ell O_2$ + aliphatic amines: tertiary	rupture of CN bond, no N-oxides formed	[12], [79]
H_2O + excess $C\ell O_2$ + phenol	Para-benzoquinone and 2-chlorobenzoquinone	[12], [79]
H_2O + $C\ell O_2$ + phenol	maleic acid and oxalic acid	[12], [79]
H_2O + $C\ell O_2$ + thiophenols	sulfonic acids	[12]
H_2O + $C\ell O_2$ + tocopherol	demethylated derivatives	[12]
H_2O + $C\ell O_2$ + anhydrides	no reaction but catalyses hydrolysis reactions	[12]
H_2O + $C\ell O_2$ + amino acids: glycine, leucine, serine, alanine, phenylalamine, valine, hydroxyproline, phenylaminoacetic acid, aspartic, glutamic acids	little, or no reaction	[12]
H_2O + $C\ell O_2$ + amino acids containing sulphur	reactive	[12]

*Table **2.2*** continued

Reactants	Products/ Description of reaction	Reference
H_2O + $C\ell O_2$ + methionine sulfoxide	sulfone	[12]
H_2O + $C\ell O_2$ + aromatic amino acids	reactive	[12]
H_2O + $C\ell O_2$ + tyrosine	dopaquinone, dopachrome	[12], [22]
H_2O + $C\ell O_2$ + tryptophan	idoxyl, isatine, indigo red and trace chlorinated products	[12], [22]
H_2O + $C\ell O_2$ + thiamine	slow reaction	[12]
H_2O + $C\ell O_2$ + keratin	hydrosoluble acids	[12]
H_2O + $C\ell O_2$ + carbohydrates CHO and CH_2OH	carboxylic functions	[12]
H_2O + $C\ell O_2$ + pectic acid	mucic acid, tartaric acid and galacturonic acid	[12]
H_2O + $C\ell O_2$ + chlorophyll and plant dyes	colour removed	[12]
H_2O + $C\ell O_2$ + latex and vinyl enamels	delays polymerisation	[12]
H_2O + $C\ell O_2$ + biacetyl	acetic acid, carbon dioxide	[12]
H_2O + $C\ell O_2$ + 2,3-butaneodiol	acetic acid and carbon dioxide	[12]
H_2O + $C\ell O_2$ + cyclohexene	aldehydes, carboxylic acids, epoxides, alcohols, halides, dienes and ketones	[12]
H_2O + $C\ell O_2$ + cyanides	oxidised	[12]
H_2O + $C\ell O_2$ + nitrites	oxidised	[12]
H_2O + $C\ell O_2$ + sulphides	oxidised	[12]
H_2O + $C\ell O_2$ + unsaturated fatty acids and their esters	typically undergo double bond oxidation	[12]
H_2O + $C\ell O_2$ + phenols	quinones, malonic acid and oxalic acid	[80], [81], [82]
H_2O + $C\ell O_2$ + lignins	quinones and carboxylic acids	[29], [83]
H_2O + $C\ell O_2$ + humic acid	quinones and carboxylic acids	[29], [83]
H_2O + $C\ell O_2$ + methoxylic groups (complex organic groups)	aliphatic hydroxylic groups	[84], [85]
H_2O + $C\ell O_2$ + methoxylic groups	aldehydes, ketones and esters (oxidises aliphatic complexes between the p-electron system of the olefin fragments	[83], [84], [85]

2.8.7 *Non-Reactive Species*

$C\ell O_2$ does not react with benzene, napthaline, ethanol, maleic acid, crotonic acid, hippuric acid, cinnamic acid, betaine, creatine, alanine, phenylalanine, valine, leucine, asparaginic acid, asparagine, glutaminic acid, serine, hydroxyproline and taurine [12], [85]. No reaction takes place when $C\ell O_2$ is in contact with aliphatically combined NH_2 groups, amido and imido compounds, HO groups in acids and alcohols [12], [83]. $C\ell O_2$ does not react with free CO_2H groups or CO_2H groups that have been esterified in a medium of mono and polybasic acids, nitrile groups, CH_2 groups that are present in a homologous series, ring structures such as C_6H_6, $C_{10}H_8$, cyclohexane, and the salts of C_5H_5N, quinoline and piperidine [12].

Under normal water treatment conditions, the majority of the aliphatic and aromatic hydrocarbons will not react with $C\ell O_2$. The exception to this rule only relates to the hydrocarbons containing specific reactive groups. These reactive groups include phenol type compounds, secondary and tertiary amines, organic sulphides and certain hydrocarbon polycyclic aromatics such as benzopyrene, anthracene and benzoathracene [84].

2.9 Water Treatment Processing

In the mid to late 1970s, numerous studies linked higher cancer mortality rates to the chlorination of potable water [60]. Trihalomethane (THM) concentrations, specifically chloroform, were found to be associated with an increase in cancer mortality [86], [87]. The formation of chloroform was a direct consequence of the reaction of chlorine and naturally occurring organics. As a result of this research, the USEPA established a maximum THM containment level for drinking water of 0.1 ppm.

$C\ell O_2$ is becoming more widely used in the water treatment industry. The first reported water treatment plant to incorporate $C\ell O_2$ was in Niagara Falls in 1944 [88]. In 1986, approximately 200-300 USA potable water treatment process plants introduced $C\ell O_2$ into their treatment cycles, whilst thousands of $C\ell O_2$ applications were recorded in Europe [51], [22].

In an aqueous medium, the species aids processes that drive coagulation and the removal of turbidity [89], [90] and prevents the formation of THMs [91].

The Poznan Water Treatment and Sewage Co in Poland uses $C\ell O_2$ as a pre-oxidation step before granular activated carbon (GAC) filtration [92] This plant has shown that even low doses of 0.2 mg $C\ell O_2$ L^{-1} can have a substantial impact on the extent to which NOM is absorbed, which in turn improves the capacity of GAC filters [92]. The molecular weight (mw) of NOM showed very slight variations. The larger molecular weight compounds were found to be more inclined to react with $C\ell O_2$ [93].

2.9.1 *Advantages and Disadvantages of the Use of $C\ell O_2$ in Water Treatment*

There are several advantages associated with the use of $C\ell O_2$ in water. A few main advantages are listed below:

- Giardia, Cryptosporidium, and other viruses are more effectively inactivated by $C\ell O_2$ than by chlorine and chloramines [94]. Also see section 2.4.
- $C\ell O_2$ oxidises iron, sulphides and manganese. **[Eq. 34 -38]**
- $C\ell O_2$ may enhance the clarification process.
- $C\ell O_2$ is easy to generate **[Refer to section 2.3.1]**
- The pH of the system has no impact on the biocide capabilities of $C\ell O_2$ [94].
- $C\ell O_2$ provides residuals for long-term disinfection because it does not hydrolyze when it enters water, but instead persists as a dissolved gas in solution and can thus act more efficiently over time [95]. $C\ell O_2$ is also more soluble than chlorine gas in water [11].
  Refer to section 2.5

Disadvantages

- The $C\ell O_2$ process forms the specific by-products chlorite ($C\ell O_2^-$) and chlorate ($C\ell O_3^-$). (These by-products are both highly toxic compounds and require Occupational Health Care during scaled processes) [60].
- The costs of sampling and laboratory testing for chlorite and chlorate are exorbitant [51], [12].
- Rental of generators and cost of the sodium chlorite are excessive [51].
- Safety precautions are required whilst measuring chlorine dioxide gas, since it is explosive [51], [12]
- $C\ell O_2$ decomposes in sunlight, so it must be produced in close proximity to the application [94].

2.9.2 *Toxicity of $C\ell O_2$*

Chlorite ($C\ell O_2^-$) causes hemolytic stress in animals when consumed in food at low levels of 50 ppm. [23]. The drinking water standard for total $C\ell O_2$, chlorite ($C\ell O_2^-$) and chlorate ($C\ell O_3^-$) was therefore limited to 1.0 ppm, taking into account individuals prone to oxidative stress [7], [96], [23].

2.9.3 *$C\ell O_2$ Residuals*

Monitoring of $C\ell O_2$ residuals in a water treatment plant environment can be problematic. The Palin DPD method [97] is used to measure $C\ell O_2$ residuals. This test usually gives a higher residual reading for $C\ell O_2$ than for chlorine. According to these results, one would expect chlorine to have a higher oxidizing potential than $C\ell O_2$. This, however, is not the case with respect to reactions (40) and (41).

$$C\ell O_2 + 4H^+ + 5\,\bar{e} \rightarrow C\ell^- + 2H_2O \qquad E_o = 1.95\ V \qquad (40)$$

$$C\ell_2 + 2\bar{e} \rightarrow 2\,C\ell^- \qquad E_o = 1.36V \qquad (41)$$

Hence $C\ell O_2$ is the stronger oxidising agent. To clarify the discrepancy in findings acquired using Palin's DPD method and reactions (42) and (43), one must make the assumption that $C\ell O_2$ is reduced as follows:

$$C\ell O_2 + \bar{e} \rightarrow C\ell O_2^- \qquad E_o = 1.15V \qquad (42)$$

$C\ell O_2$ has two distinct oxidising capacities [98], [10].

When there are adequate hydronium ions present, $C\ell O_2$ proceeds to reduce to chlorite (equation 39), which in turn reduces to chloride (equation 44).

$$C\ell O_2^- + 4H^+ + 4\bar{e} \rightarrow C\ell^- + 2H_2O \qquad (43)$$

The conversion of chlorite to chloride only occurs at low pH as described in reaction (4). Chlorite undergoes protolysis to produce chlorous acid at pH 6–8 (reaction 44) [99].

$$C\ell O_2^- + H^+ \leftrightarrow HC\ell O_2 \qquad k = 0.93x10^2 \text{ Molar (M)} \qquad (44)$$

The equilibrium concentrations of chlorous acid and chlorite at pH 7 are 1:100,000 [98].

Chlorite is only partially protolyzed. If chlorous acid prevails, it might be disproportionate to products as shown in reaction (41).

$$HC\ell O_2 + 3H^+ + 4\bar{e} \rightarrow C\ell^- + 2H_2O \qquad E_o = 1.57 \text{ V.} \qquad (45)$$

$$4HC\ell O_2 \rightarrow 2C\ell O_2 + H^+ + C\ell^- + HC\ell O_3 + H_2O \qquad (46)$$

The absence of chlorate ($C\ell O_3^-$) following the addition of $C\ell O_2$ [98] is possibly due to analytical challenges in detecting trace levels of chlorate in close proximity of other chlorine containing species. However, if chlorous acid is present in water with a pH of 6 to 8, a disproportionation reaction is perhaps most likely to occur (reaction 46). As a result, the situation above suggests that Palin's DPD approach produces chlorite residuals rather than $C\ell O_2$ residuals.

The following can be postulated regarding the reactivity of $C\ell O_2$ in water with oxidizable organic matter at pH 6–8, according to Myhrstad, and Samdal [98], Nawrocki et al, [100]:

1. A reduction of $C\ell O_2$ to chlorite (reaction 38)
2. Protolysis to a very limited extent of chlorite to chlorous acid (reaction 40)
3. Disproportionation of chlorous acid in $C\ell O_2$ and chloride (reaction 42)

The above would apply to most South African raw water treatment processes. As a result, $C\ell O_2$ degrades in two stages:

1. The conversion of $C\ell O_2$ to chlorite

2. Chlorite ion reduction occurs when the reductant produces a low redox potential and exists in the presence of excess hydrogen ions [101], [12].

2.10 Primary Photo Processes of Electronically Excited OCℓO in Water Solution

The symmetric **OCℓO** and the asymmetric **CℓOO** are the two isomeric forms of $C\ell O_2$. The CℓOO isomer is extremely reactive, thermodynamically more stable than OCℓO by around 3 kcal/mol [102], [55], [103] and challenging to examine spectroscopically.

OCℓO is kinetically stable at ambient temperature and does not react thermally with water over several days [104], [105]. Excitation of the $C\ell O_2$ molecule usually occupies three reactive states namely: $^2B_2$, $^1A_1$ and $^2A_1$. The two competitive pathways depicted in reactions 47 & 48, represents the photochemistry of excited-states of $C\ell O_2$:

$$OC\ell O + h\upsilon \rightarrow OC\ell + O \quad (47)$$

$$C\ell OO \rightarrow C\ell + O_2 \quad (48)$$

There has been limited research on the rate at which OCℓO decays via isomerization in aqueous medium and the potential impact of solvent on its reactivity [106], [107]. Given the dynamic nature of the solvent cage, a branching ratio is anticipated to exist between the two pathways. Both the liquid's static and dynamic qualities affect the branching ratio. Since the charge distribution of the reactive $^2B_2$ and $^2A_1$ states differs from one another and from the $^2A_2$ state with Franck-Condon population, this interaction will be very sensitive to the liquid's dielectric properties [102], [108].

The photochemistry of OCℓO yields the following chemical species in the absence of a solvent reaction: CℓO, O, Cℓ, O_2 and CℓOO. When photochemistry of OCℓO in water takes place at ambient temperature, excitation of the $^2A_2$ - $^2B_1$ absorption band at 355 nm occurs. 90% of the OCℓO molecule undergoes dissociation and 10% undergoes isomerisation [109], [110]. Competitive bond dissociation creates CℓO + O and isomerization creates CℓOO from the excited OCℓO molecule. The isomerized product that thermally dissociates into Cℓ and O_2 has a first order reaction rate constant of 6.7 x 10^9 s^{-1} at ambient temperature [106], [20].

2.11 Decomposition and Mechanism of $C\ell O_2$ in Basic Medium

$C\ell O_2$ decomposes rather slowly in neutral aqueous solutions [80], whereas the presence of a base increases the rate of decay [66], [111]. The disproportionation reaction is presented in reaction (6).

Decomposition pathways [112]:

- Pathway 1: First – order in [$C\ell O_2$]: products: [$C\ell O_2^-$], [$C\ell O_3^-$]

$$C\ell O_2 + OH^- \xrightarrow{k_4} (HOC\ell(O)O)^- \quad (49)$$

$$(HOC\ell(O)O)^- + C\ell O_2 \xrightarrow{k_2 fast} HOC\ell(O)O + C\ell O_2^- \quad (50)$$

$$HOC\ell(O)O + OH^- \xrightarrow{k_3 fast} C\ell O_3^- + H_2O \quad (51)$$

- Pathway 2: First-order in [$C\ell O_2$]: products: $C\ell O_2^-$ and O_2

$$C\ell O_2 + OH^- \xrightarrow{k_4} (OC\ell OOH)^- \quad (52)$$

$$(OC\ell OOH)^- + C\ell O_2 \xrightarrow{k_5 fast} OC\ell OOH + C\ell O_2^- \quad (53)$$

$$OC\ell OOH + OH^- \xrightarrow{k_6 fast} HOC\ell O + HOO^- \quad (54)$$

$$HOO^- + 2C\ell O_2 + OH^- \xrightarrow{k_7 fast} 2C\ell O_2^- + O_2 + H_2O \quad (55)$$

$$HOC\ell O + OH^- \xrightarrow{k_8 fast} C\ell O_2^- + H_2O \quad (56)$$

- Pathway 3: Second – order in [$C\ell O$]: products: [$C\ell O_2^-$] = [$C\ell O_3^-$]

$$C\ell O_2 + C\ell O_2 \xrightarrow{k_9} C\ell_2O_4 \quad (57)$$

$$C\ell_2O_4 + OH^- \xrightarrow{k_{10}} HOC\ell(O)O + C\ell O_2^- \quad (58)$$

$$HOC\ell(O)O + OH^- \xrightarrow{k_3 fast} C\ell O_3^- + H_2O \quad [112] \quad (59)$$

Reaction Mechanism

$(HOC\ell(O)O)^-$ is produced by pathway 1 when OH^- adducts with the $C\ell$ in $C\ell O_2$. Similar adducts have been postulated for $C\ell O_2$ + HO_2^- reactions [113]. The reaction between $C\ell$ and OH is weak but considerable, according to an ab initio computation involving the $(HOC\ell(O)O)^-$ adduct [114]. $C\ell O_2^-$ and $HOC\ell O_2$ are produced in the next subsequently rapid electron-transfer step (k_2), which also rapidly produces OH^- (k_3) to give $C\ell O_3^-$. Equimolar $C\ell O_2^-$ and $C\ell O_3^-$ are formed in a first order reaction involving [$C\ell O_2$] and [OH^-].

An electron transfer that is facilitated by the presence of base occurs during the k_2 step of the reaction [112]. It is assumed that pathway 2 involves OH^- combining with a $C\ell O_2$ oxygen atom to produce an adduct to produce the reactive intermediate $(OC\ell OOH)^-$ (k_4). A weak link exists between an OOH segment and an $OC\ell$ segment, the latter of which has a net charge of -0.553 (Figure 2.3).

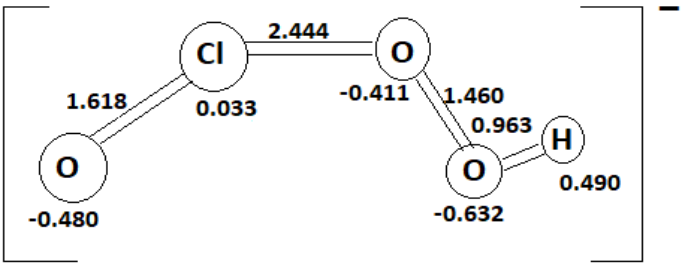

Figure-**2.3**: Equilibrium geometries (bond distances in Å) and atomic charges for the steady-state species (OCℓOOH). [112]

This adduct can swiftly transfer electrons to a second $C\ell O_2$ (k_5) to produce $C\ell O_2^-$ and OCℓOOH. HOCℓO and HOO^- (k_6) are formed when the latter species reacts favourably with OH^-. The interaction of HOO^- and $C\ell O_2$ results in $C\ell O_2^-$ and O_2, wherein k_7 denotes a succession of steps [115]. The stoichiometry for the pathway 2 reaction is presented in reaction (56). Further substantiation of processes using a base-assisted electron transfer are illustrated by the reactions in steps k_4 and k_5. The formation of $(OC\ell OH)^-$ is a potential intermediate, according to *Ab Initio* calculations (Figure-2.4).

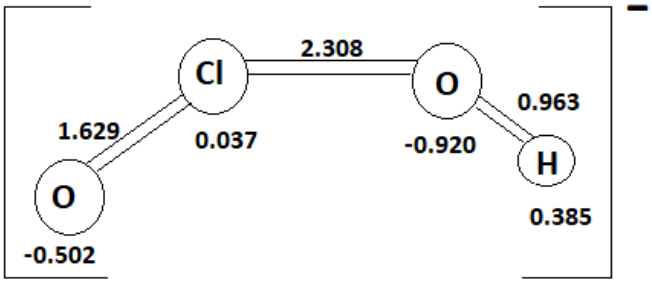

Figure-**2.4**: Equilibrium geometries (bond distances in Å) and atomic charges for the steady state species $(OC\ell OH)^-$. [112]

A second-order reaction in $C\ell O_2$ depicted in pathway 3 is shown to proceed through an intermediate $C\ell_2O_4$ which is in pre-equilibrium with two $C\ell O_2$ molecules (k_9/k_{-9}). The $C\ell_2O_4$ intermediate is similar to the BrO_2^-, $C\ell O_2$ [114] and Br_2O_4 intermediates hypothesised by Halperin and Taube [116]. Another instance of a base-assisted electron transfer occurs in step k_{10} when $C\ell_2O_4$ reacts with OH^-, this time between two weakly linked $C\ell O_2$ molecules.

2.12 Chlorine Oxide Species (This study)

Sixty (60) chlorine oxide species have been identified for the purpose of this study. Heat of Formation values available in open literature were measured using various UV spectroscopic and quantum techniques i.e., W8 theory, G2, G3 and G4 theory and various Ab Initio methods (**Refer to Chapter 4 of this manuscript**).

The chemical formula, structure, name and published Heat of Formation (ΔH_f kcal/mol at 298 K) of the sixty (60) chlorine oxide species are tabulated in Table 2.3. Active Thermodynamic Tables

(ATcT) [117] offer a comprehensive reference for many of these chlorine oxides. For the purposes of this study, a new structural naming convention has been adopted, to accent particular atoms, in highlighting their bonding sequence and conformation/configuration within the structure. The chlorine oxide species presented in Table-**2.3** will be examined in this study.

*Table-**2.3:*** Structure, formulae and names of selected chlorine species

Formula	**Chemical Name**	**Structure**	**ΔH_f (kcal mol^{-1}) at 298K**	**Reference (ΔH_f)**
CℓO (g)	Chloro-oxidanyl	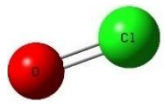	24.31	[117]
$[C\ell O]^-$ (g)	Hypochlorite	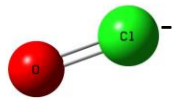	-28.26	[117]
$[C\ell O]^+$ (g)	Oxochloronium	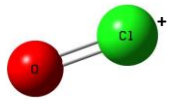	274.84	[117]
HOCℓ (g)	Hypochlorous acid	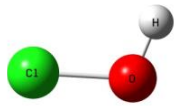	-18.35	[117]
$[HOC\ell]^+$ (g)	Hypochlorous acid cation	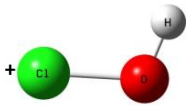	238.01	[117]
CℓOCℓO (g)	Chlorine chlorite	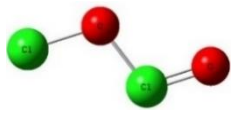	39.77	[117]

*Table-**2.3** continued*

Formula	**Chemical Name**	**Structure**	**ΔH_f (kcal mol^{-1}) at 298K**	**Reference (ΔH_f)**
$[HOC\ell]^-$ (g)	Hypochlorous acid anion	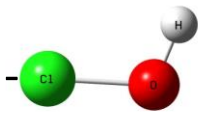	47.41	[117]
$HC\ell O$ (g)	Chlorosyl hydride	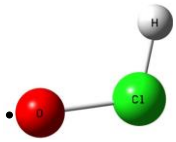	33.24	[117]
$[C\ell OH_2]^+$ (g)	Aquachlorine cation	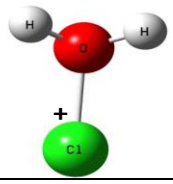	194.66	[117]
$OC\ell O$ (g)	Chlorine dioxide	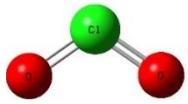	24.36	[117]
$[OC\ell O]^+$ (g)	Chloryl ion	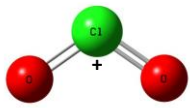	262.13	[117]
$[OC\ell O]^-$ (g)	Chlorite	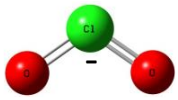	-25.74	[117]
$C\ell OO$ (g)	Chlorodioxidanyl	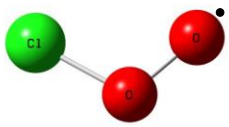	24.55	[117]
$[C\ell OO]^+$ (g)	Chlorodioxidenium	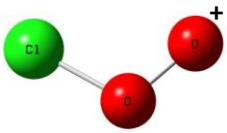	286.71	[117]

*Table-**2.3** continued*

Formula	**Chemical Name**	**Structure**	**ΔH_f (kcal mol^{-1}) at 298K**	**Reference (ΔH_f)**
$[C\ell OO]^-$(g)	Peroxyhypochlorite	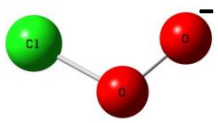	-59.28	[117]
HOCℓO (g)	Chlorous acid	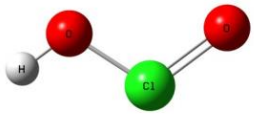	4.94	[117]
$[HOC\ell O]^+$(g)	Chlorous acid cation	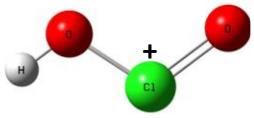	236.81	[117]
$[HOC\ell O]^-$(g)	Chlorous acid anion	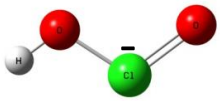	-37.33	[117]
HOOCℓ (g)	Peroxyhypochlorous acid	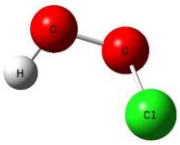	-0.31	[117]
$[HOOC\ell]^+$ (g)	Peroxyhypochlorous acid cation	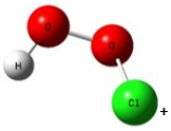	244.86	[117]
$[HOOC\ell]^-$ (g)	Peroxyhypochlorous acid anion	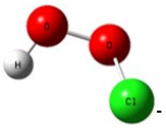	-8.12	[117]
HCℓOO (g)	Chloryl hydride	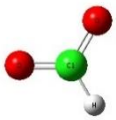	191.20	[117]

*Table-**2.3** continued*

Formula	**Chemical Name**	**Structure**	**ΔH_f (kcal mol^{-1}) at 298K**	**Reference (ΔH_f)**
CℓOCℓ (g)	Chloro hypochlorite	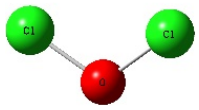	18.63	[117]
$[C\ell OC\ell]^+$ (g)	mu-Oxodichlorine cation	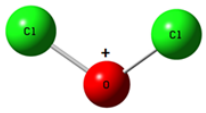	269.31	[117]
$[C\ell OC\ell]^-$ (g)	mu-Oxodichlorate anion	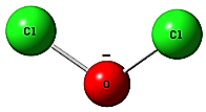	-35.30	[117]
CℓCℓO (g)	Chlorosyl chloride	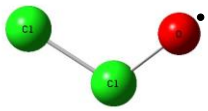	31.83	[117]
$[C\ell C\ell O]^+$ (g)	Chlorosyl chloride cation	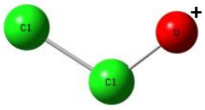	270.26	[117]
$[C\ell C\ell O]^-$ (g)	Chlorosyl chloride anion	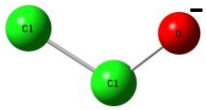	-44.14	[117]
CℓOOCℓ (g)	Chlorooxy hypochlorite		31.38	[117]
$C\ell C\ell O_2$(g)	Chloryl chloride	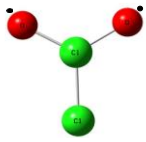	29.18	[117]

*Table-**2.3*** continued

Formula	**Chemical Name**	**Structure**	**ΔH_f (kcal mol^{-1}) at 298K**	**Reference (ΔH_f)**
$C\ell O_3$ (g)	Perchloryl	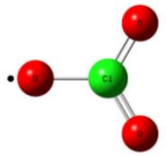	44.00	[117]
$[C\ell O_3]^+$ (g)	Perchloryl cation	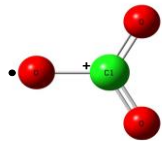	297.67	[117]
$[C\ell O_3]^-$ (g)	Chlorate	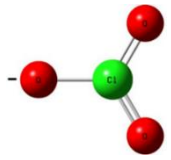	-50.86	[117]
$C\ell(O)O_2$ (g)	2-chloro ozone	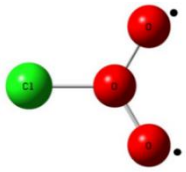	63.36	[117]
$[C\ell(O)O_2]^-$ (g)	2-chloro ozone anion	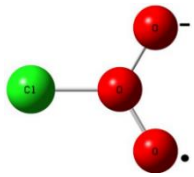	-25.22	[117]
$C\ell OOO$ (g)	1-Chloro ozone	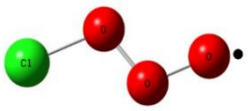	53.32	[117]
$[C\ell OOO]^-$ (g)	1-Chloro ozone anion	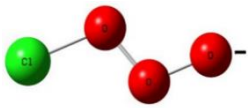	-26.62	[117]

*Table-**2.3** continued*

Formula	**Chemical Name**	**Structure**	**ΔH_f (kcal mol^{-1}) at 298K**	**Reference (ΔH_f)**
OCℓOO (g)	Chlorine oxide peroxide	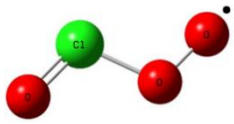	54.34	[117]
$[OC\ell OO]^-$ (g)	Peroxychlorite	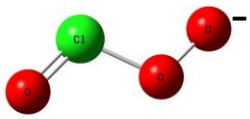	-8.19	[117]
$HOC\ell O_2$ (g)	Chloric acid	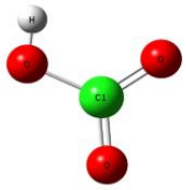	-1.19	[117]
$HC\ell O_3$ (g)	Chlorine hydride oxide	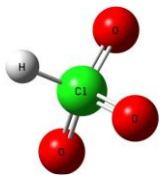	37.11	[117]
HOOOCℓ (g)	Hypochloro-peroxoous acid. Hydroxy ester	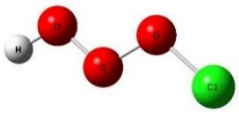	10.10	[117]
HOOCℓO (g)	Peroxychlorous acid	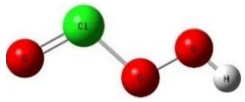	21.55	[117]
$C\ell O_4$ (g)	Perchloryloxy	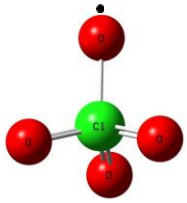	57.60	[117]
$[C\ell O_4]^-$ (g)	Perchlorate	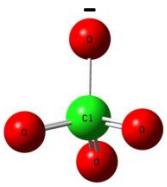	-64.99	[117]

*Table-**2.3** continued*

Formula	**Chemical Name**	**Structure**	**ΔH_f (kcal mol^{-1}) at 298K**	**Reference (ΔH_f)**
$HOC\ell O_3$ (g)	Perchloric acid	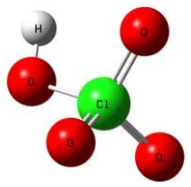	0.43	[117]
$[HOC\ell O_3]^+$ (g)	Perchloric acid cation	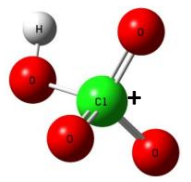	282.55	[117]
$HOOC\ell O_2$ (g)	Peroxychloric acid	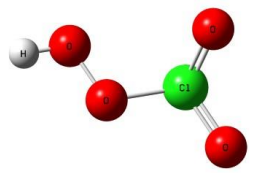	16.56	[117]
$HOOOOC\ell$ (g)		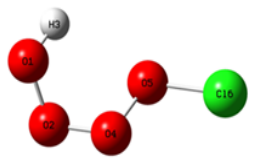	22.7	[119]
$C\ell OC\ell O_2$ (g)	Dichlorine trioxide	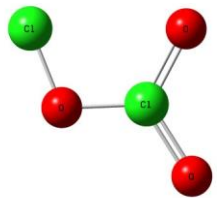	37.40	[117]
$OC\ell C\ell O_2$ (g)	Chlorineoxide	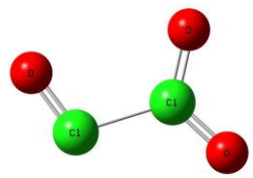	46.2	[119]

*Table-**2.3** continued*

Formula	**Chemical Name**	**Structure**	**ΔH_f (kcal mol^{-1}) at 298K**	**Reference (ΔH_f)**
$C\ell O_2C\ell O_2$ (g)		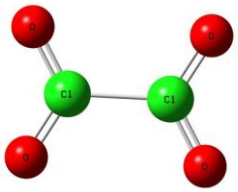 [72]	Not reported	Not analysed
$C\ell OC\ell O_3$ (g)	Chlorine perchlorate and (Chlorooxy) chlorane trioxide	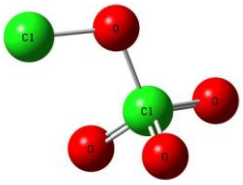	37.40	[118]
$C\ell OOC\ell O_3$ (g)	Dichlorine Pentoxide	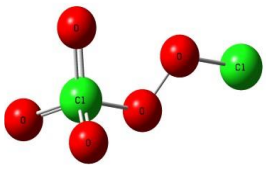 [119]	69	[118]
$C\ell O_2$-O-$C\ell O_2$ (g)	Chloryl chlorate	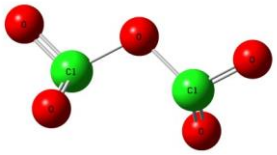 [119]	Not reported	Not reported
$[C\ell O_3C\ell O_3]^{-2}$ (g)	Oxido-[oxido(dioxo)-lambda7-chloranylidene]-dioxo-lambda7-chlorane	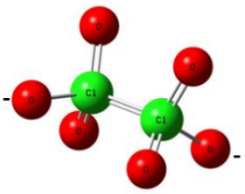 [119]	Not reported	Not reported
$C\ell O_2$-O-$C\ell O_3$ (g)	Chloryl perchlorate	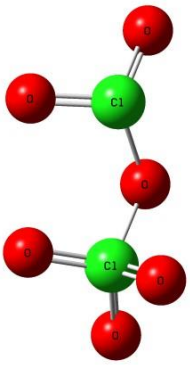	72.4	[118]

*Table-**2.3** continued*

Formula	**Chemical Name**	**Structure**	**ΔH_f (kcal mol^{-1}) at 298K**	**Reference (ΔH_f)**
$C\ell O_2$-O-O-$C\ell O_2$ (g)	Chloryloxy chlorate	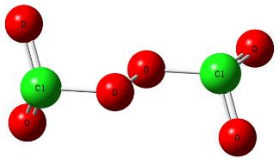 [119]	Not reported	Not reported
$C\ell O_3$-O-$C\ell O_3$ (g)	Chlorine heptoxide	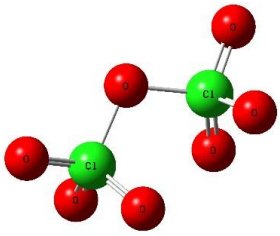 [119]	86.2	[118]
$C\ell O_3$-O-O-$C\ell O_3$ (g)	Perchloryloxy perchlorate	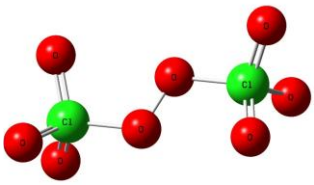 [55]	111.48*	[55]

*Heat of formation ($\Delta H_f C\ell O_3$-O-O-$C\ell O_3$) calculated from energies published by Beltran et al. (1999) [55].

2.13 References

[1] T. L. Chen, Y. H. Chen, Y. L. Zhao and P. C. Chiang, "Application of Gaseous ClO_2 on Disinfection and Air Pollution Control: A Mini Review." Aerosol and Air Quality Research, vol. 20, no. 11, pp. 2289-2298, 2020.

[2] W. Song, L. Ji, X. Zhang, C. Fu, Z. Wang and Z. Wang, "Algae-Containing Raw Water Treatment and By-Products Control Based on ClO_2 Preoxidation-Assisted Coagulation/Precipitation Process" Environmental Geochemistry and Health, vol. 44, p. 3837–3851, 2022.

[3] B. R. Deshwal and H. K. Lee, "Kinetics and Mechanism of Chloride Based Chlorine Dioxide Generation Process from Acidic Sodium Chlorate" Journal of hazardous materials, vol. 108, no. 3, pp. 173-182, 2004.

[4] "Chlorine-dioxide" Lenntech Corporation , [Online]. Available: [Accessed 2017]. http://www.lenntech.com/processes/disinfection/chemical/disinfectants-chlorine-dioxide.htm.

[5] L. O. Brockway, "The Three-Electron Bond in Chlorine Dioxide" Proceedings of the National Academy of Sciences of the United States of America. vol. 19, no. 3, pp. 303-7, 1933.

[6] L. Pauling, "General Chemistry" third edition, Dover Publications, issue number: ISBN 0-486-65622-5, 1988.

[7] E. P. United States. Environmental Protection Agency. Office of Water Programs Operations Agency, "Alternative Disinfectants and Oxidants Guidance Manual" vol. 99, no. 14, 1999.

[8] Gordon, G., Kieffer, R.G., Rosenblatt, D. H., The Chemistry of Chlorine Dioxide. Progress in Inorganic Chemistry, John Wiley & Sons, Inc, 1972.

[9] Keskinen, L.A. and Annous, B.A. Chlorine dioxide gas. Nonthermal processing technologies for food, pp.359-365, 2011.

[10] M. K. S. Monteiro, M. M. S. Monteiro, H. de Melo , A. M. J. Llanos, C. Saez, E. V. Dos Santos and M. A. Rodrigo, "A Review on the Electrochemical Production of Chlorine Dioxide from Chlorates and Hydrogen Peroxide" Current Opinion in Electrochemistry, vol. 27, p. 100685, 2021.

[11] G. Gordon and A. A. Rosenblatt, "Chlorine Dioxide: The Current State of the Art." Ozone: science & engineering, vol. 27, no. 3, pp. 203-207, 2005.

[12] H. Alliger. An Overall View of ClO_2, Melville, New York: Frontier Pharmaceutical Inc, 2001.

[13] P. Patnaik, Handbook of Inorganic Chemicals, New York: McGraw-Hill, 2003.

[14] K. Hedberg, "The Infrared Spectrum of Chlorine Dioxide" The Journal of Chemical Physics, vol. 19, p. 509, 1951.

[15] G. Gordon, "Is All Chlorine Dioxide Created Equal" Journal American Water Works Association, vol. 93, no. 4, p. 63–74, 2001.

[16] R. C. Hoehn, A. A. Rosenblatt and D. J. Gates, "Considerations for Chlorine Dioxide Treatment of Drinking Water" in American Water Works Assosciation Water Quality Technology, 1996.

[17] X. Ma, H. Chen, R. Chen and X. Hu, "Direct and Activated Chlorine Dioxide Oxidation for Micropollutant Abatement: A Review on Kinetics, Reactive Sites, and Degradation Pathway" Water , vol. 14, p. 2028, 2022.

[18] P. G. Tratnyek and J. Hoigne , "Kinetics of Reactions of Chlorine Dioxide in Water - II: Quantitative Structure-Activity Relationships for Phenolic Compounds. Water Research, vol. 28, no. 1, pp. 57-66, 1994.

[19] S. Canonica and P. G. Tratnyek, "Quantitative Structure-Activity Relationships for Oxidation Reactions of Organic Chemicals in Water" Environmental Toxicology and Chemistry: An International Journal, vol. 22, no. 8, pp. 1743-1754, 2003.

[20] V. Vaida and J. D. Simon, "The Photoreactivity of Chlorine Dioxide" Science, pp. 1443-1448, 1995.

[21] G. Gordon and A. A. Rosenblatt, "Gaseous Chlorine-Free Chlorine Dioxide for Drinking Water" in Proceedings of the 1995 Water Quality Technology Conference, Denver, CO, 1996.

[22] W. Gan, S. Huang, G. Huang, T. Bond, P. Westerhoff , J. Zhai and X. Yang, "Chlorite Formation During ClO_2 Oxidation of Model Compounds Having Various Functional Groups and Humic Substances" Water Research , vol. 159 , pp. 348-357, 2019.

[23] G. D. Simpson, R. F. Miller, G. D. Laxton and W. R. Clements, "A Focus on Chlorine Dioxide: The "Ideal" Biocide" in Corrosion-National Association of Corrosion Engineers Annual Conference-NACE, 1993.

[24] Y. Ge, X. Zhang, L. Shu and X. Yang, "Kinetics and Mechanisms of Virus Inactivation by Chlorine Dioxide in Water Treatment: A Review" Bulletin of Environmental Contamination and Toxicology , vol. 106, p. 560–567, 2021.

[25] C. Lee, C. Schmidt, J. Yoon and U. Von Gunten, "Oxidation of N-Nitrosodimethylamine (NDMA) Precursors with Ozone and Chlorine Dioxide: Kinetics and Effect on NDMA Formation Potential. Environmental Science and Technology, vol. 41, no. 6, pp. 2056-2063, 2007.

[26] R. D. Harcourt and T. M. Klapötke, "Valence Bond Structures for Molecules with 5-Electron 3-Centre Bonding Units" Computational and Theoretical Chemistry, vol. 1139, pp. 50-54, 2018.

[27] R. G. Gosavi, P. Raghunathan and O. P. Strausz, "Ab Initio Molecular Orbital Studies of Fluorine Dioxide, Chlorine Dioxide and Their Isomeric Peroxy Radical Forms" Journal of Molecular Structure: Theochem, vol. 133, pp. 25-35, 1985.

[28] R. Flesch, J. Plenge and E. Rühl, "Core-Level Excitation and Fragmentation of Chlorine Dioxide" International Journal of Mass Spectrometry, vol. 249–250, pp. 68-76, 2006.

[29] Brage C, Eriksson T, Gierer J, "Reactions of Chlorine Dioxide with Lignins in Unbleached Pulps" Holzforschung, vol. 49, p. 127–38., 1995.

[30] L. Yi, B. Baojuan, J. Liang, J. Li, B. Liu, F. Wang, C. Qin and S. Yao, "Effects of the Preferential Oxidation of Phenolic Lignin Using Chlorine Dioxide on Pulp Bleaching Efficiency" International Journal of Molecular Sciences, vol. 23, no. 21, 2022.

[31] K. Hassenberg , U. Praeger and W. B. Herppich, "Effect of Chlorine Dioxide Treatment on Human Pathogens on Iceberg Lettuce" Foods, vol. 10, no. 3, p. 574, 2021.

[32] J. Shin, B. Harte, S. Selke and Y. Lee, "Use of a Controlled Chlorine Dioxide (ClO_2) Release System in Combination with Modified Atmosphere Packaging (MAP) to Control the Growth of Pathogens." Journal of Food Quality, vol. 34, no. 3, pp. 220-228, 2011.

[33] Chlorine Dioxide Complex - An Overview & FQA. R & B Management of FL, LLC, [Online]. Available: https://www.randbmanagement.com/cidermsp/complexoverview.htm. [Accessed 4 June 2018].

[34] A. T. Al-Sa'ady, H. S. Nahar and F. F. Saffah, "Antibacterial activities of chlorine gas and chlorine dioxide gas against some pathogenic bacteria" EurAsian Journal of Biosciences, vol. 14, no. 2, 2020.

[35] D. L. Gallagher, R. C. Hoehn and R. C. Dietrich, "Sources, Occurrence, and Control of Chlorine Dioxide By-Product Residuals in Drinking Water. American Water Works Association, Denver, Sources, Occurrence, and Control of" Denver, CO, 1994.

[36] B. Mezgebe, E. Sahle-Demessie and G. A. Sorial, "Disinfection Byproducts in Drinking Water: Formation, Characterization, Control Technologies" in Contaminants in Our Water: Identification and Remediation Methods, American Chemical Society, 2020, pp. 119-142.

[37] Katz A and Narkis N, "Removal of Chlorine Dioxide Disinfection By-Products by Ferrous Salts" Water Reasearch , vol. 35, no. 1, p. 101–8., 2001.

[38] A. A. Lanrewaju, A. M. Enitan-Folami, S. Sabiu and F. M. Swalaha, "A review on disinfection methods for inactivation of waterborne viruses" Frontiers in Microbiology, vol. September 2022.

[39] K. V. Ellis, "Water Disinfection: A Review with Some Consideration of the Requirements of The Third World" Critical Reviews in Environmental Control, vol. 20, no. 5-6, pp. 341-407, 1991.

[40] W. Yang, D. Yang , S. Y. Zhu, B. Y. Chen, M. X. Huo and J. W. Li, "The Synergistic Effect of Escherichia Coli Inactivation by Sequential Disinfection with Low Level Chlorine Dioxide Followed by Free Chlorine" Journal of Water and Health, vol. 10, no. 4, p. 557–564, 2012.

[41] D. F. Bridges, A. Lacombe and V. C. H. Wu, "Fundamental Differences in Inactivation Mechanisms of Escherichia coli O157:H7 Between Chlorine Dioxide and Sodium Hypochlorite" Frontiers in Microbiology, vol. 13, 2022.

[42] P. Maris, "Modes of Action of Disinfectants" Revue Scientifique et Technique, vol. 14, no. 1, pp. 47-55, 1995.

[43] I. Ofori, S. Maddila, L. Johnson and S. B. Jonnalagadda, "Chlorine Dioxide Oxidation of Escherichia Coli in Water – A Study of the Disinfection Kinetics and Mechanism" Journal of Environmental Science and Health, Part A, vol. 52, no. 7, pp. 598-606, 2017.

[44] D. Gates , The Chlorine Dioxide Handbook, Denver, 1998.

[45] W. Gan, Y. Ge, Y. Zhong and Y. Yang, "The Reactions of Chlorine Dioxide with Inorganic and Organic Compounds in Water Treatment: Kinetics and Mechanisms" Environmental Science: Water Research & Technology, vol. 6, no. 9, pp. 2287-2312, 2020.

[46] M. E. Alvarez and R. T. O'Brien, "Mechanisms of Inactivation of Poliovirus by Chlorine Dioxide" Applied and Environmetal Microbiology, vol. 44, no. 5, pp. 1064-1071, 1982.

[47] J. Simonet and C. Gantzer, "Degradation of the Poliovirus 1 Genome by Chlorine Dioxide" Journal of Applied Microbiology, vol. 100, no. 4, pp. 862-870, 2006.

[48] "Latest Chlorine dioxide information" [Online]. Available: http://www.shareclean.net/clo2/chlorine.html.

[49] L. A. Mayack, R. J. Soracco, E. W. Wilde and D. H. Pope, "Comparative Effectiveness of Chlorine and Chlorine Dioxide Regimes for Biofouling Control" Water Research, vol. 18, no. 5, p. 593 , 1984.

[50] Z. Noszticzius, M. Wittmann, K. Kály-Kullai, Z. Beregvári, I. Kiss, L. Rosivall and J. Szegedi, "Chlorine Dioxide is a Size-Selective Antimicrobial Agent." Public Library of Science One, vol. 8, no. 11, 2013.

[51] E. M. Aieta and J. D. Berg, "A Review of Chlorine Dioxide in Drinking Water Treatment" Journal American Water Works Association, vol. 62, p. 78, 1986..

[52] H. MacKeown, J. A. Gyamfi, V. K. M. Schoutteten, D. Dumoulin, L. Verdickt, B. Ouddane and J. Criquet, "Formation and Removal of Disinfection By-Products in a Full-Scale Drinking Water Treatment Plant" Science of the Total Environment, vol. 704, p. 135280, 2020.

[53] P. J. Kemp and N. Okimoto, "Subtoxic Chlorine Dioxide Treatment to Prevent Fouling in Once Through Sea Water Cooled Surface Condensers" in Proceedings of the 2nd International Conference on Water, 1982.

[54] S. Sussman and W. J. Ward, Microbiological Control with Chlorine Dioxide Helps Save Energy, Material Performance, vol. 16, no. 7, p. 24, 1977.

[55] A. Beltran, B. Andre, J. S. Noury and B. Silvi, "Structure and Bonding of Chlorine Oxides and Peroxides: ClOx, ClOx- (x) 1-4), and Cl_2Ox (x) 1-8)" The Journal of Physical Chemistry A, vol. 103, no. 16, pp. 3078-3088, 1998.

[56] P. Yuan-sheng, W. U. Xiao-qing, L. Zhao-kun and W. Tong, "Control Effects of pε and pH on the Generation and Stability of Chlorine Dioxide" Journal of Environmental Sciences, vol. 15, no. 5, pp. 680-684, 2003.

[57] C. Korn, R. C. Andrews and M. D. Escobar, "Development of Chlorine Dioxide- Related By-Product Models for Drinking Water Treatment" Water Research, vol. 36 , no. 1, p. 330–342, 2002.

[58] K. S. Werdehoff and P. C. Singer, "Chlorine Dioxide Effects on THMFP, TOXFP and the Formation of Inorganic By-Products." Journal American Water Works Association, vol. 79, p. 107, 1987.

[59] E. Ranier and J. Swietlik, "DBPs Control in European Drinking Water Treatment Plants Using Chlorine Dioxide: Two Case Studies" Journal of Environmental Engineering and Landscape Management, vol. 18, no. 2, pp. 85-91, 2010.

[60] World Health Organization and WHO, "Guidelines for Drinking-Water Quality" World Health Organization, 2004.

[61] A. K. Horváth, I. Nagypál, G. Peintler, I. R. Epstein and K. Kustin, "Kinetics and Mechanism of the Decomposition of Chlorous Acid" The Journal of Physical Chemistry A, vol. 107, no. 36, p. 6966–6973, 2003.

[62] R. C. Brasted, Comprehensive Inorganic Chemistry, New York: D. Van Nostrand Co., 1954

[63] J. F. White, M. C. Taylor and J. P. Vincent, "Chemistry of Chlorites" Industrial & Engineering Chemistry Research., vol. 34, p. 782, 1942.

[64] F.Bohmlander, "Dissociation of Chlorous Acid" Wasser Abwasser, vol. 104, p. 518, 1963.

[65] U. von Gunten, "Oxidation Processes in Water Treatment: Are We on Track?" Environmental Science & Technology., vol. 52, no. 9, p. 5062–5075, 2018.

[66] R. L. Jolley and J. H. Carpenter, "Aqueous Chemistry of Chlorine: Chemistry, Analysis and Environmental Fate of Reactive Oxidant Species" Oak Ridge National Laboratories, 1982.

[67] R. S. ZhU and M. C. Lin, Ab Initio Study of Ammonuim Perchlorate Combustion Initiation Processes: Unimolecular Decomposition of Perchloris Acid and the Related OH + ClO_3 Reaction, Physical chemistry Communication, vol. 25, pp. 1-6, 2001.

[68] J. S. Francisco and S. P. Sander, "Existence of a Chlorine Oxide and Water ($ClO-H_2O$) Radical Complex" Journal of the American Chemistry Society, vol. 117, pp. 9917-9918 , 1995.

[69] Z.F. Xu, R. Zhu and M. Lin, "Ab Initio Studies of ClOx Reactions. Kinetics and Mechanisms for the OH +OClO Reaction" Journal of Physical. Chemistry A, vol. 107, pp. 1040-1049, 2003

[70] M. A. A. Clyne and J. A. Coxon, "Reactions of Chlorine Oxide Radicals. Part 1.Reaction Kinetics of the ClO radical" Transactions of the Faraday Society, vol. 62, pp. 1175-1189, 1966.

[71] E. G. Thorsteinsson and J. T. Gudmundsson, "The Low Pressure Cl_2/O_2 Discharge and the Role of ClO" Plasma Sources Science and Technology, vol. 19, no. 5, p. 055008, 2010.

[72] Q. Li, S. Lu, Y. Xie, P. V. Schleyer and H. F.Schaefer, Molecular Structures, Thermochemistry, and Electron Affinities for the Dichlorine Oxides:Cl_2O_n/Cl_2O_n" International Journal of Quantum Chemistry, vol. 95, p. 731–757, 2003.

[73] M. L. Alegre, M. Gerones, J. A. Rosso, S. G. Bertolotti, A. M. Braun, D. O. Martire and M. C. Gonzalez, "Kinetic Study of the Reactions of Chlorine Atoms and Cl^2•-Radical Anions in Aqueous Solutions. 1. Reaction with Benzene." The Journal of Physical Chemistry A, vol. 104, no. 14, pp. 3117-3125., 2000.

[74] D. Vione, V. Maurino, C. Minero, P. Calza and E. Pelizzetti, "Phenol Chlorination and Photochlorination in the Presence of Chloride Ions in Homogeneous Aqueous Solution" Environmental Science & Technology, vol. 39, no. 13, pp. 5066-5075, 2005.

[75] W. Gan, Y. Ge, S. Zhong and X. Yang, "The Reactions Of Chlorine Dioxide with Inorganic and Organic Compounds in Water Treatment: Kinetics and Mechanisms" Environmental. Science Water Research & Technology Journal, vol. 6, p. 2287, 2020.

[76] S. M. Husnain, A. Umar , A. Yaqub , N. Abbas and F. Shahzad, "Recent trends of MnO_2-derived adsorbents for water treatment: a review" New Journal of Chemistry, vol. 44, pp. 6096-6120, 2020.

[77] W. D. Heizer , R. S. Sandler, E. J. Seal , S. C. Murray, M. G. Busby , B. G. Schliebe and S. N. Pusek, "Intestinal Effects of Sulfate in Drinking Water on Normal Human Subjects" Digestive Diseases and Sciences, vol. 42, no. 5, pp. 1055-1061, 1997.

[78] X. Yang , W. Guo and W. Lee, "Formation of Disinfection Byproducts Upon Chlorine Dioxide Preoxidation" Chemosphere, vol. 91, p. 1477–1485, 2013.

[79] M. Xu, Y. Lin, T. Zhang, C. Hu, Y. Tang, D. J and B. Xu, "Chlorine Dioxide-Based Oxidation Processes for Water Purification：A Review" Journal of Hazardous Materials, vol. 436, p. 129195, 2022.

[80] J. Raczyk-Stanis"awiak, A. Swietlik and Dabrowska, "Biodegradability of Organic By-Products After Natural Organic Matter Oxidation with ClO_2—Case Study" Water Research , vol. 38, p. 1044–1054, 2004.

[81] C. Rav-Acha and E. Choshen, "Aqueous Reactions of Chlorine Dioxide with Hydrocarbons" Environmental Science & Technology, vol. 21, no. 11, pp. 1069-1074, 1987.

[82] J. Hoigne and Bader H, "Kinetics of Reactions of Chlorine Dioxide in Water - I. Rate Constants for Inorganic and Organic Compounds" Water Research, vol. 28, no. 1, pp. 45-56, 1994.

[83] Sun Y and D. S. Argyropoulos , "A Comparison of the Reactivity and Efficiency of Ozone, Chlorine Dioxide, Dimethyldioxirane and Hydrogen Peroxide with Residual Kraft Lignin" Holzforschung , vol. 50, p. 175–82, 1996.

[84] U. Yetis, S. Ataberk, C. F. Gokcay and S. M. Sahin, "Characterization of Effluents from Chlorine Dioxide Substitution Bleaching and Oxygen-Reinforced Extraction" Water Science and Technology, vol. 36, no. (2–3), p. 353–60, 1997

[85] J. Świetlik, U. Raczyk-Stanisławiak, S. Biłozor, W. Ilecki and J. Nawrocki, "Adsorption of Natural Organic Matter Oxidized with ClO_2 on Granular Activated Carbon" Water Research, vol. 36, no. 9, pp. 2328-2336, 2002

[86] F. J. C. Roe, "Preliminary Report of Long-Term Tests of Chloroform in Rats, Mice and Dogs. Ozone, Chlorine Dioxide and Chloramines as Alternatives to Chlorine for Disinfection of Drinking Water Water Supply Research" U.S. EPA,, Cincinnati, OH,, 1976.

[87] A. L. Srivastav, N. Patel and V. K. Chaudhary, "Disinfection By-Products in Drinking Water: Occurrence, Toxicity and Abatement" Environmental Pollution, vol. 267, p. 115474, 2020.

[88] G. C. White, Handbook of Chlorination, New York: Van Nostrand Reinhold, 1972, 744.

[89] Ghernaout, D., "The hydropnbhhilic/hydrophobic ratio vs. dissolved organics removal by coagulation. A review" Journal of King Saud University Ghernaout, D."The Hydropnbhhilic/Hydrophobic Ratio vs. Dissolved Organics Removal by Coagulation". A Review. Journal of King Saud University , Science , vol. 26, p. 169–180, 2014.

[90] Q. Shen, J. Zhu, L. Cheng, Z. Zhang and X. Xu, "Enhanced Algae Removal by Drinking Water Treatment of Chlorination Coupled with Coagulation" Desalination , vol. 271, no. 1-3, pp. 236-240, 2011.

[91] Water Treatment and Pathogen Control: Process Efficiency in Achieving Safe Drinking Water. IWA Publishing, London, United Kingdom, 2004

[92] A. Dabrowska, J. Swietlik and J. Nawrocki, "Formation of Aldehydes Upon ClO_2 Disinfection" Water Research , vol. 37, no. 5, p. 1161–9, 2003.

[93] J. Swietlik, U. Raczyk-Stanis"awiak, S. Bi"ozor, W. Ilecki and J. Nawrocki, "Adsorption Of Natural Organic Matter Oxidized with ClO_2 on Granular Activated Carbon" Water Research , vol. 36, p. 2328–2336, 2002.

[94] A. A. Khan, R. Paterson and H. Khan, "Modification and application of the Canadian Council of Ministers of the Environment Water Quality Index (CCME WQI) for the communication

of drinking water quality data in Newfoundland and Labrador" Water Quality Research Journal, vol. 93, no. 3, pp. 285-293., 2004.

[95] M. Bredács, A. Frank, A. Bastero, A. Stolarz and G. Pinter, "Accelerated aging of polyethylene pipe grades in aqueous chlorine dioxide at constant concentration." Polymer Degradation and Stability, vol. 157, pp. 80-89, 2018.

[96] N. J. Ashbolt, "Risk Analysis Of Drinking Water Microbial Contamination Versus Disinfection By-Products (DBPs)." Toxicology, vol. 198, no. 1-3, pp. 255-262, 2004.

[97] A. T. Palin, "Current DPD Methods for Residual Halogen Compounds and Ozone in Water." Journal of American Water Works Association, vol. 67, no. 1, pp. 32-33, 1975.

[98] J. A. Myhrstad and J. E. Samdal, "Behaviour and Determination of ClO_2" Journal of American Water Works Association, vol. 61, no. 4, pp. 205-208, 1969.

[99] J. V. Feuss, "Problem in Determination of Chlorine Dioxide Residual" Journal of American Water Works Association, vol. 56, p. 607, 1964.

[100] J. Nawrocki, S. Golfinopoulos and A. Nikolaou, Chlorine Dioxide. In Control of Disinfection By-Products in Drinking Water Systems, Nova Science publisher, 2007

[101] R. S. Ingols and G. M. Ridenour, "Chemical Properties of Chlorine Dioxide in Water Treatment" Journal of American Water Works Association, vol. 40, no. 11, pp. 1207-1227, November 1948.

[102] J. L. Gole, "Photochemical Isomerization of Chlorine Dioxide and the Low-Lying Electronic State of the Possible Implications for Matrix Isolation Spectroscopy" Journal of Physical Chemistry, vol. 84, p. 1333–1340, 1980.

[103] O. Ventura, K. Irving and M. Kieninger, "Basis Set Effects in the Description of the Cl-O Bond in ClO and XClO Isomers (X= H, O, Cl) Using DFT and CCSD (T) Methods." ChemRxiv, 2018.

[104] J. C. Dunn, B. N. Flanders, V. Vaida and J. C. Simon, "The Spectroscopy of OClO in Polar Liquids" Spectrochimica Acta Part A: Molecular Spectroscopy , vol. 48, no. 9, pp. 1293-1301, 1992.

[105] N. Kang, T. A. Anderson and W. A. Jackson, "Photochemical Formation of Perchlorate from Aqueous Oxychlorine Anions" Analytica Chimica Acta, vol. 567, no. 1, pp. 48-56, 2006

[106] R. C. Dunn and J. D. Simon, "Excited-State Photoreactions of Chlorine Dioxide in Water" Journal of the American Chemical Society, vol. 114, pp. 4856-4860, 1992.

[107] C. L. Thomsen, P. J. Reid and S. R. Keiding, "Quantum Yield for ClOO Formation Following Photolysis of Aqueous OClO" Journal of the American Chemical Society, vol. 122, no. 51, pp. 12795-12801, 2000.

108] J. Simon, P. Cong, H. P. Deuel, R. Doolen, R. C. Dunn and P. A. Thompson, "Dynamics of Electronic Excited States in Ssolution." American Institute of Physics -AIP Conference Proceedings, vol. 298, no. 1, pp. 141-157, 1994.

[109] E. C. Richard and V. Vaida, "The Photochemical Dynamics of the A2A2 State of Chlorine Dioxide" Journal of Chemical Physics, vol. 94, no. 1, pp. 163-171, 1991.

[110] S. C. Hayes, P. M. Wallace, J. C. Bolinger and P. J. Reid, "Investigating the phase-dependent photochemical reaction dynamics of chlorine dioxide using resonance Raman spectroscopy" International Reviews in Physical Chemistry, vol. 21, no. 3, pp. 405-432, 2002.

[111] S. Navalon, M. Alvaro and H. Garcia, "Reaction of Chlorine Dioxide with Emergent Water Pollutants: Product Study of the Reaction of Three B-Lactam Antibiotics with ClO_2" Water Research, vol. 42, no. 8-9, pp. 1935-1942, 2008.

[112] I. N. Odeh, J. S. Francisco and D. W. Margerum, "New Pathways for Chlorine Dioxide Decomposition in Basic Medium" Inorganic Chemistry, vol. 41, pp. 6500-6506, 2002..

[113] Y. Ni and X. Wang, "Mechanism and Kinetics of Chlorine Dioxide Reaction with Hydrogen Peroxide under Acidic Conditions" The Canadian Journal of Chemical Engineering., vol. 75, pp. 31-36, 1996.

[114] L. Wang, J. S. Nicoson, K. E. Huff Hartz, J. S. Francisco and D. W. Margerum, "Bromite Ion Catalysis of the Disproportionation of Chlorine Dioxide with Nucleophile Assistance of Electron-Transfer Reactions between ClO_2 and BrO_2 in Basic Solution" Inorganic Chemistry, vol. 41, pp. 108-113., 2002.

[115] J. Hoigne and H. Bader, "Kinetics of Reactions of Chlorine Dioxide (OClO) in Water. I. Rate Constants for Inorganic and Organic Compounds" Water Research., vol. 28, pp. 45-55, 1994.

[116] J. Halperin and H. Taube, "The Transfer of Oxygen Atoms in Oxidation—Reduction Reactions. III. The Reaction of Halogenates with Sulfite in Aqueous Solution" Journal of the American Chemical Society, vol. 74, pp. 375-380, 1952.

[117] B. Ruscic and D. H. Bross, "Active Thermochemical Tables (ATcT) values based on ver. 1.122p of the Thermochemical Network" 2020. [Online]. Available: https://atct.anl.gov/Thermochemical%20Data/version%201.122p/index.php. [Accessed 4 June 2020].

[118] J. E. Sicre and C. J. Cobos, "Thermochemistry of the higher chlorine oxides ClO x (x ¼ 3, 4) and Cl_2O x (x ¼ 3–7)" Journal of Molecular Structure (Theochem) , vol. 620 , p. 215–226, 2003.

[119] National Library of Medicine, "National Library of Medicine" [Online]. Available: https://pubchem.ncbi.nlm.nih.gov/compound/11159534. [Accessed 5 May 2021].

CHAPTER 3: CHEMICAL APPROACH AND COMPUTATIONAL STRATEGY

3.1 Introduction

Some of the chlorine dioxide ($C\ell O_2$) species investigated, are classified as ionic and radicals and are involved in extensive intra- and inter-molecular interactions in aqueous medium. Although Heats of Formation for most of the species were available from the open literature, it was important to construct chemical structures and derive their optimum geometries, validated against reported energies to be applied in all subsequent calculations. It was therefore important to elucidate their thermochemical properties, applying an empirical supported first principal computational approach.

The study involved a few technical stages:

a) Force field parameter preparation
b) Model preparation
c) Model optimization
d) GCMC Canonical ensemble simulations (radical and neutral species only)
e) Ab Initio and semi-empirical derivation of Heats of Formation
f) Species based thermodynamics to extract reaction schemes.

Simulations performed on extended (Grand ensemble) model representations, have been undertaken to determine the optimum potential energy model stages. This was followed by semi-empirical and *Ab Initio* quantum chemical optimizations (***MOPAC*** *and* ***VASP*** software) to derive thermochemical properties.

This was done to verify the authenticity and achievable electronic structures of the compounds, against published energy figures and furthermore correlate their ensemble chemical properties against single molecular figures, as proof of a technique to determine organic compound characteristics.

Model preparation Stage

A group of chlorine oxide species listed towards the end of Chapter 2, was selected for this study. The group comprised of neutral, radical and ionic species (+ve and -ve) with some extended compounds, hosting a higher oxygen content, including a number of hydrogen derivatives of $C\ell O_2$.

a) Periodic models were constructed using the MedeA-3.3.1 software, followed by a *VASP* (DFT) refinement cycle (conditions listed), used in all further software simulations
b) Molecular models were prepared with the *GaussView-6* model preparation interface of the *Gaussian-16* software suite

3.1.1 *Initial Stage*

The empirical *pcff*+ [8] force field, lacked some parameters for a number of the chlorine oxide species, in support of *Grand Canonical* ensemble simulations and several force field parameters were "borrowed" and derived from the *cvff* and *pcff* force field repositories to complement the *pcff*+ set.
All adjusted *pcff*+ force field entries are presented in Tables- (**5.1–5.6**).

3.1.2 *GEMC Simulation stage*

For all neutral and radical samples, *GIBBS* GEMC (GCMC) ensemble model simulations were undertaken, to portray realistic and effective inter-molecular interactions that take place between species.

3.1.3 *Semi-empirical Stage*

The GEMC models extracted at the minima Internal Energy (U) of the simulated ensemble and beyond the minimum Saddle Points for each of the neutral species (considered to be their optimum model sizes) were subjected to ***MOPAC*** (semi-empirical quantum) analyses, to determine their ΔH_f (reported as for single species). The ΔH_f of the simulated optimum ensemble models, was computed applying all seven Hamiltonians of the ***MOPAC-16*** software.

3.1.4 *Ab Initio simulation Stage*

Ensemble models of structures from the ***GIBBS*** *Grand Canonical* ensemble outcome, were transferred to the ***VASP*** and ***MOPAC*** software, for a final 'bulk' structural optimization at the electronic level. Heats of Formation (ΔH_f) derived from these simulations were verified against some of the available, literature referenced energies, as validation of their geometries and stereochemistry. Charged ClO_2 species, not possible to be exposed to force field simulations, were optimized through ***Gaussian-16*** calculations, applying B3LYP theory and the cc-pv5z basis set, to determine their Heats of Formation as single molecular entities.
All these species have computationally been treated in the gas phase, for the thermodynamic derivations to be reported as single species (molecules) in a vacuum environment. It remains to compensate for coulomb and dipole-dipole interactions, van der Waals dispersion and inter-species hydrogen bonding in an attempt to present a true representation of their energies of formation.

3.1.5 *Final Stage*

Finally, the ***FactSage*-7.3** species-based thermodynamic software was used to determine the prevalent species of chlorine dioxide in an aqueous medium. A consolidated set of chemical reaction schemes were derived to demonstrate the major reactions involved and highlights specific product species, considered to be harmful during scaled water purification processes.

3.2 Computational Software Programs

The software programs and related techniques that were used to refine and optimize model structures and determine thermochemical properties, are listed below:

- *MedeA (GIBBS-9.7.4)* 1998-2017 -- *GIBBS* ensemble Monte Carlo simulation. This statistical-mechanical method predicts the equilibrium conditions of interaction at a molecular level [1], confined to periodic simulation space.
- *MedeA* (*VASP*-6.2.1) --The Vienna *Ab Initio* Simulation Package (*VASP*) was used to conduct DFT electronic structure refinement, for to derive at thermochemical properties [2]
- *MedeA* (*VASP*-5.4) –*Mulliken* molecular partial charge distributions
- *MedeA* (*MOPAC-2016*, v.17.048) – Semi-empirical quantum chemical software system which incorporates molecular orbital theory, combined with force field structural. support. The system was used to calculate thermochemical properties of species and Bader (partial) charges [3]
- GaussView-6 -- A software modelling interface, applied to prepare Gaussian models for numeric analysis [4]
- *Gaussian-16*, Rev.C.01 -- Computational software to conduct *Ab Initio* single molecular calculations to predict Thermochemical properties and structure refinement [5]
- *FactSage-7.3* -- Thermochemical software package to predict water-based species interactions [6] and extract chemical reaction schemes.

3.3 GIBBS-9.7.4 (GIBBS ensemble Monte Carlo)

Single monomeric chlorine oxide species were exposed to an Isobaric-Isothermal ***GIBBS*** ensemble (GEMC) simulation, applying Grand Canonical Monte Carlo (GCMC) methodology. This represents a statistical mechanical periodic ensemble at constant T and P, where the number of molecular entities (introduced as single molecular periodic models) *N*, is preserved throughout each simulation cycle. It is frequently referred to as an NPT ensemble [7] but in this instance, with a stepwise increment of single species to a maximum pre-defined population. The objective being to reach a sustained but minimum potential energy, which ultimately should present the optimum model size. The initial Grand Scale periodic cell dimensions were permitted to be adjusted as well. NPT ensembles were constructed, permitting between five to one hundred molecules in a single global periodic environment.

The Potential Energy (U_i) for the ensemble model was determined at each optimum step, followed by further additions of species and the trajectory energy graphically displayed to determine the minimum (optimum) internal energy point. This technique was used to mimic chemically realistic inter- and intra-molecular interactions in a confined chemical space (at the molecular dynamics level of simulation), as opposed to merely analysing them as single molecular structures. The optimum

ensemble model step was extracted and subjected further to ***VASP*-6.2.1** [2] and ***MOPAC-2016*** [3] refinement and analyses, to obtain thermochemical properties.

Table-**3.1:** *GIBBS* (GEMC) Conditions Applied for GCMC Simulation

GIBBS Execution Conditions	
Initialize: Non-Bond	Lennard Jones (6-9)
Electrostatic Sums:	Ewald
ensemble: Fixed ($) T,a P	NPT (298K, 1 Atm.)
Steps (Per species addition):	1000
Periodic initial Cell size:	10x10x10 Å
Internal moves:	0.2 Å
Pivoting around centre:	0.2 Å

The process flow that was adopted to run *GIBBS* Monte Carlo and the parameters activated at each stage, are tabulated below:

Initialise
Non-bond Lennard Jones (6-9)
Electrostatics: Ewald
Random seed: -1

Single Phased properties ensemble: NVT temperature: $T

Run	
N- Steps	1000
Intervals	
Writing the main averages	1000
Writing the configuration	10000
Adjusting displacement amplitude	20000
Writing the restart file	-1
Steps between checking for stopping	-1
Writing intermediate configurations	10
Writing the trajectory file	10

Move Probabilities

Internal moves	
Internal moves	0.2
internal rotation	0.2
pivoting around the centre	0.2
reptation of linear molecules	0
concerted rotation	0
double bridging	0
internal double rebridging	0
stretching (atomic translation)	0

Insertion test	
insertions and deletions	0

Rigid Moves	
rigid translation:	0.2
rigid translation and rotation	0
rigid rotation	0
Exchange two molecules	0

*Figure-**3.1**:* MedeA GIBBS Monte Carlo (GEMC) Process Flow

3.4 *Gaussian-16* (Single molecular optimization)

The structures of all the species in this study were first optimised using *Hybrid Density Functional Theory* (DFT) applying a small basis set of: 6-311++G (3d2f,3p2d). The B3LYP method (Becke's three-parameter nonlocal exchange functional with the correlation functional of Lee, Yang, and Parr) using basis set (cc-pv5z) w then applied to determine optimum species energies.

3.4.1 *DFT Approach -- Gaussian*

Three (3) options are presented to compute DFT frontier molecular orbitals:

a) Unrestricted Hartree Fock (UHF) method
b) Restricted Hartree Fock (RHF) method
c) Restricted Open Shell Hartree Fock (ROHF) approach

UHF uses a separate orbital for each electron, even if they are paired (in this study this was applied to ions, excited states and radicals) [9]. Energies and optimisation of geometries were performed at DFT (Density Functional Theory) levels, using Pople´s higher basis set (aug-cc-pv5z) and Dunning´s correlation.

3.4.2 *DFT and Ab Initio structure refinement*

The *Gaussian-16* software supports a non-periodic (Molecular) model environment. All single model species were prepared with the *GaussView-6* software [10], [11]. For *Gaussian-16* calculations, theory level CCSD (T) has shown to provide for the most accurate thermochemical properties [10], but is computationally resource demanding, especially when combined with higher basis sets [12]. Computational conditions applied for *Gaussian-16* analyses, are presented in Table- 3.2

*Table-**3.2**:* Executional Conditions Applied for *Gaussian* Analysis

Gaussian Execution Conditions	Selection
Optimization Conditions:	**OPT** selected plus **FREQUENCY**
Temperature:	298.15K
Pressure:	1 atm
Spin polarization: Restricted Open Shell HF	**ROHF**: Charged and Radical Species
Spin polarization: Unrestricted Hartree Fock	**UHF**: Open shell, Radical, Charged species
Spin polarization: Restricted Hartree Fock	**RHF**: Neutral Species
Theory:	Hartree Fock
basis set:	cc-pV5Z
Charge:	To specify for charged species
Theory:	DFT
Functional:	B3LYP, CCSD
basis set:	cc-pV5Z
Spin:	Selected

It was furthermore required to apply an additional calculation step (externally applied to *Gaussian* derived electronic energies [13]) to obtain the Heats of Formation (ΔH_f 298) and is briefly outlined below and in the Appendix.

A similar approach was followed to determine Gibbs Free Energy of Formation (ΔG_f 298).

3.4.3 *Heats of Formation Calculation (Transformed Gaussian-16 Computations)*

The enthalpies of formation of the species was calculated at **0K** [$\Delta H_f(0K)$] and **298K** [$\Delta H_f(0K)$]

First calculate ΔH_f (*M*, **0K**) for each molecule [14]:

$$\Delta H_f(M, \mathbf{0K}) = \sum_{atoms} x\, \Delta H_f(X, 0K) - \sum D_0(M)$$

$$= \sum_{atoms} x\, \Delta H_f(X, 0K) - [\sum x \varepsilon_0(X) - \varepsilon_0(M) - \varepsilon_{ZPE}(M)]$$

Where:

M = Molecule

X	=	Element which makes up *Molecule (M)*
x	=	The number of atoms of X in M
$\sum D_0$ (M)	=	Atomization energy of the molecule
(ε_0, M)	=	Total energies of the molecule
ε_{ZPE} (M)	=	Zero-point energy of the molecule [14]

The ΔH_f (M, **0K**) energy obtained was then used to calculate ΔH_f (M, **298K**) for each molecule [14]:

$$\Delta H_f \text{ (M, } \mathbf{298K}) = \Delta H_f\ (M, 0K) + [\Delta H_{f\,\mathrm{M}}\ (298\ K) - \Delta H_f\ (M, 0K)] - \sum_{atoms} x\ [\Delta H_f\ x(298\ K) - \Delta H_f\ x(0K)]$$

The complete suite of ΔH_f calculations, using the energies of species obtained at the B3LYP (cc-PV5Z) level of theory, is outlined in the Appendix section (A4) of this document as a working example, to fully perceive the calculations undertaken.

3.5 MOPAC-2016 computations

MOPAC-2016 (Version: 20.302W) was used to compute Heats of Formation of the single species selected for this study. Relevant charges were assigned to ionic species and subjected for refinement as non-periodic structures. *MOPAC* is a semi-empirical quantum chemistry program and is based on neglect of diatomic differential overlap (NDDO) approximation as defined by Dewar and Thiel [15]. Seven (7) different semi-empirical Hamiltonians are in *MOPAC-2016* namely:

Austin Model 1 (AM1)
Recife Model 1 (RM1)
Parametric Method 3 (PM3)
Parametric Method 6 (PM 6)
Parametric Method 7 (PM7)
Modified Neglect of Diatomic Overlap (MNDO)
Modified Neglect of Diatomic Overlap with D Atomic Orbitals (MNDOD)

- MNDO was among the earliest semi-empirical NDDO methods developed for quantum calculations. The key benefit of MNDO over former methods, was that parameter values were enhanced to emulate molecular properties instead of atomic properties [16]
- AM1 was developed as an improvement of MNDO, since it has the ability to replicate hydrogen bonds and estimate accurate activation energies for reactions [17]
- RM1 parameters were developed to reproduce experimental properties: such as ionization potentials, geometry, enthalpies of formation, electronic charges and dipole moments [18]

- PM3 theory is based on the equation and formalism similar to the AM1 method. PM3 functionality methodically defines intermolecular hydrogen bonding in small polar molecules [19]
- MNDOD replaced and improved on the Modified Intermediate Neglect of Diatomic Overlap (MINDO) method.
- PM6 is a re-parameterized version of the NDDO method.
- PM7 is improved form the PM6 method of the neglect of diatomic differential overlap (NDDO) theory, developed for large systems. Atomic parameters were enhanced with a ~10% reduction in average errors in organic compounds [15].

MOPAC-2016 computational steps applied, are presented in Table-3.3

*Table-**3.3**:* MOPAC conditions applied for analysis

*MOPAC E*xecution Conditions	
Hamiltonians applied:	AM1/MNDO/MNDOD PM3/PM6/RM1/PM7
SCF convergence:	0.01 kcal/mol
Structure Optimize:	Normal
Wave function:	Automatic
Periodic Cell:	Optimize
Starting Hessian:	Automatic
Convergence:	Normal
Iterations:	10 000
Initial Temp:	50K
Final Temp:	300K

The overall workflow used to execute *MedeA* (*MOPAC-2016)* is presented in Figure-3.2.

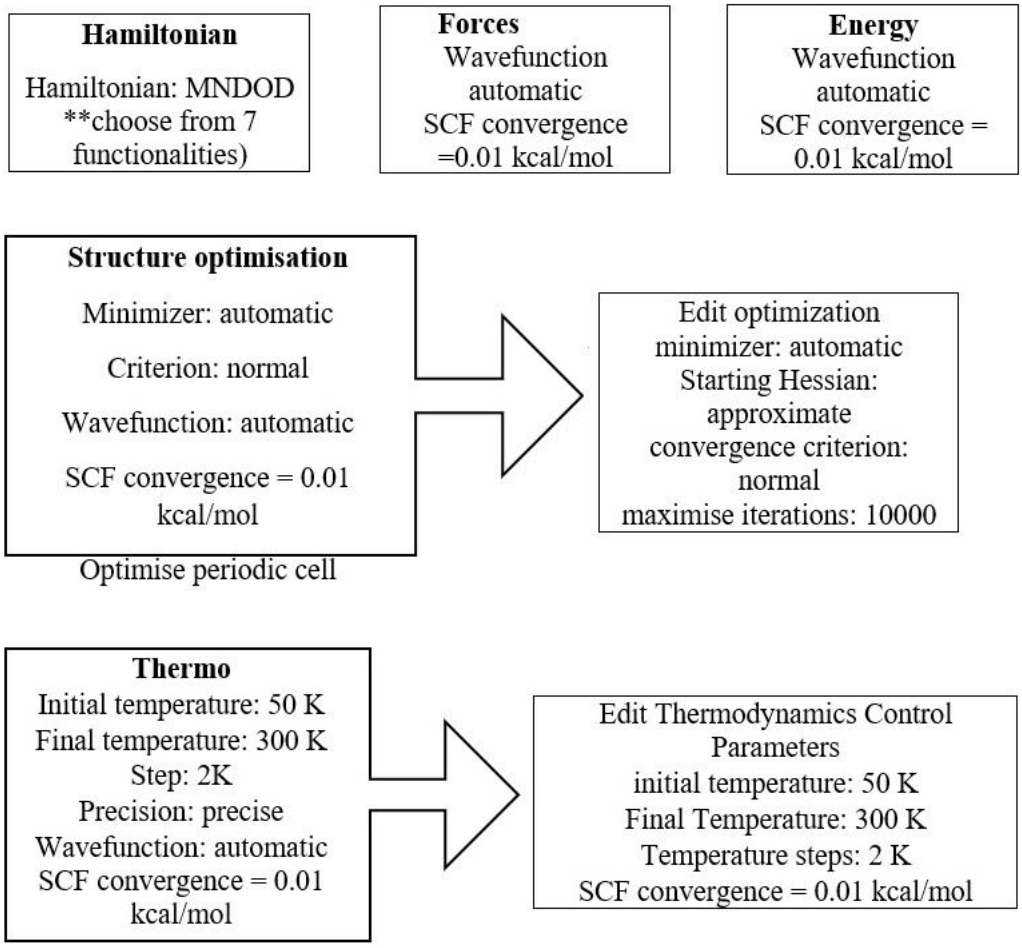

*Figure-**3.2**: MedeA/MOPAC-2016*

Single neutral periodic species were first optimised with *MedeA*-3-3.1/(*VASP*-6.2.1) and the resultant model then exposed to the single point meta-generalized gradient approximation (Meta-GGA) scan method. Both computations used the same parameters with the exception of the calculation module where the DFT Exchange Correlation (GGA-BLYP) was used for optimisation and the GGA-SCAN functional was used for single point analysis.

3.6 *VASP*-6.2.1 Computations

VASP-6.2.1 was used to compute the thermochemistry of neutral and radical single molecular species (confined to periodic space) with all atomic positions relaxed and unit-cell dimensions refined, as pre-condition for refinement of the larger ensemble models. No *van der Waals* dispersion corrections were applied. Computations were undertaken at the DFT theory level, applying both LDA (*Linear Density Approximation*) and Exchange Correlations (GGA-BLYP) and (GGA-PBE) for potential approximations, applied for full structural refinement at group symmetry *P1(1)*. Energies of Formation were determined with a Projector Augmented Wave (PAW) plane-wave cut-off of 400 eV, increased to compensate for cell-shape and cell-volume optimization. All *VASP-6.2.1* calculations were employed with the same input parameters, presented in Table-3.4.

*Table-**3.4**:* *VASP*-6.2.1 Conditions Applied for DFT Analysis

(Remaining Conditions taken as default)

VASP Execution Conditions	Single Molecule	Ensemble Models
Theory: Functional	DFT	DFT
Exchange Correlation: *Becke-3-LYP*	GGA-BLYP	GGA-BLYP
Perdue Burke Ernzerhof	GGA-PBE	GGA-PBE
Cell size:	15x15x15 Å	*GIBBS* optimized model
Cell Optimize:	No	No
Volume Change:	No	No
Relax Atoms:	Yes	No
Energy of Formation:	Yes	Yes
Augmented PAW plane-wave cut off:	280-400 eV	280-400 eV
Brillouin zone (k-mesh) spacing:	0.5 $Å^{-1}$	0.5 $Å^{-1}$
Mesh points:	2x2x2 $Å^{-1}$	2x2x2 $Å^{-1}$
Smearing: Methfessel-Paxton (width)	0.2 eV	0.2 eV
Energy response surface: Optimized	Conjugate Gradient (CG)	Conjugate Gradient (CG)
Vd Waals Dispersion:	No	No
SCF convergence:	1x 10^{-5} eV	1x 10^{-5} eV
Max. iterations:	120	120

The parameter flowchart applied for *MedeA/VASP-6.2.1* computations are presented in Figure-3.4 and Figure-3.5.

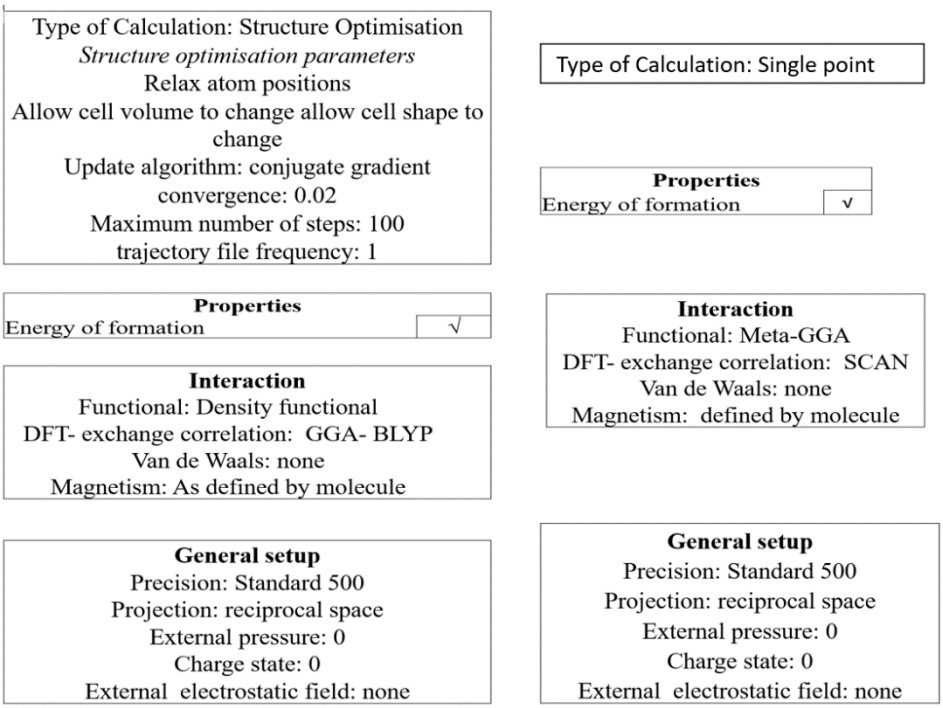

*Figure-**3.3**:* Calculation Module of VASP-6

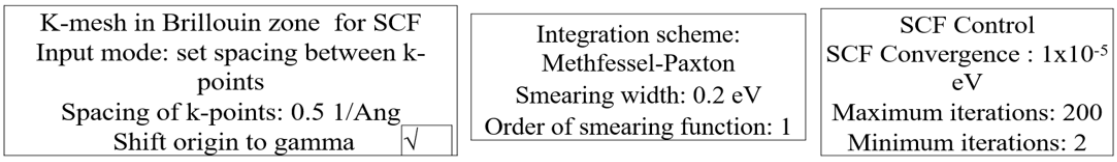

*Figure-**3.4**:* SCF Module of VASP-6

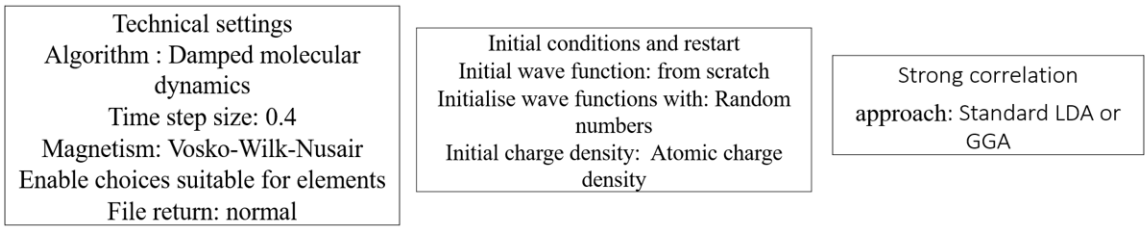

*Figure-**3.5**:* Advanced Restart Module of VASP-6

3.7 References

[1] Rueil-Malmaison & Laboratoire de Chimie-Physique, Universite Paris Sud, CNRS, "MedeA-3.3.1 (GIBBS-9.7.4) -- Gibbs ensemble Monte Carlo simulation," Rueil-Malmaison & Laboratoire de Chimie-Physique, France, 1998-2017.

[2] Prof. J. Hafner by G. Kresse and J. Furthmüller., "MEDEA VASP v6.3 Vienna Ab-initio Simulation Package,," Vienna Ab-initio Simulation Package, 2020. [Online]. Available: http://cms.mpi.univie.ac.at/vasp/.. [Accessed June 2021].

[3] J. J. P. Stewart, "MOPAC2016 17.048," Stewart Computational Chemistry, Colorado Springs, CO, USA, 2016. [Online]. Available: http://openmopac.net/. [Accessed June 2020].

[4] R. Dennington, T. A. Keith and J. M. Millam, "GaussViewer version 6.1," Semichem Inc, Shawnee Mission, KS, 2016.

[5] L. A. Curtiss, "Gaussian-4 theory," Journal of Chemical Physics, vol. 126, no. 8, 2007.

[6] C. W. Bale, P. Chartrand, S. A. Degterov, G. Eriksson, K. Hack, R. B. Mahfoud, J. Melançon, A. D. Pelton and S. Petersen, FactSage 7.3, Thermfact amd GTT-Technologies, 2019.

[7] A. Kadoura, A. Salama, S. Sun and A. Sherik, "An NPT Monte Carlo Molecular Simulation-Based Approach to Investigate Solid-Vapor Equilibrium_ Application to Elemental Sulfur-H2S System," Procedia Computer Science, vol. 18, p. 2109 – 2116, 2013.

[8] H. Sun, S. J. Mumby, J. R. Maple and A. T. Hag, "An ab Initio CFF93 All-Atom Force Field for Polycarbonates," Journal of the American Chemical Society, vol. 116, no. 7, p. 2978–2987, 1994.

[9] A. Tomberg, "Gaussian 09W Tutorial: An Introduction to Computional Chemistry using Gaussian 09 and Avagadro," Barett Group, [Online]. Available: https://barrett-group.mcgill.ca/tutorials/Gaussian%20tutorial.pdf. [Accessed 25 April 2021].

[10] O. Ventura, K. Irving and M. Kieninger, "basis set Effects in the Description of the Cl-O Bond in ClO and XClO Isomers (X=H,O,Cl) Using DFT and CCSD(T) Methods," ChemRxiv, 13 April 2018. [Online]. Available: www.ChemRxiv.com. [Accessed 5 August 2020].

[11] J. E. Sicre and C. J. Cobos, "Thermochemistry of the Higher Chlorine Oxides ClO x (x ¼ 3, 4) and Cl2O x (x ¼ 3–7)," Journal of Molecular Structure (Theochem) , vol. 620 , p. 215–226, 2003.

[12] K. P. Somers and J. M. Simmie, "Benchmarking Compound Methods (CBS-QB3, CBS-APNO, G3, G4,W1BD) against the Active Thermochemical Tables: Formation

Enthalpies of Radicals," Journal of Physical Chemistry A, vol. 119, pp. 8922-8933, 2015.

[13] Gaussian:
M. J. Frisch, G. W. Trucks, H. B. Schlegel, G. E. Scuseria, M. A. Robb, R. A. Cheeseman, J. R. Cheeseman, G. Scalmani, V. Barone, G. A. Petersson, H. Nakatsuji, X. Li, M. Caricato, A. V. Marenich, J. Bloino, B. G. Janesko, R. Gomperts, B. Mennucci, H. P. Hratchian, J. V. Ortiz, A. F. Izmaylov, J. L. Sonnenberg, D. Williams-Young, F. Ding, F. Lipparini, F. Egidi, J. Goings, B. Peng, A. Petrone, T. Henderson, D. Ranasinghe, V. G. Zakrzewski, J. Gao, N. Rega, G. Zheng, W. Liang, W. Hada, M. Ehara, K. Toyota, R. Fukuda, J. Hasegawa, M. Ishida, T. Nakajima, Y. Honda, O. Kitao, H. Nakai, T. Vreven, K. Throssell, J. A. Montgomery, Jr., J. E. Peralta, F. Ogliaro, M. J. Bearpark, J. J. Heyd, E. N. Brothers, K. N. Kudin, V. N. Staroverov, T. A. Keith, R. Kobayashi, J. Normand, K. Raghavachari, A. P. Rendell, J. C. Burant, S. S. Iyengar, J. Tomasi, M. Cossi, J. M. Millam, M. Klene, C. Adamo, R. Cammi, J. W. Ochterski, R. L. Martin, K. Morokuma, O. Farkas, J. B. Foresman and D. J. Fox, "Gaussian 16, Revision C.01," Gaussian, Inc., Wallingford CT, 2016.

[14] J. W. Ochterski, "Thermochemistry in Gaussian," Gaussian Inc, 2 June 2000. [Online]. Available: www.gaussian.com . [Accessed 8 June 2019].

[15] James J. P. Stewart , "MOPAC®," James Stewart Computational Chemistry 2007, 2007. [Online]. Available: http://openmopac.net/. [Accessed 03 August 2021].

[16] J. P. Stewart, "Optimization of Parameters for Semiempirical Methods V: Modification of NDDO approximations and application to 70 elements," Journal of Molecular Modeling volume , vol. 13, p. 1173–1213, 2007.

[17] M. J. Dewar, E. G. Zoebisch, E. F. Healy and J. P. Steward, "AMI: A New General Purpose Quantum Mechanical," Journal of the American Chemical Society, vol. 107, no. 13, pp. 3902-3909, 1985.

[18] N. B. Lima , G. B. Rocha, R. O. Freire and A. M. Simas, "RM1 Semiempirical Model: Chemistry, Pharmaceutical Research, Molecular Biology and Materials Science," Journal of the Brazilian Chemical Society, vol. 30, no. 4, 2019.

[19] M. W. Jurema and G. C. Shields, "Ability of the PM3 Quantum-Mechanical Method to Model Intermolecular Hydrogen Bonding between Neutral Molecules," 31 July 1993. [Online]. Available: http://mercuryconsortium.org/shields/pubs/JuremaS1993.pdf. [Accessed 27 August 2021]

CHAPTER 4: COMPUTATIONAL RESULTS: SINGLE MOLECULES

4.1 Introduction

The results presented in this Chapter, reflect on the correlation between the different software systems to derive at Heats of Formation, as one measure of conformity to optimum molecular geometries and effective electronic structure. The optimum structural property for each species was important to apply to a Grand Ensemble Canonical Simulation but scaled to atomic structural representations applying empirical force field parameters.

4.2 *Gaussian* Computations

Ab Initio open literature investigations utilised a collection of computational software systems such as: *Gaussian, Molpro, OpenMP* (parallel version of Mihaly Kallay's general coupled cluster code *MRCC* [1]). Application of these computational software systems are all compute resource demanding and come with innumerable challenges and usually require extended cluster computational hardware.

These factors probably justify why only a selected few $C\ell O_2$ species have been selected and studied by computational means up to now.

Chlorine oxide species present a significant class of organic molecules, described by complex covalent bonding (and in some instances dative bonding) between highly electronegative atoms. Additionally, some molecules have unpaired electrons (resulting in open shell geometries) which usually result in strong lone-pair repulsions, or in cases of hydrogen derivative species, in strong inter-molecular hydrogen bonding. The O-Cℓ bond creates a challenge for single referenced electron correlation methods, as these species are usually dominated by severe non-dynamical correlation (NDC) effects [1] and spin contamination, with resultant polarization.

Structural properties required to calculate geometries, spectroscopic properties and energy characteristics of molecules, are obtained from theoretical methods utilising one-electron basis set theory.

Many researchers have discussed some of the complexities associated with these studies, especially in relation to the calculation of Enthalpies of Formation and typical atmospheric kinetic models [2], [3], [1].

Heats of formation (ΔH_f) were calculated for single species (identified in chapter 2 from open literature), using DFT/B3LYP unrestricted level of theory, with Prof John Pople´s basis set (cc-pV5Z) programmed into the *Gaussian-16* program.

- An external (to *Gaussian*) calculation step was required to derive at Heats of Formation and Free Energies of Formation [4]. Tables-A4.1 and A4.2 in the Appendix of this manuscript outlines the steps to follow in deriving at final Heats of Formation and Free Energies of Formation, from all *Gaussian*-16 simulations for chlorine oxide species.

- Tabulated Heats of Formation derived with the *Gaussian*-16 software are listed in Table-**4.4**
- Literature referenced, alternative techniques utilized to derive at Heats of Formation for most of the $C\ell O_2$ species, are listed in Table-**4.1** (below)

*Table-**4.1**:* Literature referenced alternative computational and experimental methods used to obtain ΔH_f energies. (The structure of $C\ell_2O_3$ and its isomer $C\ell OC\ell O_2$ was referenced to Clark and Francisco [5]

Investigator		
(CℓO)	ΔH_f (kcal/mol)	Method
Jr. M. W. Chase	24.19 [6]	Determined experimentally
Abramowitz and Chase	24.27 [7]	Determined experimentally by spectroscopy
Karton et al.	24.28 [1]	W8 theory
Ventura et al.	24.88 [2]	G4 theory
Ruscic et al.	24.31 [8] [9] [10]	ATcT thermochemical network (TN)
(OCℓO)	ΔH_f (kcal/mol)	Method
Xu et al.	23.70 [11]	G2M//B3LYP/6-311+G(3df.2p)
Abramowitz and Chase	23.17 [7]	Determined experimentally by spectroscopy
Karton et al.	23.67 [12]]	W8 theory
Ventura et al.	27.2 [2]	Ab initio method: CCSD(T) aug-cc-pV6Z
Ruscic et al.	24.36 [8] [9] [10]	ATcT thermochemical network (TN)
(CℓOO)	ΔH_f (kcal/mol)	Method
Zhu and Lin	23.8 [13]	G2M//B3LYP/6-311G(3df. 2p)
Abramowitz and Chase	21.5 [7]	Determined experimentally by spectroscopy
Karton et al.	24.30 [12]	W8 theory
Ventura et al.	24.30 [2]	Ab initio method: CCSD(T) aug-cc-pV6Z
Ruscic et al.	24.56 [8] [9] [10]	ATcT thermochemical network (TN)

*Table-**4.1*** continued

Investigator		
(HOCℓ)	ΔH_f (kcal/mol)	Method
Zhu and Lin	-17 [13]	G2M//B3LYP/6-311G(3df. 2p)
Ventura et al.	-18 [2]	Ab initio method: CCSD(T) aug-cc-pV6Z
Karton et al.	-18 [12]	W4 theory
Ruscic et al.	-18.36 [8] [9] [10]	ATcT thermochemical network (TN)
($C\ell O_3$)	ΔH_f (kcal/mol)	Method
Zhu and Lin	47.2 [13]	G2M//B3LYP/6-311G(3df. 2p)
Sicre and Cobos	49.3 [14]	G3M//B3LYP/6-311G(3df. 2p)
Sicre and Cobos	57.0 [14]	G1 and isodesmic reaction
Karton et al.	50.9 [12]	W4 theory
Ruscic et al.	44.46 [8] [9] [10]	ATcT thermochemical network (TN)
($C\ell O_4$)	ΔH_f (kcal/mol)	Method
Sicre and Cobos	65.2 [14]	G2M//B3LYP/6-311G(3df. 2p)
Sicre and Cobos	66.4 [14]	Ab initio: B3LYP/6-311+G(3d2f)
Ruscic at al.	57.6 [8] [9] [10]	ATcT thermochemical network (TN)
(CℓOCℓ)	ΔH_f (kcal/mol)	Method
Jr. M. W. Chase	22 [13]	Determined experimentally
Karton et al.	18.82 [12]	W4 theory
Abramowitz and Chase.	31.77 [7]	Determined experimentally by spectroscopy
Klobas and Wilmouth.	31.03 [15]	Determined from the slope of the van't Hoff plot in the third law analysis.
($C\ell_2O_3$)	ΔH_f (kcal/mol)	Method
Clark and Francisco	46.2 [5]	G1 and G2 theory
	44.9 [5]	
Sicre and Cobos	37.8 [14]	Ab initio techniques: B3LYP 6-311+G(3d2f)
	53.9 [14]	G2 theory
Burkholder et al.	35.8 [16]	Determined with UV spectroscopy
(HOCℓO)	ΔH_f (kcal/mol)	Method
Karton et al.	5.0 [12]	W4 theory
Clark and Francisco	11.9 [5]	G2 theory
Ruscic at al.	4.94 [8] [9] [10]	ATcT thermochemical network (TN)
(HOCℓOO)	ΔH_f (kcal/mol)	Method
Xu et al.	0.1 [11]	G2M//B3LYP/6-311+G(3df.2p)
Karton et al.	-2.6 [1]	W4 theory
Ruscic at al.	-1.10 [8] [9] [10]	ATcT thermochemical network (TN)
(HOOCℓO)	ΔH_f (kcal/mol)	Method
Xu et al.	20.6 [11]	G2M//B3LYP/6-311+G(3df.2p)
Ruscic at al.	21.54 [8] [9] [10]	ATcT thermochemical network (TN)

*Table-**4.1*** continued

Investigator		
($HOOC\ell O_2$)	ΔH_f (kcal/mol)	Method
Xu et al.	0.1 [11]	G2M//B3LYP/6-311+G(3df.2p)
Colussi and Grela	-4.2 [17]	Determined with UV spectroscopy
Ruscic at al.	16.55 [8] [9] [10]	ATcT thermochemical network (TN)
($HOC\ell O_3$)	ΔH_f (kcal/mol)	Method
Xu et al.	3.2 [11]	G2M//B3LYP/6-311+G(3df.2p)
Clark and Francisco	10.80 [5]	G2 theory
Colussi and Grela	-1.5 [17]	Determined with UV spectroscopy
Ruscic et al.	0.43 [8] [9] [10]	ATcT thermochemical network (TN)

Unrestricted Hartree Fock (UHF) spin polarization restriction was applied on radical and charged species, with *Restricted Hartree Fock* (RHF) applied to neutral species. *Restricted Open Shell Hartree Fock* (ROHF) ruling was used for some charged species in an attempt to compensate for spin polarization.

Although a significant group of chlorine oxide related species exist, a few have been studied computationally, possibly owing to the complexity of their bonding character. Many researchers have attempted to compute the thermochemical properties of a few chlorine oxide species [1] [2] [5][6] [7] citing discrepancies in their energy values. A list of reported energies and the methods used to derive at them, are presented below in Table-**4.2.**

- The ΔH_f of twenty (20) SINGLE species were considered unacceptable, since these values show a difference in energy, exceeding 8.5 kcal/mol correlated against Literature Reference ΔH_f energies. This equates to thirty-three (33) percent of the species producing unacceptable results.
- The computed ΔH_f of thirteen (13) species showed differences in energy, between the calculated and the reference energies that lie between 3.5 - 8.5 kcal/mol hence twenty-two (22) percent produced fair results.
- Accurate results were obtained for thirty-five (35) percent of the species
- The *Gaussian* (DFT/B3LYP) theory supported by the (*cc-pV**5**Z)* basis set, was found by many researchers to be sufficiently accurate, but noted the (*cc-pV**6**Z)* basis set to be more acceptable for these compounds [2]
- ***Gaussian*-09** supports computations with the (*cc-pV**6**Z)* basis set on 3rd row elements [18]. However, this basis set is not supported in the later *Gaussian-16* [18].

- ***Gaussian-16*** theory level CCSD (T) gave the most accurate thermochemical properties [2], but found to be computationally resource demanding, especially when combined with higher basis sets [19].

4.3 MOPAC Computations

The Heats of Formation (ΔH_f) for the set of sixty (60) species were calculated, applying each of the seven (7) *MOPAC* Hamiltonians. Different ΔH_f energies were obtained for each compound. The author of the *MOPAC* program, Dr James (Jim) Stewart [20] very kindly corrected the number of orbitals assigned, to deal with effective electron population and charge distribution in each ionic species. Although reference ΔH_f of a few species are unknown, the result (applying the different Hamiltonians) corresponding to the most sterically correct geometry were finally accepted.

The ΔH_f results for the studied set of species computed with *MOPAC-2016* are tabulated in Table 4.2 and were used in determining Free Energies of Formation, Entropy and Heat Capacity properties.

*Table-**4.2:*** Calculated Heats of Formation (kcal/mol) with MOPAC-2016, applying all the supported Hamiltonians for single species (in 'vacuum'). Entries in bold were selected as Heats of Formation. Entries closest to reference values were selected as the final Heat of Formation values.

		Hamiltonian (ΔH_f kcal/mol)						
Molecule Formula	Reference	AM1	MNDO	MNDOD	PM3	PM6	PM7	RM1
CℓO	24.31 [8]	31.09	34.84	17.73	8.27	**25.47**	21.57	12.83
$[C\ell O]^-$	-28.26 [8]	-15.27	-7.78	-35.81	-32.98	**-24.00**	-31.23	-20.98
$[C\ell O]^+$	274.84 [8]	321.72	334.48	316.78	238.35	284.77	276.94	**279.73**
CℓOO	24.56 [8]	44.45	22.24	**23.28**	13.51	19.07	7.35	-1.15
$[C\ell OO]^-$	-59.28 [8]	-42.04	-44.04	-43.15	-40.56	-32.58	-41.39	**-53.36**
$[C\ell OO]^+$	286.71 [8]	277.39	299.61	**293.61**	264.05	249.24	259.35	272.89
CℓOCℓ	18.62 [8]	**19.45**	31.26	16.02	-16.25	8.53	4.89	9.1
$[C\ell OC\ell]^-$	-35.28 [8]	-39.81	-30.51	**-36.72**	-53.84	-60.37	-61.23	-57.16
$[C\ell OC\ell]^+$	269.14 [8]	284.81	302.43	**261.74**	213.39	237.23	247.28	244.88
CℓCℓO	31.81 [8]	55.03	73.16	28.63	9.18	**37.78**	40.13	17.28
$[C\ell C\ell O]^-$	-44.11 [8]	-32.32	-39.71	**-43.69**	-62.98	-56.57	-49.02	-75.53
$[C\ell C\ell O]^+$	270.09 [8]	285.23	307.67	264.74	234.68	256.85	**271.85**	240.95
$C\ell C\ell O_2$	29.16 [8]	132.97	170.87	38.44	-55.80	**28.98**	46.02	19.42
CℓOOO	53.29 [8]	42.54	**45.51**	41.66	4.03	9.07	10.83	30.75
$[C\ell OOO]^-$	-25.00 [8]	-13.25	-6.47	-4.21	-35.61	-9.43	-53.81	**-25.06**
$C\ell(O)O_2$	63.37 [8]	**63.42**	63.96	62.96	74.32	83.95	61.23	63.47
$[C\ell(O)O_2]^-$	-25.22 [8]	-8.12	-12.12	-10.55	-12.99	**-35.34**	-53.81	-14.77
$C\ell O_3$	44.46 [8]	153.42	171.64	38.79	-21.19	**39.31**	53.10	158.13
$[C\ell O_3]^-$	-50.83 [8]	72.95	130.44	**-55.19**	-155.81	-65.04	-59.67	-41.97
$[C\ell O_3]^+$	297.67 [8]	497.19	530.66	**300.82**	**300.82**	324.37	339.03	386.74

*Table-**4.2*** Continued

Molecule Formula	Reference	Hamiltonian (ΔH_f kcal/mol) AM1	MNDO	MNDOD	PM3	PM6	PM7	RM1
$C\ell O_4$	57.60 [8]	219.47	249.03	79.10	**46.14**	136.89	92.82	163.42
$[C\ell O_4]^-$	-64.98 [8]	166.46	238.88	-80.38	-128.15	**-72.82**	-82.73	2.47
$C\ell OC\ell O$	41.80 [8]	82.39	117.00	36.38	-4.37	38.19	33.41	**42.73**
$C\ell OOC\ell$	31.37 [15]	**33.69**	41.70	36.71	2.33	16.00	14.64	18.80
$C\ell OC\ell O_2$	37.80 [16]	150.69	212.90	**38.45**	-83.71	22.17	26.44	48.41
$C\ell OC\ell O_3$	37.40 [14]	267.68	325.67	50.07	-112.63	54.44	**49.52**	66.97
$C\ell O_2C\ell O_2$	N/R	275.27	350.88	103.16	-112.63	**50.72**	74.49	68.02
$C\ell O_2$-O-$C\ell O_2$	N/R	283.17	397.84	**41.27**	-198.43	18.51	**22.32**	49.18
$C\ell OOC\ell O_3$	69 [14]	227.59	303.20	**73.94**	-20.74	78.4	68.99	111.43
$C\ell O_2$-O-$C\ell O_3$	72.40 [14]	403.53	509.39	**47.01**	-119.90	44.94	37.45	154.79
$C\ell O_3$-O-$C\ell O_3$	86.20 [14]	526.16	623.36	57.12	-26.25	**76.7**	59.59	260.46
$C\ell O_2$-O-O-$C\ell O_2$ [22]	N/R	214.46	363.24	82.18	-143.74	62.83	**79.42**	105.24
$C\ell O_3$-O-O-$C\ell O_3$ [22]	111.40 [22]$	128.12	585.97	**108.37**	44.32	137.16	128.12	182.76
$[C\ell O_3C\ell O_3]^-$ [2] [18]	N/R	212.66	578.86		-120.01	44.91	37.45	**106.06**
$OC\ell O$	24.36 [8]	97.57	142.95	**25.47**	43.1	80.35	41.21	90.43
$[OC\ell O]^-$	-25.74 [8]	22.37	54.39	-33.48	-36.85	-16.07	**-23.14**	2.2
$[OC\ell O]^+$	262.13 [8]	385.36	418.23	270.55	188.61	**266.34**	279.2	284.22
$OC\ell OO$	54.31 [8]	3.33	18.82	1.71	4.02	26.69	**44.72**	-8.60
$[OC\ell OO]^-$	-8.19 [8]	-22.07	2.48	-25.07	-23.26	1.52	**-12.15**	-24.39
$OC\ell C\ell O_2$	46.20 [5]	196.34	243.10	82.73	-83.71	22.18	27.21	**50.13**
$[C\ell OH_2]^+$	194.66 [8]	207.65	201.43	**197.10**	183.5	201.92	200	207.75
$HOC\ell$	-18.36 [8]	-21.78	-15.68	-15.67	-34.30	**-17.81**	-23.08	-20.93
$[HOC\ell]^-$	47.38 [8]	-48.80	-61.54	**-9.02**	-55.81	-65.41	-63.2	-60.86
$[HOC\ell]^+$	237.86 [8]	**244.01**	253.76	219.18	201.4	215.87	220.85	224.08
$HOC\ell O$	4.94 [8]	35.04	69.25	-1.73	-25.15	9.49	**6.77**	12.76
$[HOC\ell O]^-$	-37.31 [8]	-22.66	-13.62	**-34.19**	-48.81	-49.98	-47.06	-42.32
$[HOC\ell O]^+$	236.82 [8]	265.87	293.57	221.29	177.25	222.4	**223.62**	233.62
$HOC\ell O_2$	10.90 [23]	106.10	165.03	**-3.27**	-108.27	-12.98	-10.91	5.86
$HOC\ell O_3$	0.43 [8]	223.17	277.8	**3.71**	-26.48	16.03	7.49	110.80
$[HOC\ell O_3]^+$	0.43 [8]	401.01	430.41	304.78	**273.23**	303.74	325.2	344.25

*Table-**4.2*** Continued

Molecule Formula	Reference	Hamiltonian (ΔH_f kcal/mol)						
		AM1	MNDO	MNDOD	PM3	PM6	PM7	RM1
HOOCℓ	282.36 [8]	9.72	9.23	5.81	-13.83	-1.6	0.47	**-0.68**
$[HOOC\ell]^-$	-0.32 [8]	**-39.22**	-61.72	-56.94	-52.75	-53.14	-52.6	-58.96
$[HOOC\ell]^+$	-8.12 [8]	251.3	259.09	252.98	227.53	223.78	230.67	**244.23**
HOOCℓO	27.30 [23]	49.08	82.04	17.76	-7.17	30.06	**23.08**	22.05
$HOOC\ell O_2$	16.55 [8]	114.9	174.77	19.82	-80.24	**19.25**	21.63	35.03
HOOOCℓ	14.00 [23]	13.6	14.86	**11.88**	-6.34	7.94	3.80	1.65
HOOOOCℓ	22.70 [5]	29.39	29.21	27.10	5.81	**24.78**	17.94	11.62
HCℓO	33.24 [8]	43.63	76.22	21.77	10.50	27.70	**30.43**	34.08
$HC\ell O_2$	45.65 [8]	121.11	177.07	31.72	-70.49	37.56	**49.06**	47.7
$HC\ell O_3$	57.10[23]	106.1	302.02	**45.70**	-11.39	73.01	77.41	5.86

*N/R - not reported

$ Indicates that the ΔH_f *(298K)* of $C\ell O_3$-O-O-$C\ell O_3$ is calculated from Energies by Beltran et al., (1999) [22]

Additional properties i.e., Spin Multiplicity, Point groups, Entropy and Heat Capacities (Cp) at 298K, were calculated with *MOPAC-2016* are listed in Table 4.3. These chemical properties are required as supporting data for the population of the *FactSage* database (chapter 7).

*Table-**4.3:*** Entropy, Heat capacities, Point Groups and Multiplicities

Molecule Formula	S (J/mol K)	Cp (J/mol K)	Multiplicity (Spin State)	Point Group
CℓO	215.09	30.78	2	C*v
$[C\ell O]^-$	215.64	31.01	1	C*v
$[C\ell O]^+$	213.25	21.66	1	C*v
CℓOO	256.64	40.54	2	C2v
$[C\ell OO]^-$	265.18	46.01	1	C2v
$[C\ell OO]^+$	258.75	35.69	1	C2v
CℓOCℓ	264.16	43.33	1	C2v
$[C\ell OC\ell]^-$	279.21	48.37	2	C2v
$[C\ell OC\ell]^+$	262.36	42.76	2	C2v
CℓCℓO	272.67	45.19	1	Cs
$[C\ell C\ell O]^-$	293.01	49.86	2	Cs
$[C\ell C\ell O]^+$	275.27	47.94	2	Cs
$C\ell C\ell O_2$	296.4	61.96	1	Cs

*Table-**4.3*** continued

Molecule Formula	S	Cp	Multiplicity	Point Group
CℓOOO	297.01	52.81	2	C1
$[C\ell OOO]^-$	286.06	56.29	1	C1
$C\ell(O)O_2$	323.26	63.22	2	C2v
$[C\ell(O)O_2]^-$	300.27	62.35	1	C2v
$C\ell O_3$	280.33	62.65	2	D3h
$[C\ell O_3]^-$	264.82	56.18	1	D3h
$[C\ell O_3]^+$	273.42	35.56	1	D3h
$C\ell O_4$	308.9	79.68	2	C2v
$[C\ell O_4]^-$	265.7	63.11	1	Td
CℓOCℓO	302.40	62.52	1	C1
CℓOOCℓ	289.38	57.09	1	C2
$C\ell OC\ell O_2$	308.11	69.63	1	Cs
$C\ell OC\ell O_3$	335.93	86.60	1	C1
$C\ell O_2C\ell O_2$	340.46	96.51	1	D2h
$C\ell O_2$-O-$C\ell O_2$	332.84	99.84	1	D2h
$C\ell OOC\ell O_3$	359.09	102.89	1	C1
$C\ell O_2$-O-$C\ell O_3$	367.43	111.22	1	C1
$C\ell O_3$-O-$C\ell O_3$	369.09	126.94	1	D3h
$[C\ell O_3C\ell O_3]^{-2}$	403.99	126.56	1	D3d
$C\ell O_2$-O-O-$C\ell O_2$	403.86	129.85	1	C2h
$C\ell O_3$-O-O-$C\ell O_3$	471.17	164.93	1	C1
OCℓO	250.18	38.97	2	C2v
$[OC\ell O]^-$	253.39	42.54	1	C2v
$[OC\ell O]^+$	272.24	32.61	1	C2v
OCℓOO	368.09	67.23	2	Cs
$[OC\ell OO]^-$	302.31	65.09	1	Cs
$OC\ell C\ell O_2$	340.18	77.86	1	Cs
$[C\ell OH_2]^+$	246.18	27.56	2	C2v
HOCℓ	236.16	36.05	1	Cs
$[HOC\ell]^+$	235.36	35.62	2	Cs
HOCℓO	263.60	47.48	1	Cs
$[HOC\ell O]^-$	283.68	57.80	2	Cs
$[HOC\ell O]^+$	271.55	52.30	2	Cs
$HOC\ell O_2$	288.18	62.57	1	Cs

*Table-**4.3*** continued

Molecule Formula	S (J/mol K)	Cp (J/mol K)	Multiplicity (Spin State)	Point Group
$HOC\ell O_3$	307.07	74.37	1	Cs
$[HOC\ell O_3]^+$	312.33	80.74	2	Cs
$HOOC\ell$	263.45	49.09	1	Cs
$[HOOC\ell]$-	270.30	52.15	2	Cs
$[HOOC\ell]^+$	266.73	51.32	2	Cs
$HOOC\ell O$	293.57	65.99	1	C1
$HOOC\ell O_2$	322.75	82.36	1	C1
$HOOOC\ell$	286.64	58.79	1	C1
$HOOOOC\ell$	329.09	84.55	1	C1
$HC\ell O$	237.13	38.579	1	Cs
$HC\ell O_2$	253.22	47.44	1	C2v
$HC\ell O_3$	264.06	50.98	1	C3v

MOPAC Hamiltonians: MNDOD, PM6 and PM7, accounted for 35.60 %, 22 % and 25 %, accurate ΔH_f energies respectively. Final (geometry optimized) MOPAC Heats of Formation energies are reported jointly in Table-**4.4**, with the Gaussian (single) molecule energies.

MOPAC-2016 surprisingly, offered excellent results:

- Approximately 21 % of the calculated ΔH_f obtained were between 6 to 10 kcal/mol higher than the reference values.
- The calculated ΔH_f of five species calculated (highlighted in yellow in Table- 4.5) were beyond the limit of the reference values and classified as unacceptable
- The remainder of the calculated ΔH_f were within 5 kcal/mol of the reference ΔH_f and acceptable.
- Finite ΔH_f energies for $[C\ell O_3C\ell O_3]^{-2}$. $C\ell O_2$-O-$C\ell O_2$. $C\ell O_2C\ell O_2$ and $C\ell O_2$-O-O-$C\ell O_2$ could not be confirmed with no reference ΔH_f energies being available.

4.4 *VASP* Computation (including all consolidated results)

The ΔH_f energies of neutral *single* models, were calculated using *VASP-6.2.1* applying two functionals: GGA-BLYP and GGA-PBE. All neutral single species exposed to *VASP*-6.2.1 calculations, were confined to periodic cell conditions under Space Group symmetry restrictions of P**1**(1).

Periodic cell parameters assigned were increased to 15x15x15 Å to ensure a true single molecular environment persists. The GGA-BLYP functional produced accurate energies and the calculated

(single molecule) *VASP*-6.2.1 ΔH_f energies are presented in *Table-**4.4*** which also summarises **all** results obtained for single molecule species (from the *MOPAC* Software)

*Table-**4.4***: Heats of Formation (ΔH_f*298K*) of single chlorine oxide species calculated with the *Gaussian-16* (DFT B3LYP/cc-pV5Z) and MOPAC-2016 software

Species	Literature Reference ΔH_f (298K)	*Gaussian-16* (DFT B3LYP, cc-pV5Z) ΔH_f (298K)	MOPAC-2016 (derived) ΔH_f (298K)	VASP-6.2.1 GGA-BLYP	VASP-6.2.1 GGA-PBE
				ΔH_f (298K)	
CℓO [8]	24.31 [8]	29.71	25.47	25.91	26.62
$[C\ell O]^-$ [8]	-28.26 [8]	-23.46	-24.00		
$[C\ell O]^+$ [8]	274.84 [8]	278.18	276.94		
CℓOO [8]	24.56 [8]	21.50	23.28	23.74	23.06
$[C\ell OO]^-$ [8]	-59.28 [8]	-54.75 #	-53.36		
$[C\ell OO]^+$ [8]	286.71 [8]	299.79	293.61		
CℓOCℓ [8]	18.62 [8]	21.03	19.45	16.13	16.27
$[C\ell OC\ell]^-$ [8]	-35.28 [8]	-35.26	-36.72		
$[C\ell OC\ell]^+$ [8]	269.14 [8]	269.03	261.74		
CℓCℓO [8]	31.81 [8]	34.64	37.80	23.94	21.79
$[C\ell C\ell O]^-$ [8]	-44.11 [8]	-54.10 #	-43.69		
$[C\ell C\ell O]^+$ [8]	270.09 [8]	275.83	271.85		
CℓCℓOO [8] *# $[C\ell C\ell O_2]$	29.16 [8]	36.79	28.96	9.75	5.83
CℓOOO [8]	53.29 [8]	67.80	45.51	65.8	66.06
$[C\ell OOO]^-$ [8]	-25.00 [8]	-21.93	-25.06		
CℓO(O)O [8]*# $[C\ell(O)O_2]$	63.37 [8]	69.46	63.47		
$[C\ell O(O)O]^-$ [8]*# $[C\ell(O)O_2]^-$	-25.22 [8]	-21.95	-35.34		
$C\ell O_3$ [8]	44.46 [8]	47.79	39.31	72.17	61.87
$[C\ell O_3]^-$ [8]	-50.83 [8]	**-35.31**	-55.19		
$[C\ell O_3]^+$ [8]	297.67 [8]	**329.73**	300.82		
$[C\ell O_4]$ [8]	57.60 [8]	**74.64**	46.14	62.99	45.53
$[C\ell O_4]^-$ [8]	-64.98 [8]	**-42.11**	-72.83		
CℓOCℓO [8]	41.80 [8]	54.98	38.19	15.54	13.52
CℓOOCℓ [8]	31.37 [15]	38.67	33.69	31.38	10.86
$C\ell OC\ell O_2$ [8]	37.80 [16]	48.86 **	38.45	40.46	34.81
$C\ell OC\ell O_3$ [8]	37.40 [14]	65.77	49.52		
CℓOOCℓOO [21]* $[C\ell O_2C\ell O_2]$	N/R	69.78	50.72	21.63	16.32
$C\ell O_2$-O-$C\ell O_2$ [21]	N/R	81.21	41.27	104.5	90.07

*Table-**4.4*** Continued

Species	Literature Reference ΔH_f (298K)	*Gaussian-16* (DFT B3LYP, cc-pV5Z) ΔH_f (298K)	MOPAC-2016 (derived) ΔH_f (298K)	VASP-6.2.1 GGA-BLYP	VASP-6.2.1 GGA-PBE
				ΔH_f (298K)	
$C\ell_2O_5$ [14] *# [$C\ell OOC\ell O_3$]	69 [14]	72.17	73.94	49.87	33.22
$C\ell_2O_6$ [14] *# [$C\ell O_2$-O-$C\ell O_3$]	72.4 [14]	85.24 *	**47.01**	28.78	15.45
$C\ell_2O_7$ [14]*# $C\ell O_3$-O-$C\ell O_3$	86.2 [14]	89.64 *	76.70	77.53	44.22
$C\ell O_2$-O-O-$C\ell O_2$ [21]	N/R	104.17 **	79.42	105.61	25.24
$C\ell_2O_8$ [22] *# $C\ell O_3$-O-O-$C\ell O_3$	111.40 [22]$	118.45	108.37		
[$C\ell O_3$-$C\ell O_3$]$^{-2}$ [21]	N/R	105.74	106.06		
$OC\ell O$ [8]	24.36 [8]	23.89	25.47	21.04	66.92
[$OC\ell O$]$^-$ [8]	-25.74 [8]	-16.29	-23.14		
[$OC\ell O$]$^+$ [8]	262.13 [8]	278.24	266.34		
$OC\ell OO$ [8]	54.31 [8]	51.63	44.72	36.12	33.65
[$OC\ell OO$]$^-$ [8]	-8.19 [8]	-9.89	-12.15		
$OC\ell C\ell O_2$ [8]	46.2 [5]	**146.67 #**	50.13	43.07	35.69
[$C\ell OH_2$]$^+$ [8]	194.66 [8]	202.38	197.10		
$HOC\ell$ [8]	-18.36 [8]	-16.43 *	-17.81	-18.04	-19.28
[$HOC\ell$]$^-$ [8]	47.38 [8]	54.25	**-9.02 ****		
[$HOC\ell$]$^+$ [8]	237.86 [8]	239.06	244.01		
$HOC\ell O$ [8]	4.94 [8]	13.01	6.77	6.15	1.9
[$HOC\ell O$]$^-$ [8]	-37.31 [8]	-57.33 #	-34.19		
[$HOC\ell O$]$^+$ [8]	236.82 [8]	238.93	233.62		
$HOC\ell(O)O$ [8] *# [$HOC\ell O_2$]	10.90 [23]	11.18 **	**-3.27**	13.7	7.84
[$HOC\ell O_3$] [8]	0.43 [8]	12.13 **	3.71	9.09	-10.44
[$HOC\ell O_3$]$^+$ [8]	0.43 [8]	325.73 #	273.23		
$HOOC\ell$ [8]	282.36 [8]	2.60 *	-0.68	2.97	0.97
[$HOOC\ell$]$^-$ [8]	-0.32 [8]	-10.60	**-39.22**		
[$HOOC\ell$]$^+$ [8]	-8.12 [8]	253.27 #	244.23		
$HOOC\ell O$ [23]	27.30 [23]	27.78 *	23.08	27.49	21.73
$HOOC\ell(O)O$ [8]*# [$HOOC\ell O_2$]	16.55 [8]	**37.26 ****	19.25	5.08	-37.37
$HOOOC\ell$ [8]	14.00 [23]	**27.44 ***	11.88	3.39	-0.53
$HOOOOC\ell$ [5]	22.70 [5]	28.18	24.78	12.92	8.31
$HC\ell O$ [8]	33.24 [8]	33.89 *	30.45	31.05	28.15
$HC\ell O_2$ [8]	45.65 [8]	48.31 *	49.06	88.98	81.31
$HC\ell O_3$ [23]	57.1 [23]	46.07 *	45.70	42.49	25.82

N/R - not reported

*# Highlights the naming convention adopted for this study

***** Restricted: DFT/B3LYP/cc-pv5z

**Restricted open shell. DFT/B3LYP/cc-pv5z
Unrestricted: DFT/B3LYP/6-311++G(3d2f,3p2d)
$ Indicates that the ΔH_f *(298K)* of $C\ell O_3$-O-O-$C\ell O_3$ is calculated from Energies by Beltran et al., 1999 [22]

Some discrepancies observed for both *Gaussian* and *MOPAC* single molecule species, are highlighted as bold text. Comparison of ΔH_f obtained with three computational programs i.e., *Gaussian-16, MOPAC-2016* and *VASP-6.2.1* resulted in variable results for the species:

$C\ell O_2$-O-$C\ell O_2$, $[C\ell O_3 C\ell O_3]^{-2}$, $C\ell O_2$-O-O-$C\ell O_2$, and $C\ell O_2 C\ell O_2$.

Further investigations are required to elucidate these variations, probably related to spin polarization and/or improved atom potentials.

4.5 Conclusion

A noticeable variation in spin-states were observed for higher-order $C\ell O_2$ species structures, applying both the *Gaussian* and *MOPAC* software programs. This was specifically prevalent for species hosting a higher oxygen content, which resembles a complex array of internal open shell connectivity and spin polarization. This must not be conceived as flaws in the software algorithms, but rather considered as a result of slight alterations in electronic structural configurations, adopted by the software algorithms. Species of this nature (with intrinsic radical and charge dissipation character) are particularly vulnerable, to produce varying spin conditions. Both *Gaussian*-16 and *MOPAC-2016* performed well in terms of the computational determination of the Heat of Formation, which could comfortably be utilised in the subsequent extraction of chemistry reaction schemes.

4.6 References

[1] A. Karton, S. Parthiban and J. M. Martin, “Post-CCSD(T) ab Initio Thermochemistry of Halogen Oxides and Related Hydrides XOX, XOOX, HOX, XOn, and HXOn (X) F, Cl), and Evaluation of DFT Methods for These Systems,” Journal of Physical Chemistry A, vol. 113, p. 4802–4816, 2009.

[2] O. Ventura, K. Irving and M. Kieninger, “Basis Set Effects in the Description of the Cl-O Bond in ClO and XClO Isomers (X=H,O,Cl) Using DFT and CCSD(T) Methods,” ChemRxiv, 13 April 2018. [Online]. Available: www.ChemRxiv.com. [Accessed 5 August 2020].

[3] D. W. Rogers, A. A. Zavitsas and Y. N. Matsunaga, “Determination of Enthalpies (‘Heats’) of Formation,” Wiley Interdisciplinary Reviews: Computational Molecular Science, vol. 3, pp. 21-36, 2013.

[4] Gaussian: M. J. Frisch, G. W. Trucks, H. B. Schlegel, G. E. Scuseria, M. A. Robb, R. A. Cheeseman, J. R. Cheeseman, G. Scalmani, V. Barone, G. A. Petersson, H. Nakatsuji, X. Li, M. Caricato, A. V. Marenich, J. Bloino, B. G. Janesko, R. Gomperts, B. Mennucci, H. P. Hratchian, J. V. Ortiz, A. F. Izmaylov, J. L. Sonnenberg, D. Williams-Young, F. Ding, F. Lipparini, F. Egidi, J. Goings, B. Peng, A. Petrone, T. Henderson, D. Ranasinghe, V. G. Zakrzewski, J. Gao, N. Rega, G. Zheng, W. Liang, W. Hada, M. Ehara, K. Toyota, R. Fukuda, J. Hasegawa, M.Ishida, T. Nakajima, Y. Honda, O. Kitao, H. Nakai, T. Vreven, K. Throssell, J. A. Montgomery, Jr., J. E. Peralta, F. Ogliaro, M. J. Bearpark, J. J. Heyd, E. N. Brothers, K. N. Kudin, V. N. Staroverov, T. A. Keith, R. Kobayashi, J. Normand, K. Raghavachari, A. P. Rendell, J. C. Burant, S. S. Iyengar, J. Tomasi, M. Cossi, J. M. Millam, M. Klene, C. Adamo, R. Cammi, J. W. Ochterski, R. L. Martin, K. Morokuma, O. Farkas, J. B. Foresman and D. J. Fox, “Gaussian 16, Revision C.01,” Gaussian, Inc.,, Wallingford CT, 2016.

[5] J. Clark and J. S. Francisco, “Study of the Stability of Cl2O3 Using Ab Initio Methods,” Journal of Physical Chemistry A, vol. 101, p. 7145., 1997.

[6] M. W. Chase, Jr. , “NIST-JANAF Thermochemical Tables,” American Chemical Society, American Institute of Physics for the National Institute of Standards and Technology, Washington, DC : New York, 1998.

[7] S. Abramowitz and M. W. Chase, “Thermodynamic Properties of Gas Phase Species of Importance to Ozone Depletion,” Pure Applied Chemistry, vol. 63, no. 10, pp. 1449-1454, 1991.

[8] B. Ruscic and D. H. Bross, “Active Thermochemical Tables (ATcT) values based on ver. 1.122r of the Thermochemical Network,” 2021. [Online]. Available: https://atct.anl.gov/Thermochemical%20Data/version%201.122r/index.php. [Accessed 4 June 2021].

[9] B. Ruscic, R. E. Pinzon, G. v. Laszewski, D. Kodeboyina, A. Burcat, D. Leahy, D. Montoya and A. F. Wagner, “Active Thermochemical Tables: Thermochemistry for the 21st Century.,” Journal of Physics: Conference Series, vol. 16, pp. 561-570, 2005.

[10] B. Ruscic, R. E. Pinzon, M. L. Morton, G. v. Laszewski, S. Bittner, S. G. Nijsure, K. A. Amin, M. Minkoff and A. F. Wagner, “Introduction to Active Thermochemical Tables: Several "Key" Enthalpies of Formation Revisited.,” Journal of Physical Chemistry A, vol. 108, pp. 9979-9997, 2004.

[11] Z.F. Xu, R. Zhu and M. Lin, “Ab Initio Studies of ClOx Reactions. 3. Kinetics and Mechanisms for the OH +OClO Reaction,” Journal of Physical Chemistry A, vol. 107, pp. 1040-1049, 2003.

[12] A. Karton, E. Rabinovich, J. M. Martin and B. Ruscic, “W4 theory for Computational Thermochemistry: In Pursuit of Confident Sub-kJ/mol Predictions,” The Journal of Chemical Physics 4, vol. 125, pp. 144108-17, 2006.

[13] R. S. Zhu and M. C. Lin, “Ab Initio study of Ammonuim Perchlorate Combustion Initiation Processes: Unimolecular Decomposition of Perchloris Acid and the Related OH + ClO3 Reaction,” The Journal of Chemical Physics Communications, vol. 25, pp. 1-6, 2001.

[14] J. E. Sicre and C. J. Cobos, “Thermochemistry of the Higher Chlorine Oxides ClO x (x ¼ 3, 4) and Cl2O x (x ¼ 3–7),” Journal of Molecular Structure (Theochem) , vol. 620 , p. 215–226, 2003.

[15] J. E. Klobas and D. M. Wilmouth, “UV Spectroscopic Determination of the Chlorine Monoxide (ClO)/ Chlorine Peroxide (ClOOCl) Thermal Equilibrium Constant,” Atmospheric Chemistry and Physics, Discussions, p. 1120, 2018.

[16] J. B. Burkholder, R. K. Talukdar, A. R. Ravishankara, and S. Solomon, “Temperature Dependence of the HNO3 UV Absorption Cross Sections,” Journal of Geophysical Research, vol. 98, p. 22937–22948, 1993.

[17] A. J. Colussi and M. A. Grela, “Kinetics and thermochemistry of chlorine-and nitrogen-containing oxides and peroxides,” The Journal of Physical Chemistry A, vol. 97, p. 3775, 1993.

[18] Gaussian, “Gaussian,” Gaussian International, [Online]. Available: https://gaussian.com/. [Accessed 08 06 2019].

[19] K. P. Somers and J. M. Simmie, “Benchmarking Compound Methods (CBS-QB3, CBS-APNO, G3, G4,W1BD) against the Active Thermochemical Tables: Formation Enthalpies of Radicals,” Journal of Physical Chemistry A vol. 119, pp. 8922-8933, 2015.

[20] James J. P. Stewart , “MOPAC®,” James Stewart Computational Chemistry 2007, 2007. [Online]. Available: http://openmopac.net/. [Accessed 03 August 2021].

[21] National Library of Medicine, “National Library of Medicine,” [Online]. Available: https://pubchem.ncbi.nlm.nih.gov/compound/11159534. [Accessed 5 May 2021].

[22] A. Beltran, J. Andres, S. Noury and B. Silvi, “Structure and Bonding of Chlorine Oxides and Peroxides: ClOx, ClOx- (x) 1-4), and Cl2Ox (x) 1-8),” Journal of Physical Chemistry A , vol. 103, pp. 3078-3088, 1999.

[23] J. S. Francisco and S. P. Sander, “Structures, Relative Stabilities, and Vibrational Spectra of Isomers of HClO3,” Journal of Physical Chemistry A., vol. 100, pp. 573-579, 1996

CHAPTER 5: ENSEMBLE MODEL COMPUTATIONS

5.1 Introduction

The first critical and significantly important aspect in simulation at the force field level of molecular space definition, is the specification of suitable empirical force field parameters. The *MedeA*/*GIBBS* software features a built-in algorithm to assign appropriate force field parameters to a predefined model (periodic or molecular) and is based on molecular geometry and α-β bonding from every atom, within a specified cut off distance from each atom. Cut off distances of 3.5Å are typically permitted around each atom. Atom type assignments associated with immediate 3D-neighbours are therefore effectively considered. For organic structures all facets of torsion; bond angles (typical); bond lengths; long-distance interactions; coulomb forces; bond character/type (to restrain bond distance); bond increments; and vd Waals interactions are accounted for and have to be assigned as a completed set, prior to any simulation. This represents a molecular mechanical representation at the atomic-level [1], side stepping the *Ab Initio* details of electron-electron and electron-nucleon interactions.

The force field concept relates to classical mechanics and is a collection of equations and associated parameters, designed to reproduce molecular geometry and selected properties, normally derived from a vast set of known structures [2]. The force field method uses a set of empirical formulae to portray the interatomic interactions in an averaged fashion [3]. This method is used as an excellent averaged molecular structural representation tool, when electron (or charge) distribution is not considered or required and can successfully describe properties of interest and as a result are computationally less demanding.

The technique is sufficiently accurate and powerful, to optimize a molecular (or periodic) structure to within an acceptable energy regime, for quantum chemistry to take over.

5.2 MedeA GIBBS ensemble (NPT)

Panagiotopoulos [4] proposed the concept of Gibbs ensemble Monte Carlo (GEMC) simulations in 1987, which entailed a method of directly computing the phase coexistence properties of either pure fluids or mixtures [4]. The technique is dependent on a confined model space and is undertaken in a periodic (Grand Cell) environment. GEMC has an advantage over other conventional methods since two-phase equilibrium properties can be calculated without requiring a Free Energy value [4]. In this case, each chlorine oxide species was built as a periodic model, force field parameters assigned and executed as a single-phase system in a GEMC ensemble simulation.

5.2.1 *Chemical Approach*

Single monomeric chlorine oxide species were exposed to an isobaric-isothermal Gibbs ensemble (GEMC) simulation, applying Grand Canonical Monte Carlo (GCMC) methodology at constant temperature (T) & pressure (P). The number of molecular entities *N* is preserved throughout each

simulation cycle. It is frequently referred to as an NPT ensemble [5] but in this instance, with a stepwise increment of single species to a maximum defined population. The initial periodic cell dimensions were therefore permitted to be optimized at each molecular addition, in shape and size.

The concept of employing the Grand Canonical ensemble in this study, was based on the capability to simulate realistic inter- and intra-molecular interactions in a defined chemical environment, as opposed to merely consider **single molecular moieties.**

The following sequence presents the adjustment of force field parameters to support the $C\ell O_2$ species in empirical simulations.

5.2.2 Polymer Consistent Force-Field (pcff+) Parameterisation

5.2.2.1 Atom types

c - generic sp3 carbon

o - generic sp3 oxygen in alcohol, ether, or acid group

h - generic hydrogen

oh - oxygen bonded to hydrogen

ho - hydrogen bonded to oxygen

h* - hydrogen bonded to fluorine, nitrogen, oxygen

cl – chlorine atom

cl4 - chlorine in $C\ell O_4^-$ aniono_1r - oxygen in $C\ell O_4^-$ anion

p - general phosphorous atom

s2 -Sulphur in SO_2

o1 -oxygen in NO_2

Equivalence parameters

Equivalence parameters are presented in Table 5.1.

*Table-**5.1**:* Equivalence Parameters

Type	Non-Bond	Bond	Angle	Torsion	OOP	Force field Reference
cl4	cl4	cl4	cl4	cl4	cl4	cvff file
o_1r	o_1r	o_1r	o_1r	o_1r	o_1r	cvff file
oh	oh	oh	oh	oh	oh	This work
ho	ho	ho	ho	ho	ho	This work
h*	h*	h*	h*	h*	h*	This work

5.2.2.2 Bond Increments parameters

Bond increments describe the charge distribution formed during the bonding of two atoms. The assignment of the atomic charges of a molecule into bond increments, creates a set of general rules, based on the type of atoms in the bond [6].

I and J are the atom types of the bonded atoms [8]. Delta IJ and Delta JI (presented as partial atomic charges measured in elementary charge unit e) refers to the change in atomic charges depending on the direction of the charge i.e., I to J or from J to I [8].

Bond increments parameters are presented in Table 5.2.

*Table-**5.2**:* Bond Increment Parameters

I	J	Delta-IJ	Delta-JI	Force field reference
cl4	o_1r	0.3864	-0.6364	pcff file
cl	o	0.3864	-0.6364	This work
h*	o	0.4100	-0.4100	pcff file
cl	o_1r	0.3864	-0.6364	This work

Entries for bond increments: **cl [o]** and **cl [o_1r]** constants have been borrowed from the *cvff* force field set for: **cl4 [o_1r].** No other constants have been published to support this study. Bond lengths for **cl [o]** = 1.7 Å, **cl4 [o_1r]** = 1.4 Å and **cl [o_1r]** = 1.6 Å [7].

5.2.2.3 Quartic bond parameters

The quartic bond-stretching potential is presented by:

$$E = K2 * (R - R0)^2 + K3 * (R - R0)^3 + K4 * (R - R0)^4$$

Where:

R is the current bond length and R_0 the reference bond length in angstroms.

K_2, K_3 and K_4 are the coefficients for the quadratic, cubic and quartic terms in units of kcal/mol $Å^{-2}$, kcal $mol^{-}Å^{-3}$ and kcal/mol $Å^{-4}$ respectively.

I and *J* are the atom types of the bonded atoms [8].

Quartic bond parameters are presented in Table 5.3.

*Table-**5.3**:* Quartic Bond Parameters

I	J	R 0	K2	K3	K4	Force field Reference
cl	o	1.6500	307.0632	0.0	0.0	cvff file
h	o	0.9600	493.8480	0.0	0.0	cvff file
cl4	o_1r	1,4523	419.3650	-838.7299	978.5182	cvff file
cl	o_1r	1.679	419.3650	-838.7299	978.5182	This work
cl4	oh	1.641	419.3650	-838.7299	978.5182	This work
o	o	1.2080	833.6868	0,.00	0.00	cvff file
o	o_1r	1.3603	833.6868	0,.00	0.00	This work
o_1r	o_1r	1.3227	833.6868	0,.00	0.00	This work

- Entries for the: **cl [o_1r]** and **cl4 [oh]** constants have been extracted from the **cl4 [o_1r]** entry in *pcff*+. The relevant bond lengths (R0) were obtained from literature [7].
- Entries for the: **o [o_1r]** and **o_1r [o_1r]** constants have been extracted from the o - o entry in *pcff*+. The relevant bond lengths (R0) were obtained from literature [9].

5.2.2.4 Quartic bond angle parameters

The quartic angle is defined as follows in *pcff*+:

$\triangle = \boldsymbol{\theta} - \boldsymbol{\theta_0}$

$E = K2 * \triangle^2 + K3 * \triangle^4$

$\triangle^3 + K4 * \triangle^4$

Where:

$\triangle$ is used to represent Delta, the changed angle value

$\boldsymbol{\theta_0}$ is the equilibrium value of the angle.

Theta (θ) is the current bond angle, Theta0 (θ_0) is the reference bond angle in degrees.

The usual half factor is included in K [10].

K_2, K_3 *and* K_4 are quadratic force constants in units of: kcal/mol rad^{-2}.

I,J,K are the atom types involved in the angle.

Quartic angle parameters are presented in Table 5.4.

*Table-**5.4**:* Quartic Angle Parameters

I	J	K	Theta0	K2	K3	K4	Force field reference
o1=	s2=	o1=	119.300	115.2627	-35.6278	-26.1261	cvff file
o	cl	o	115.400	115.2627	-35.6278	-26.1261	This work
*	p	*	109.5000	45.0000	0.0	0.0	pcff file
o	cl	oh	109.5000	45.0000	0.0	0.0	This work
*	o	*	109.5	60.000	0.0	0.0	pcff file
cl	o_1r	cl4	111,9	60.000	0.0	0.0	This work
cl4	o_1r	o_1r	110,3	60.000	0.0	0.0	This work
cl4	o_1r	o	110.4700	60.000	0.0	0.0	This work
cl	o	o_1r	111,74	60.000	0.0	0.0	This work
cl4	o_1r	cl4	119,11	60.000	0.0	0.0	This work
cl4	oh	ho	105	60.000	0.0	0.0	This work
o_1r	cl4	o_1r	112.2363	108.1226	-24.1496	-23.3346	pcff file
o_1r	cl4	oh	104,2	108.1226	-24.1496	-23.3346	This work
o	cl	o_1r	104,6	108.1226	-24.1496	-23.3346	This work

- Constants from the SO_2 (*cvff* file entry) were borrowed for the **o-cl-o** quartic angle and was found to be an appropriate chemical fit for CℓO species.
- The actual quartic angle from literature [7] was substituted for Theta0.

  Constants and Theta0 from the * [p] * entry were borrowed for the **o – cl - oh** quartic angle.

  cl was substituted for ‘p’. ‘o’ and ‘oh’ were substituted for *.

  Constants from the * [o] * entry were borrowed for the following quartic angle entries:
- cl [o_1r] cl4 o_1r was substituted for ‘o’. cl and cl4 were substituted for *
- cl4 [o_1r] cl4 o_1r was substituted for ‘o’. cl4 and cl4 were substituted for *
- cl4 [o_1r] o_1r o_1r was substituted for ‘o’. cl4 and o_1r were substituted for *
- cl4 [o_1r] o o_1r was substituted for ‘o’. cl4 and o were substituted for *
- cl [o] o-1r cl and o_1r were substituted for *
- cl [oh] ho oh was substituted for ‘o’. cl was substituted for *
- cl [o_1r] cl4: The quartic angle for cl - o – cl bond was extracted from literature [7] and was substituted for $\boldsymbol{\theta_0}$
- cl4 [o_1r] o_1r: The quartic angle for cl - o – o bond was extracted from literature [11] and was substituted for $\boldsymbol{\theta_0}$
- cl4 [o_1r] o: The quartic angle for cl - o – o bond was extracted from literature [9] and was substituted for $\boldsymbol{\theta_0}$

- cl [o] o-1r: The quartic angle for cl - o – o bond was extracted from literature [9] and was substituted for $\boldsymbol{\theta}_0$
- cl [oh] ho: The quartic angle for cl -o – h bond was extracted from literature [7] and was substituted for $\boldsymbol{\theta}_0$

Constants from the o_1r [cl4] o_1r entry were borrowed for the following Quartic angles:

a) o [1r – cl4] oh ! oh was substituted for 'o_1r'
b) o [cl] o_1r ! o was substituted for 'o_1r'
c) o_1r [cl4] oh ! Quartic angle, from literature [11] and was substituted for $\boldsymbol{\theta}_0$
d) o [cl – o] 1r ! Quartic angle was extracted from literature [9] was substituted for $\boldsymbol{\theta}_0$

5.2.2.5 Wilson out of plane parameters

The Wilson out-of-plane potential is defined according to the angle between one bond from the central atom and the plane defined by the other two bonds [8]. The format of the out-of-plane potential (Wilson definition) section is:

$$E = K * (Chi - Chi0)^2$$

Where:

I,J,K and l are the atom types of the four atoms involved in the out-of-plane term.

J being the central atom: Chi (χ_0) is the reference angle in degrees [8].

Wilson out of plane parameter are presented in Table 5.5.

*Table-**5.5***: Wilson out of Plane Parameters

I	J	K	L	K-Chi	Chi0	Force field Reference
*	p	*	*	0.000	0.000	cvff file
o	cl	o	o	0.000	0.000	This work
o	cl	o	oh	0.000	0.000	This work
o	cl	o	h	0.000	0.000	This work
o	cl	o	cl	0.000	0.000	This work
cl4	o_1r	o_1r	cl4	0.000	0.000	This work
o_1r	cl4	o_1r	cl4	0.000	0.000	This work
cl	o	o_1r	cl4	0.000	0.000	This work

The constants from entry *** -p- * - *** were used for all Wilson out of plane entries, **cl** was substituted for **p.** The relevant atoms were substituted for *.

5.2.2.6 Torsion parameters

The three-term cosine expansion of the torsion potential is:

$$E = \sum(n=1,3)\ \{V(n) * [\ 1 - \cos\ (n*Phi - Phi0(n))\ ]\}$$

Where:

V_1, V_2 and V_3 are the barrier heights in kcal/mol

Phi (ϕ) is the current torsion angle.

ϕ_{01}, ϕ_{02} and ϕ_{03} are the reference torsion angles in degrees.

(The reference angles are usually 0° or 180°)

(The atoms are bonded to each other in the order *I-J-K-L)* [10].

Torsion parameters are presented in Table 5.6.

*Table-**5.6**:* Torsion Parameters

I	J	K	L	V(1)	Phi1(0)	V(2)	Phi2(0)	V(3)	Phi3(0)	Force field Reference
*	c	o	*	0	0	0	0	0.13	0	cvff file
o	cl	o	o	0	0	0	0	0.13	0	This work
o	cl	o	h	0	0	0	0	0.13	0	This work
o	cl	oh	ho	0	0	0	0	0.13	0	This work
o_1r	cl4	o_1r	cl	0	0	0	0	0.13	0	This work
o_1r	cl4	o_1r	cl4	0	0	0	0	0.13	0	This work
o_1r	cl4	o_1r	o	0	0	0	0	0.13	0	This work
o_1r	cl4	oh	ho	0	0	0	0	0.13	0	This work
o	cl	o_1r	cl4	0	0	0	0	0.13	0	This work
o	cl	o	oh	0	0	0	0	0.13	0	This work
o	cl	oh	o	0	0	0	0	0.13	0	This work
o	cl	o	cl	0	0	0	0	0.13	0	This work
o	cl	o	o_1r	0	0	0	0	0.13	0	This work
o_1r	cl4	o_1r	o_1r	0	0	0	0	0.13	0	This work
*	o	o	*	0	0	0	0	1	0	cvff file
cl4	o_1r	o_1r	cl4	0	0	0	0	1	0	This work
cl	o	o_1r	cl4	0	0	0	0	1	0	This work

The constants from *** - cl – o - *** and *** - o – o - *** in *pcff+* were used for torsion entries derived for the chlorine species.

5.3 Heats of Formation

5.3.1 Ensemble Models -- Potential Energy of Chlorine Species

GEMC Simulations were undertaken for all neutral and radical species, assuming that a good approximation of molecular geometries has been achieved, irrespective of the uneven electron population for radicals. The potential energy (Ui) for each ensemble model was determined at each step of addition of molecular units, followed by a dynamic step and the minimized energy extracted.

A typical GIBBS (GEMC) energy profile for Cl_2O_2 is graphically presented in Figure-**5.1** to demonstrate the effective inflection point, when the interaction of a sufficient number of molecules have reached a global equilibrium.

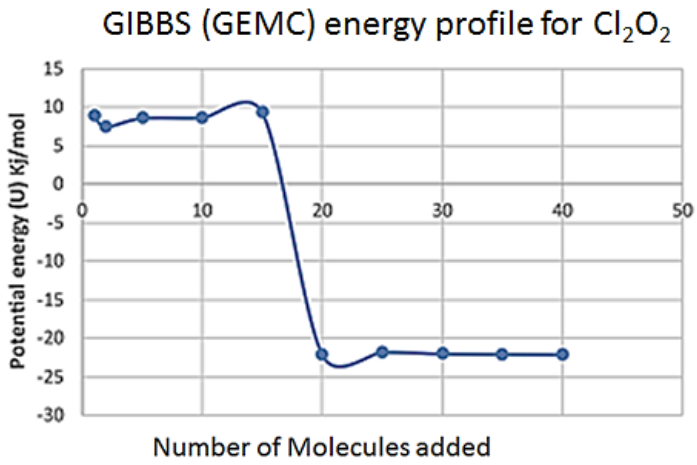

*Figure-**5.1**:* GEMC Potential Energy profile for $C\ell_2O_2$

The model ensemble energies were recorded at:

a) The minimum point
b) Before the minimum point
c) Beyond the minimum Internal Energy

Neutral species structures were successfully computed under GEMC with the exception of $HC\ell O$, $HC\ell O_2$ and $HC\ell O_3$ due to lacking force field parameters.

It must further be noted that applying MOPAC Hamiltonians to describe an optimum model status, may differ with **single–molecular** models (in vacuum or periodic) and rely on optimum basis sets to effectively describe an **ensemble model.**

Table-**5.7** displays the *MOPAC* calculated ΔH_f energies for the ensemble models. Reference ΔH_f energies are listed as well. In cases where no reference ΔH_f was available, the more consistent energy obtained through different Hamiltonians was reported.

In Table-**5.7** the ensemble model energies noted as: “Model before minimum (U)”, “Model at minimum (U)” and “Model after minimum (U)” are shown. These are listed to demonstrate that a global minimum had been reached. Optimum ΔH_f energies from selected *MOPAC* Hamiltonians, are given in the last column.

*Table-**5.7**:* Heat of Formation of ensemble neutral models applying the seven Hamiltonians in MOPAC-2016

		HEAT OF FORMATION (kcal/mol)							ΔH_f (Calculated)		
Ensemble model Energy nodal points	Literature Ref. ΔH_f (kcal/mol)	AM1	MNDO	MNDOD	PM3	PM6	PM7	RM1	Model	Functional	ΔH_f (kcal/mol)
OCℓO before minimum (U)		151.31	218.44	72.68	47.97	83.88	83.49	91.26	Single Molecule		25.47
OCℓO at minimum (U)	24.36	92.06	104.09	20.13	-109.64	4.85	-13.7	-9.66		MNDOD	
OCℓO after minimum (U)		41.56	84.09	21.51	-64.49	34.29	-11.09	16.62	ensemble Model		**20.13**
CℓOOCℓ before minimum (U)		30.4	87.26	27.62	17.91	23.1	18.85	15.64	Single Molecule		33.69
CℓOOCℓ at minimum (U)	31.38	30.48	33.36	35.36	18.62	21.22	10.08	13.56		AM1	
CℓOOCℓ after minimum (U)		29.45	32.27	33.88	17.05	19.91	9.47	12.79	ensemble Model		**30.48**
CℓO before minimum (U)		31.05	35.85	18.98	5.81	21.61	15.6	7.23	Single Molecule	PM6	25.47
CℓO at minimum (U)	24.31	41.64	48.48	21.87	-24.47	5.73	8.18	11.66			
CℓO after minimum (U)		34.26	50.35	22.81	-14.95	15.34	6.35	9.14	ensemble Model	MNDOD	**21.87**
CℓOCℓO_2 before minimum (U)		154.97	215.95	55.61	-74.72	26.31	32.35	51.75	Single Molecule		37.59
CℓOCℓO_2 at minimum (U)	37.4	144.69	215.39	39.25	-167.11	-13.23	-23.35	6.34		MNDOD	
CℓOCℓO_2 after minimum (U)		143.07	214.92	40.16	-187.73	-17.67	-27.37	9.65	ensemble Model		**39.25**
CℓO_2-O-CℓO_2 before minimum (U)		284.64	398.04	40.83	-198.48	18.06	22.26	50.42	Single Molecule		50.55
CℓO_2-O-CℓO_2 at minimum (U)	N/R	268.89	400.56	27.67	-381.76	-53.16	-75.27	-2.92		RM1	
CℓO_2-O-CℓO_2 after minimum (U)		268.36	396.55	27.17	-392.01	-64.15	-79.88	-6.2	ensemble Model		**50.42**

*Table-**5.7*** Continued

Ensemble model. Energy nodal points	Literature Ref. ΔH_f (kcal/mol)	HEAT OF FORMATION (kcal/mol) AM1	MNDO	MNDOD	PM3	PM6	PM7	RM1	ΔH_f (Calculated) Model	Functional	ΔH_f (kcal/mol)
$C\ell O_2$-O-O-$C\ell O_2$ before minimum (U)		111.44	197.15	40.35	-72.25	31.78	36.10	52.88	single molecule	RM1	79.42
$C\ell O_2$-O-O-$C\ell O_2$ at minimum (U)	N/R	104.97	150.25	37.26	-163.38	-4.55	-9.21	23.46			
$C\ell O_2$-O-O-$C\ell O_2$ after minimum (U)		102.55	153.47	36.89	-158.55	-4.99	-8.56	25.31	ensemble model	AM1	**104.97**
$C\ell OOC\ell O_3$ before minimum (U)		193.21	236.12	73.95	-199.46	48.78	65.84	129.36	single molecule		73.84
$C\ell OOC\ell O_3$ at minimum (U)	69.00	171.61	252.84	83.87	-371.14	53.66	10.89	11.96		PM7	
$C\ell OOC\ell O_3$ after minimum (U)		158.03	249.98	84.47	-359.16	47.16	55.19	27.74	ensemble model		**65.84**
$C\ell O_2$-O-$C\ell O_3$ before minimum (U)		276.34	347.19	87.40	13.02	67.15	58.41	156.56	single molecule	MNDOD	47.01
$C\ell O_2$-O-$C\ell O_3$ at minimum (U)	72.4	284.29	358.71	92.12	12.30	67.28	60.18	157.11			
$C\ell O_2$-O-$C\ell O_3$ after minimum (U)		283.84	357.55	92.37	10.85	67.22	59.65	157.25	ensemble model	PM6	**67.28**
$C\ell O_3$-O-$C\ell O_3$ before minimum (U)		135.89	261.66	56.45	-260.12	78.94	83.52	33.03	single molecule		77.47
$C\ell O_3$-O-$C\ell O_3$ at minimum (U)	82.6	150.33	261.66	91.78	-310.25	33.56	-5.52	53.61		PM6	
$C\ell O_3$-O-$C\ell O_3$ after minimum (U)		160.17	261.66	65.69	-324.62	34.88	-8.48	49.11	ensemble model		**78.94**
$C\ell C\ell O$ before minimum (U)		55.88	78.87	50.01	18.98	44.74	38.43	34.93	single molecule	MNDOD	28.63
$C\ell C\ell O$ at minimum (U)	31.84	55.44	83.91	54.73	18.64	43.58	34.08	34.41			
$C\ell C\ell O$ after minimum (U)		56.58	82.00	52.48	19.28	44.85	36.56	35.28	ensemble model	RM1	**34.41**
$C\ell OO$ before minimum (U)		5.56	20.78	23.28	12.02	0.74	7.36	0.60	single molecule		23.28
$C\ell OO$ at minimum (U)	24.56	33.71	50.53	28.26	18.95	21.89	15.91	0.40		MNDOD	
$C\ell OO$ after minimum (U)		5.19	24.18	28.52	13.57	-4.44	-5	-36.79	ensemble model		**28.26**
$HOC\ell$ before minimum (U)		-13.71	3.25	0.03	-31.1	-27	-28.18	-20.71	single molecule		-17.81
$HOC\ell$ at minimum (U)	-18.36	-16.57	-0.39	-3.40	-32.76	-18.56	-31.99	-22.44		PM6	
$HOC\ell$ after minimum (U)		-16.19	1.49	-0.44	-32.09	-17.51	-31.19	-21.68	ensemble model		**-18.56**

*Table-**5.7*** Continued

Ensemble model Energy nodal points	Literature Ref. ΔH_f (kcal/mol)	HEATS of FORMATION (kcal/mol)							ΔH_f (calculated)		
		AM1	MNDO	MNDOD	PM3	PM6	PM7	RM1	Model	Functional	ΔH_f (kcal/mol)
HOCℓO before minimum (U)		50.01	75.94	11.18	-10.42	21.31	14.43	29.56	single molecule		6.77
HOCℓO at minimum (U)	4.94	52.05	85.54	23.18	-11.19	18.9	6.49	28.78		PM7	
HOCℓO after minimum (U)		52.44	86.12	25.76	-7.95	22.08	8.52	30.63	ensemble model		**6.49**
HOCℓO_3 before minimum (U)		220.98	281.3	1.17	-126.05	-9.49	-25.44	28.42	single molecule		3.71
HOCℓO_3 at minimum (U)	0.43	28.42	282.58	3.17	-143.86	-16.06	-30.61	26.02		MNDOD	
HOCℓO_3 after minimum (U)		81.54	287.76	3.17	-110.97	-11.02	-36.04	73.5	ensemble model		**3.17**
HOCℓO_2 before minimum (U)		146.79	193.2	-2.82	-14.77	44.4	-10.18	98.57	single molecule		-3.27
HOCℓO_2 at minimum (U)	1.1	144.9	198.6	-11.67	-11.25	46.15	-66.3	99.02		MNDOD	
HOCℓO_2 after minimum (U)		141.66	195.54	-11.32	-22.53	38.45	42.84	93.79	ensemble model		**-2.82**
HOOCℓO_2 before minimum (U)		29.78	174.26	16.04	-163.7	-8.4	100.99	5.64	single molecule	PM6	19.25
HOOCℓO_2 at minimum (U)	16.56	63.52	175.04	19.33	-179.74	-18.81	-29.29	1.17			
HOOCℓO_2 after minimum (U)		35.75	174.91	18.63	-183.26	-22.65	-33.78	3.22	ensemble model	MNDOD	**19.33**
HOOCℓ before minimum (U)		-0.88	0.91	3.94	-18.27	-1.6	-5.07	-9.32	single molecule	RM1	-0.68
HOOCℓ at minimum (U)	-0.32	-3.56	3.94	4.65	-19.01	-4.83	-17.56	-23.33			
HOOCℓ after minimum (U)		-4.1	5.19	6.28	-19.04	-5.73	-18.4	-21.61	ensemble model	AM1	**-3.56**

*Table-**5.7*** Continued

Ensemble model Energy nodal points	Literature Ref. ΔH_f (kcal/mol)	AM1	MNDO	MNDOD	PM3	PM6	PM7	RM1	Model	Functional	ΔH_f (kcal/mol)
			HEATS of FORMATION (kcal/mol)						ΔH_f (calculated)		
HOOOCℓ before minimum (U)		14.5	15.02	12.55	-4.73	7.89	3.70	1.12	single molecule	MNDOD	11.88
HOOOCℓ at minimum (U)	10.11	10.68	19.89	21.80	-4.49	1.75	-9.77	-5.37			
HOOOCℓ after minimum (U)		10.9	20.15	22.84	-5.34	0.85	-10.46	-9.51	ensemble model	AM1	**10.68**
$C\ell O_3$-O-O-$C\ell O_3$ before minimum (U)		428.47	514.59	132.79	75.26	116.31	107.13	225.37	single molecule	MNDOD	108.37
$C\ell O_3$-O-O-$C\ell O_3$ at minimum (U)	111.40	430.80	519.64	126.35	66.72	107.45	100.03	223.79			
$C\ell O_3$-O-O-$C\ell O_3$ after minimum (U)		432.53	522.22	130.02	68.53	109.60	102.64	223.43	ensemble model	PM6	**107.45**
CℓOCℓ before minimum (U)		19.52	31.39	16.29	-16.12	8.63	4.78	9.91	single molecule		19.45
CℓOCℓ at minimum (U)	18.64	19.73	37.35	29.9	-14.13	7.79	-5.91	-8.92		AM1	
CℓOCℓ after minimum (U)		19.48	36.6	29.55	-14.16	6.47	-6.05	-12.53	ensemble model		**19.73**
CℓOCℓO before minimum (U)		40.67	58.77	18.76	-1.73	19.57	16.76	20.2	single molecule	PM6	38.19
CℓOCℓO at minimum (U)	39.77	38.48	60.19	23.07	-39.03	4.78	4.16	8.12			
CℓOCℓO after minimum (U)		37.77	59.33	21.97	-21.21	6.25	4.03	9.06	ensemble model	AM1	**38.48**

*Table-**5.7*** Continued

Ensemble model. Energy nodal points	Literature Ref. ΔH_f (kcal/mol)	HEAT OF FORMATION (kcal/mol) AM1	MNDO	MNDOD	PM3	PM6	PM7	RM1	ΔH_f (Calculated) Model	Functional	ΔH_f (kcal/mol)
CℓOOO before minimum (U)		42.65	46.29	41.71	3.83	8.47	12.92	32.68	single molecule	MNDO	45.51
CℓOOO at minimum (U)	53.32	41.35	48.32	50	6.86	2.21	1.56	7.88			
CℓOOO after minimum (U)		41.93	71.23	70.42	18.06	40.91	28.27	26.19	ensemble model	MNDOD	**50**
OCℓCℓO_2 before minimum (U)		127.51	243.82	83.73	-83.46	43.96	97.34	49.71	single molecule	RM1	50.13
OCℓCℓO_2 at minimum (U)	46.2	110.92	245.76	52.86	-187.61	-8.77	-13.24	2.74			
OCℓCℓO_2 after minimum (U)		142.52	226.62	52.67	-184.16	-6.96	-24.39	10.67	ensemble model	MNDOD	**52.86**
CℓOCℓO_3 before minimum (U)		211.01	262.07	58.84	7.15	37.93	29.62	106.24	single molecule	PM7	49.49
CℓOCℓO_3 at minimum (U)	37.4	211.78	261.91	61.21	8.08	39	30.43	107.32			
CℓOCℓO_3 after minimum (U)		212.09	263.52	61.86	8.75	39.43	31.15	107.58	ensemble model	PM6	**39**
CℓO_2CℓO_2 before minimum (U)		132.01	166.67	51.62	-46.3	22.6	21.51	60.74	single molecule	RM1	68.02
CℓO_2CℓO_2 at minimum (U)	N/R	66.55	145.42	104.12	-117.22	-8.09	-11.98	11.84			
CℓO_2CℓO_2 after minimum (U)		68.11	154.04	24.57	-113.87	-9.69	-11.87	106.43	ensemble model	AM1	**66.55**
CℓO_4 before minimum (U)		233.59	237.17	35.74	-87.59	70.83	61.15	147.87	single molecule	PM3	46.14
CℓO_4 at minimum (U)	57.6	227.73	243.25	77.65	-99.56	64.97	48.92	125.1			
CℓO_4 after minimum (U)		228.67	244.04	78.66	-95.81	114.7	48.23	120.66	ensemble model	PM7	**48.92**
CℓO_3 before minimum (U)		153.68	154.08	38.84	-23.37	48.62	53.19	81.31	single molecule	PM6	39.31
CℓO_3 at minimum (U)	44	99.55	216.84	20.17	-166.07	1.04	-16.84	41.52			
CℓO_3 after minimum (U)		151.65	164.93	27.25	-136.88	-4.2	-16.94	50.98	ensemble model	RM1	**41.52**

Optimum GEMC **ensemble** models extracted at the energy intervals outlined above, were subjected to *MOPAC-2016* computation to determine the ΔH_f Heats of Formation.

ΔH_f energies for **ensemble** models and **single** species using *MOPAC* analysis for CℓOCℓ, CℓOCℓO, CℓOCℓO_2, HOCℓO_3, HOOCℓ, HOOCℓO, HOOCℓO_2 and HOOOCℓ produced similar results.

- The majority of the ensemble model analyses offered overall Heat of Formation values similar to reference values when compared to single species energies for: CℓOO, CℓCℓO, CℓOOO, CℓO_3, CℓOOCℓ, CℓOCℓO_3, CℓO_2-O-CℓO_3, OCℓOO, CℓO_3-O-CℓO_3, HOCℓO, HOCℓ, HOCℓO_2 and HOOOOCℓ
- A few single species i.e., CℓO, CℓCℓO_2, Cℓ(O)O_2, CℓO_4, CℓOOCℓO_3 and OCℓO were the exception, producing results that matched reference values more closely than ensemble models.

A summary of the single molecular and ensemble model *MOPAC-2016* Heats of Formation obtained from ensemble model simulations, are presented in Table-**5.8** below.

*Table-**5.8**:* Heat of Formation Derived from ensemble Model Space (GEMC Derived) Calculated with MOPAC-2016.

ensemble Models	ΔH_f (calculated)			
	MODEL Space	MOPAC Hamiltonian	ΔH_f (kcal/mol)	Literature Ref. ΔH_f (kcal/mol)
CℓO	single ensemble	PM6 MNDOD	25.47 21.87	24.31 [12]
CℓOO	single ensemble	MNDOD MNDO	23.28 24.18	24.56 [12]
CℓOCℓ	single ensemble	AM1 AM1	19.45 19.73	18.62 [12]
CℓCℓO	single ensemble	MNDOD RM1	28.64 34.41	31.84 [12]
CℓCℓO_2	single ensemble	PM6 MNDOD	28.96 22.34	29.16 [12]
CℓOOO	single ensemble	MNDO MNDOD	45.54 50.00	53.29 [12]

*Table-**5.8*** Continued

Ensemble Models	ΔH_f (calculated)			
	MODEL Space	MOPAC Hamiltonian	ΔH_f (kcal/mol)	Literature Ref. ΔH_f (kcal/mol)
Cℓ(O)O_2	single ensemble	MNDOD MNDOD	63.00 66.14	63.37 [12]
CℓO_3	single ensemble	PM6 RM1	39.31 41.52	44.30 [12]
CℓO_4	single ensemble	PM3 PM7	50.54 48.92	57.60 [12]
CℓOCℓO	single ensemble	PM6 AM1	38.19 38.48	41.80[12]
CℓOOCℓ	single ensemble	AM1 AM1	33,69 30.48	31.37 [13]
CℓOCℓO_2	single ensemble	MNDOD MNDOD	38.45 39.25	37.80 [14]
CℓOCℓO_3	single ensemble	PM7 PM6	49.52 39.00	37.40 [14]
CℓO_2CℓO_2	single ensemble	MNDOD AM1	103.16 66.55	Not reported
CℓO_2-O-CℓO_2	single ensemble	RM1 RM1	50.55 50.42	Not reported
CℓOOCℓO_3	single ensemble	PM7 PM7	69.23 65.84	69.00 [14]
CℓO_2-O-CℓO_3	single ensemble	MNDOD PM6	46.97 67.28	72.40 [15]
CℓO_3-O-CℓO_3	single ensemble	PM6 PM6	77.66 78.94	82.60 [15]
CℓO_2-O-O-CℓO_2	single ensemble	RM1 AM1	79.42 104.97	Not reported
CℓO_3-O-O-CℓO_3	single ensemble	PM6 PM6	108.37 107.45	111.40 [9] $^{\$}$
OCℓO	single ensemble	MNDOD MNDOD	25.47 20.13	24.36 [12]

*Table-**5.8*** Continued

Ensemble Models	ΔH_f (calculated)			
	MODEL Space	MOPAC Hamiltonian	ΔH_f (kcal/mol)	Literature Ref. ΔH_f (kcal/mol)
OCℓOO	single ensemble	PM6 MNDOD	26.69 53.73	54.3 [12]
OCℓCℓO_2	single ensemble	RM1 RM1	50.13 49.71	46.2 [14]
HOCℓ	single ensemble	PM6 PM6	-17.81 -18.56	-18.36 [12]
HOCℓO	single ensemble	PM7 PM7	0.22 6.49	4.94 [12]
HOCℓO_2	single ensemble	MNDOD MNDOD	-3.18 -2.82	-1.10 [12]
HOCℓO_3	single ensemble	MNDOD MNDOD	3.71 3.17	0.43 [12]
HOOCℓ	single ensemble	RM1 AM1	-0.68 -0.88	-0.32 [12]
HOOCℓO	single ensemble	RM1 MNDOD	22.05 22.7	21.54 [12]
OOCℓO_2	single ensemble	PM6 MNDOD	19.27 19.33	16.55 [12]
HOOOCℓ	single ensemble	MNDOD AM1	11.88 10.68	10.11 [12]
HOOOOCℓ	single ensemble	PM6 PM6	24.78 21.58	22.7 [14]

$ Indicates that the ΔH_f *(298K)* of CℓO_3-O-O-CℓO_3 is calculated from energies by Beltran et al. (1999) [9].

Ensemble models subjected to *MOPAC-2016* analyses consistently, produced acceptable results. Over 60 % producing acceptable results compared to energies obtained for their single molecule counterparts.

No reference ΔH_f energies for CℓO_2-O-CℓO_2 and CℓO_2-O-O-CℓO_2 were available from the Open Literature. Calculated values of 50.42 kcal/mol and 104.97 kcal/mol were assigned respectively for these ensemble analyses. These energies were consistently obtained, by applying a number of Hamiltonians (*MOPAC*) which produced similar results or a result closest in value to their single

molecules counterparts. The energy of the single molecule analysis was selected based on which Hamiltonian produced the most sterically correct structure.

5.3.2 GEMC Results

ΔH_f energies obtained applying the GEMC ensemble model approach, consistently produced results that matched reference values and should in general be applied to derive at effective chemical properties.

5.4 Conclusion

Application of the GEMC (GCMC) approach in calculation the Heats of Formation for this group of CℓO2 species has proven to be successful. But the technque relies on an appropriate set of force field parameters. Extending the molecular/compound description (even in vacuum space) validates the importance of a multiple molecular ensemble. In this study, the extraction of confirmed Heats of Formation proved invaluable. Extending the technique to other compounds and substances, cannot be claimed to offer the same result. It will however be beneficial in extending the force field tables to include parameters for ions and radicals, specifically for a selection of species supporting open shell electron configurations.

A Species-based level of thermodynamics can now be undertaken with confidence.

5.5 References

[1] H. Sun, "COMPASS: An ab Initio Force field Optimized for Condensed-Phase Applications. Overview with Details on Alkane and Benzene Compounds," The Journal of Physical Chemistry B, vol. 102, pp. 7338-7364, 1998.

[2] "Wednesday-ForceFields.pdf," [Online]Available: https://www.ks.uiuc.edu/Training/Workshop/SanFrancisco/lectures/Wednesday-ForceFields.pdf. [Accessed 23 August 2018].

[3] U. Burkert and N. L. Allinger, Molecular Mechanics, Washington DC: ACS Monograph 77, 1989.

[4] A. Z. Panagiotopoulos, "Direct determination of phase coexistence properties of fluids by Monte Carlo simulation in a new ensemble," Molecular Physics, vol. 61, no. 4, pp. 813-826, 1987, 61, 813.

[5] A. Kadoura, A. Salama, S. Sun and A. Sherik, "An NPT Monte Carlo Molecular Simulation-Based Approach to Investigate Solid-Vapor Equilibrium_ Application to Elemental Sulfur-H_2S System," Procedia Computer Science, vol. 18, p. 2109 – 2116, 2013.

[6] J. D. Yesselman, D. J. Price, J. L. Knight and C. L. Brooks III, "Match: An Atom- Typing Toolset for Molecular Mechanics," Journal of Computational Chemistry, vol. 33, no. 2, p. 189–202, 2012.

[7] B. Casper, H. Willner, H. S. Muller, H. G. Mack and H. Opperhammer, "Molecular Structures of Perchloric Acid and Halogen Perchlorates $ClOClO_3$ and $FOClO_3$," Journal Physical Chemistry, vol. 98, pp. 8339-8342, 1994.

[8] Micro-Star Int'l Co., Ltd, "CDiscovery Files: Molecular simulations," 26 September 1997. [Online] https://saf.bio.caltech.edu/hhmi_manuals/insight970/cdiscover9709/d_files.html. [Accessed 5 September 2019].

[9] A. Beltran and B. Andre, "Structure and Bonding of Chlorine Oxides and Peroxides: ClOx, ClOx- (x) 1-4), and Cl_2Ox (x) 1-8)," The Journal of Physical Chemistry A, vol. 103, pp. 3078-3088, 1998.

[10] LAMMPS ORG, "Lammps Manual," 2021 August 2021. [Online]. Available: https://docs.lammps.org. [Accessed 2021 September 6].

[11] A. D. Boese and J. M. L. Martin, "Anharmonic force fields of $HClO_4$ and Cl_2O_7," Journal of Molecular Structure, p. 780–781, 2006.

[12] B. Ruscic and D. H. Bross, "Active Thermochemical Tables (ATcT) Values Based on ver. 1.122r of the Thermochemical Network," 2021. [Online] Available: https://atct.anl.gov/Thermochemical 20Data/version 201.122r/index.php. [Accessed 4 June 2021].

[13] R. P. Thorn Jr, L. J. Stief and S. C. Kuo, R. B. Klemm, “Ionization Energy of Cl_2O and ClO, Appearance Energy of ClO+ (Cl_2O), and Heat of Formation of Cl_2O,” The Journal of Physical Chemistry, vol. 100, pp. 14178-14183, 1996.

[14] J. Clark and J. S. Francisco, “Study of the stability of Cl_2O_3 using ab initio methods,” The Journal of Physical Chemistry A, vol. 101, p. 7145, 1997.

[15] J. E. Sicre and C. J. Cobos, “Thermochemistry of the higher chlorine oxides ClO x (x ¼ 3, 4) and Cl_2O x(x ¼ 3–7),” Journal of Molecular Structure (Theochem) , vol. 620 , p. 215–226, 2003.

CHAPTER 6: BONDING CHARACTER OF CHLORINE OXIDE

6.1 Introduction

The CℓO group of species, exhibits a unique bonding combination of chlorine (a strong electronegative atom) with oxygen (a paramagnetic element). The atomic stoichiometry of having to consider these two elements in the construction of $C\ell O_2$ and its subspecies, including the isometric extension into larger sub-species with higher oxygen atom content, poses a complex bonding character to decipher. Effective atom electron potentials pose a further complication for quantum chemical analysis, with basis sets approximating (assumed) near acceptable structural geometries. The quantum chemical analyses undertaken, demonstrated a clear ability of the software systems applied (*Gaussian*, *MOPAC* and *VASP*), to produce promising results in structural geometries, and thermochemical properties which are agreement with available referenced values. This verification step helps one to carry out the species level water interactions outline in chapter 7 with confidence.

6.2 Variation in Heats of Formation

A selected few species are displayed in Table-**6.1** depicting their bond distances and atomic partial charges, demonstrating the intrinsic charge distributions in these complex compounds.

*Table-**6.1:*** Selected few species extracted, to demonstrate their varying partial charge distributions (Mulliken) and bonding character in relation to their molecular spin states. Atom connectivity is presented in parenthesis. (A species naming convention has been adopted to portray bond sequencing)

Species	Molecular Structure	Atomic Partial Charges	Spin State	Bond Distances (Å) (Atom Connectivity)
HOCℓO	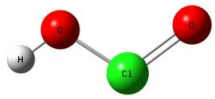	O1: -0.26 Cℓ: 0.34 O2: -0.33 H: 0.24	singlet	Cℓ-O1 = 1.51 Cℓ-O2 = 1.77 O2-H = 0.98 (O1-**Cℓ**-O2-H)
CℓOOCℓ		Cℓ1: 0.05 O1: -0.03 O2: -0.08 Cℓ2: 0.06	singlet	Cℓ1-**O1** = 1.82 **O1-O2** = **1.32** (Bridge) Cℓ2-**O2** = 1.82 (**Cℓ**-O1-O2-**Cℓ**)
HOOCℓO	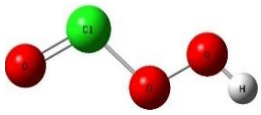	O3: -0.33 Cℓ: 0.53 O2: -0.22 O1: -0.32 H: 0.34	singlet	Cℓ-O3 = 1.51 Cℓ-O2 = 1.84 O2-O1 = 1.46 O1-H = 0.98 (O3-**Cℓ**-O2-O1-H)

Table-6.1 continued

Species	Molecular Structure	Atomic Partial Charges	Spin State	Bond Distances (Å) (Atom Connectivity)
HOOOCℓ	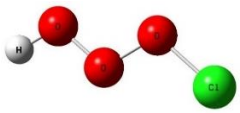	Cℓ: 0.1 O3: -0.09 O2: -0.07 O1: -0.27 H: 0.34	singlet	Cℓ-O3 = 1.81 **O3-O2** = **1.35** (Bridge) O2-O1 = 1.48 O1-H = 0.98 (O3-**Cℓ**-O2-O1-H)
HOOOOCℓ	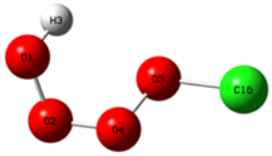	Cℓ: 0.24 O4: -0.25 O3: -0.021 O2: 0.022 O1: -0.54 H: 0.59	singlet (triplet)	Cℓ-O4 = 1.63 O4-O3 = 1.75 **O3-O2** = **1.26** (Bridge) O2-O1 = 1.57 O1-H = 0.98 (**Cℓ**-O4-O3-O2-O1-H)
$C\ell OOC\ell O_3$	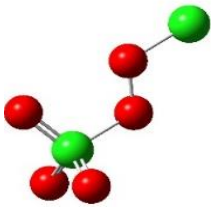	Cℓ1: 0.93 O1: -0.11 O2: -0.30 O3: -0.32 O4: -0.25 O5: 0.061 Cℓ2: -0.0056	singlet	Cℓ1-**O1** = 1.65 **O1-O2** = 1.44 (Bridge) Cℓ2-**O2** = 1.95 Cℓ2-O3 = 1.44 Cℓ2-O4 = 1.47 Cℓ2-O5 = 1.44 (**Cℓ1**-O1-O2-**Cℓ2**-O3{O4}{O5})
$C\ell O_3$-O-$C\ell O_3$	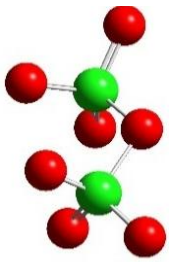	Cℓ1: 0.99 O1: -0.28 O2: -0.28 O3: -0.28 O4: -0.26 Cℓ2: -0.99 O5: -0.30 O6: -0.28 O7: -0.28	singlet	Cℓ1-O1 = 1.44 Cℓ1-O2 = 1.44 Cℓ1-O3 = 1.48 Cℓ1-**O4** = 1.90 Cℓ2-**O4** = 1.94 Cℓ2-O5 = 1.42 Cℓ2-O6 = 1.42 Cℓ2-O7 = 1.46 (**Cℓ1**-O1{O2}{O3}-**O4-Cℓ2**-O5{O6}{O7})
$C\ell O_2$-O-O-$C\ell O_2$	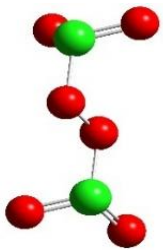	Cℓ1: 0.28 O1: -0.20 O2: -0.21 O3: 0.13 Cℓ2: 0.28 O4: 0.13 O5: -0.21 O6: -0.20	singlet	Cℓ1-O1 = 1.46 Cℓ1-O2 = 1.54 Cℓ1-**O3** = 1.97 **O3-O4** = 1.32.(Bridge) Cℓ2-**O4** = 1.97 Cℓ2-O5 = 1.46 Cℓ2-O6= 1.54 (O1{O2}-**Cℓ1-O3-O4-Cℓ2**{O5}O6)

*Table-**6.1*** continued

Species	Molecular Structure	Atomic Partial Charges	Spin State	Bond Distances (Å) (Atom Connectivity)
$C\ell O_3$-O-O-$C\ell O_3$	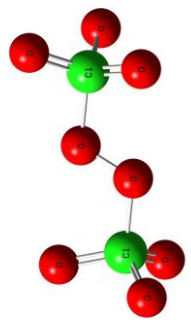	Cℓ1: 1.02 O1: -0.14 O5: -0.30 O6: -0.29 O7: -0.30 Cℓ2: 1.02 O2: -0.14 O8: -0.29 O9: -0.30 O10: -0.30	singlet	Cℓ1-O5 =1.37 Cℓ1-O6 =1.37 Cℓ1-O7 =1.374 Cℓ1-**O1** =1.64 **O1-O2** = 1.36 (Bridge) Cℓ2-**O2** =1.64 Cℓ2-O8 =1.37 Cℓ3-O9 =1.37 Cℓ4-O10 =1.37 (**Cℓ1**-O5{O6){O7}-**O1-O2-Cℓ2**-O8{O9}{O10})
$C\ell O_2$-O-$C\ell O_3$	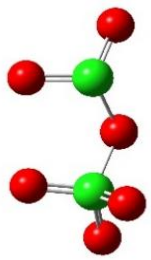	Cℓ1: 0.97 O1: -0.28 O2: -0.25 Cℓ2: 0.78 O3: -0.26 O4: -0.35 O5: -0.29 O6: -0.31	singlet	Cℓ1-O1 = 1.41 Cℓ1-O2 = 1.43 Cℓ1-**O3** = 1.82 Cℓ2-**O3** = 1.93 Cℓ2-O4 = 1.90 Cℓ2-O5 = 1.43 Cℓ2-O6 = 1.77 (**Cℓ1**-O1{O2}-**O3-Cℓ2**-O4{O5}{O6})
HCℓO		Cℓ: 0.41 O: -0.47 H: 0.064	singlet	Cℓ-O = 1.56 Cℓ-H = 1.32 (H-**Cℓ**-O)
$HC\ell O_2$	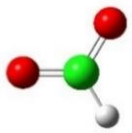	Cℓ: 0.32 O1: -0.46 O2: -0.46 H: 0.14	singlet	Cℓ-O1 = 1.47 Cℓ-O2 = 1.47 Cℓ-H = 1.36 (H-**Cℓ**-O1{O2})
$HC\ell O_3$	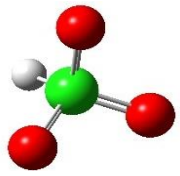	Cℓ1: -0.94 O1: -0.33 O2: -0.33 O3: -0.33 H: 0.058	singlet (doublet)	Cℓ-O1 = 1.42 Cℓ-O2 = 1.42 Cℓ-O3 = 1.42 Cℓ-H = 1.33 (H-**Cℓ**-O1{O2}{O3})

A comprehensive collection of partial charges derived for all chlorine oxide species in this study, can be found in Table-**A6** (APPENDIX).

The hydrogen terminated species, HOOOO**Cℓ**, HOOO**Cℓ**, HOO**Cℓ**O and HO**Cℓ**O all display varying atomic partial charges at the chlorine positions, ranging from **0.96 ε** to **0.07 ε** --- the larger partial charges observed for chlorine bounded by two oxygen atoms. This large variation can be ascribed to varying bonding character, adopted with the central and neighbouring oxygen atoms. The assignment of

two possible spin-states (singlet and triplet) for HOOOO**Cℓ,** can be tied to this vast variation in partial charge distribution. For HOOOO**Cℓ,** HOOO**Cℓ** and **Cℓ**OO**Cℓ** a bridging double bond is observed (1.26 Å, 1.35 Å and 1.32 Å respectively) between the central two oxygen atoms, clearing the one major paramagnetic contribution, leaving chlorine and/or oxygen atoms on either end, to share a bond in a closed shell condition (as a dative bond). This can result in either a triplet for HOOOO**Cℓ** or a singlet state, in which case a partial double-bond charge distribution has to be at play with the two atoms neighbouring the central double bond.

It is furthermore significant to observe the large partial charges (**0.97** and **0.86**) for the two chlorine atoms in the two structures (HO**Cℓ**O and HOO**Cℓ**O respectively) flanked on either side by oxygen atoms. The unique assignment of a singlet spin state for both these species, displaying a reduced bond distance of 1.51 Å (a typical Cℓ-O bond distance) between their terminal oxygen atoms and the chlorine atoms (considered as double bonds) may dictate the residual charge distribution on the inner oxygen atoms.

The complex construction of electron sharing and resulting bond character, is demonstrated in Table-**6.1** for these species and may be the reason for their vulnerability to dissociate in media such as water, imposing a dipole moment of 1.85 Debye, through dipole-dipole interaction and charge transfer. This large bond distance observed between oxygen, bonded to two chlorine atoms, noted as ‘bridge’ bonding is noticeable in all structures, clearly assigned to single bond character.

Figure-6.1 presents a composite graph of all Heats of Formation values derived. empirical construction of the ionic species, supported by force field structure conditioning, were not possible and these were calculated as single species entities. Varying spin conditions were applied in all cases, also considering different basis sets. Table-4.3 (chapter 4) lists the observed spin-states.
Singlet and doublet spin conditions were considered during the calculations.

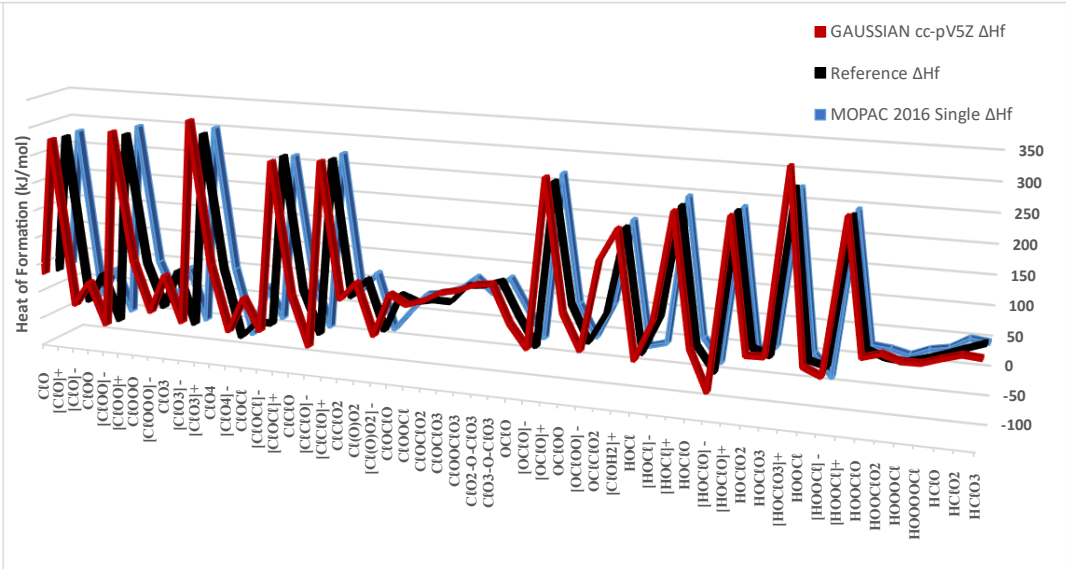

*Figure-**6.1**:* Composite graph presenting Heats of Formation for all species investigated

Two outlier results are observed for species: $[C\ell O_3]^+$ and $[OC\ell O]^+$ under the DFT/BLYP functional. It is apparent from Figure-6.1 that the higher-oxygen hosted species, show a lower Heat of Formation (mid-section of the graph). This is most probably as a result of the intricate paramagnetic character of oxygen (as bridging atom, with covalent character) distributed across a complex electronic delocalized bond structure.

Kosmas, A.M.; 2007 [1] found that multivalent bonding is usually characteristic of a strong ionic nature that influences thermodynamic stabilisation trends and the structural character of a molecule. Their research proposed that the relative and thermodynamic stability of various halogen molecules resulted from the combination of three factors:

- electrostatic nature of the halogen-oxygen fragments
- electronegativity of the halogen. In this study, we consider the electronegativity of chlorine and oxygen with assigned electronegativity of 3.16 and 3.44 respectively [1].
- degree of halogen valence in the formation of the hypervalent bonds

6.2.1 *Hypervalency of Halogen-O Species and Bonding Character*

When a Cℓ−O bond comprises of a terminal oxygen atom (signified as bivalent or trivalent terminal bonding in this study), the corresponding halogen atom is classified as hypervalent, since it contains an excess of eight electrons in the valence shell [2]. Lee et al. [2] found that the bonds between multivalent halogen atoms and terminal oxygen atoms undergo tightening of bond distances (shorter bond lengths). The larger halogen−O bond distances are characteristic for bonds where halogen and oxygen atoms are bridged (in these cases flanked by two chlorine atoms, imposing a dual influence of electronegativity [this work]) whilst the shortest halogen−O bond distances have been found to correspond to hypervalent structures [1]. This characterisation is prevalent in all species presented in Table-**6.1**. Considering

($C\ell OOC\ell O_3$) as Cℓ1-O1-O2-Cℓ2-O3{O4}{O5} which has two types of O-Cℓ bonds, i.e., a **bridged bond** between Cℓ2-O2 atoms at 1.95 Å, a bond distance of ±1.4 Å for the **terminal Cℓ2**-O3{O4}{O5} bonds and 1.65 Å between the single-valent bonded terminal **Cℓ1**-O1**.**

$HC\ell O$, $HC\ell O_2$ and $HC\ell O_3$ are hypervalent configurations [1] (solely due to their terminal oxygen atoms) whose instability is attributed to an electropositive charged hypervalent halogen (Table-**6.1**), being associated to the electropositive H-atom, which appears to affect the relative stability order and is attributed to the degree of valency on the halogen [1].

Lee et al.,[2] and suggested that the multi-valency of a halogen is due to one, two, or three lone-pair valence electrons achieving significant degrees of *d*-character, resulting in multiple pd-hybrid halogen bonds. He examined $C\ell XO_2$, and HXO type molecules (X = Cℓ) and found that these molecules undergo pd hybridization. This hybridization process entails *p* - *d* orbital promotion of lone-pair electrons. This imparts the hypervalent character to the chlorine molecule thereby allowing the formation of more than one bond thus increasing the electron count. This type of hypervalent bonding for a halogen is characterized by a large ionic component [2]. This large ionic component imparts high thermodynamic stability to $-XO_Z$, and HXO type molecules.

Lee et al., proved that "-XOz are very stable while the -XO species usually are less stable than the normal valent isomer -OX" (z = number of oxygen molecules and X = Cℓ) [2]. This change in stability in the *sp* hybridisation process occurs since the *d* shell becomes partially occupied which lowers its energy. This lower energy equates to more stability. This stability trend is clearly seen in the mid-section of the Figure-6.1 which represents $-XO_2$ type molecules such as $C\ell OOC\ell$, $C\ell O_2$-O-O-$C\ell O_2$, $C\ell O_2$-O-$C\ell O_3$ and the HXO type molecules such as $HOOC\ell O$, $HOOOC\ell$, $HOOOOC\ell$, $HC\ell O$, $HC\ell O_2$ and $HC\ell O_3$. The higher stability of the mentioned chlorine oxides is represented by the low Heats of Formation values.

Single Cℓ-O bonds are ionic (dative) in nature and as stated earlier, their thermodynamic stability is affected by various factors, one being electronegativity. Examination of the atomic charges of Cℓ in Cℓ=O bonds (Table-**6.1**) reveals that the poly-oxide species possess highly electropositive charged chlorine atoms. This electro-positivity indicates that these species are prone to chemical attack from radicals and most likely explains why the Cℓ=O bonds are easily broken and break up into small components becoming available for use in other chemical processes.

6.3 Conclusion

$C\ell O_2$ compounds and its associated sub-species display a peculiar bonding character. The combination of strong electronegativity (chlorine) in the presence (directly bonded) to elements with an unpaired electron configuration (oxygen) and in this case, enclosed into relatively small molecular structures, results in a complicated bonding arrangement. This is further demonstrated by the thermochemical instability of some of the species (indicated by their high Heat of Formation Figure-**6.1)** in forming excess amounts of O_2, $C\ell^-$, $C\ell_2$, $[C\ell O_2]^-$ and $[C\ell O_3]^-$ which ultimately, could play a major role in pathogen control.

6.4 References

[1] A. M. Kosmas, “Theoretical Investigation of Halogen-oxygen. Bonding and its Implications in Halogen Chemistry and Reactivity,” Bioinorganic Chemistry and Applications, vol. 2007, p. 9, 2007.

[2] T. J. Lee, C. E. Dateo and J. E. Rice, “An Analysis of Chlorine and Bromine Oxygen Bonding and Its Implications for Stratospheric Chemistry,” Molecular Physics, vol. 96, no. 4, p. 633–643, 1999.

CHAPTER 7: SPECIES BASED THERMODYNAMICS IN AQUEOUS MEDIUM

7.1 Objective

The ultimate objective was to demonstrate the optimum conditions for specific species identified, to persist in an aqueous medium, to play a role in pathogen control in water treatment.

- Extract the main chemical reaction schemes
- Identify the $C\ell O_2$ species behavior in an aqueous medium

7.2 Species-based Thermodynamics

FactSage is an amalgamation of two popular thermochemistry computational software packages namely: FACT-Win (formerly *F*A*C*T*) and *CHEMSAGE* (formerly *SOLGASMIX*) [1]. The initial programs were used to calculate thermochemical properties for pure substances and ideal gases. *FactSage* contains two types of thermochemical databases i.e.:

- A pure substances database
- A solution database

The "*Facility for the Analysis of Chemical Thermodynamics"* (FACT) solution databases is updated frequently via globally funded research programs [1].

The Gibbs energy minimisation module of *FactSage*, 'EQUILIB' which determines the concentration of compounds in an equilibrium state, was used to predict the sustainability of the studied chlorine species in aqueous medium at standard temperature and pressure All chlorine species (with confirmed and/or attainable Heats of Formation for 'unknowns') were added to the *FactSage* compound database. Selected thermochemical properties Cp, ΔH_f and S derived in this study by semi-empirical and *Ab Initio* supported techniques for single molecules (ensuring correlation with ensemble derived energies) were populated into the compound database. Each species was reacted with H_2O in a mole ratio of water: species of 1:1 and the resultant product species recorded. Resultant mole fractions for products, lower than 10^{-5} were discarded. The product species that resulted from reaction with H_2O is tabulated in the Appendix, Table-**A7**.

The following product species were found to be prevalent in most aqueous reactions: O_2, $[C\ell OH_2]^+$, $C\ell^-$, and $[C\ell O_4]^-$. These species persist in the aqueous environment and act as precursors for further chlorine oxide interactions.

7.3 Populating the *FactSage* Software Database

The *FactSage* database was populated with: *GIBBS* Free Energies, Heats of Formation and Heat Capacities, of all chlorine oxide species studied – listed in Table-**7.1**

NOTE:

The *FactSage* software (in its current status -- Sept. 2022) applying the *EQUILIB* module, does not support the option to invoke (select) ionic species, but will report on their contribution (prior populating the database via the *COMPOUND* Module).

This imposed a restriction on the analysis of comprehensive chlorine oxide and sub-species analyses, which prompted the alternative approach of exposing each individual (neutral) species to water, in a 1:1 mol ratio. A detailed list of a predominant species, resulting from interaction of single species with water analyses are listed in Table-**A7** (Appendix). This was used to derive at a comprehensive set of reaction schemes, in demonstrating the significant formation of specifically $\mathbf{O_2}$, $\mathbf{C\ell^-}$, $\mathbf{[C\ell O_2]^-}$, $\mathbf{[C\ell O_3]^-}$ as species known, to be involved in pathogen control.

The individual Free Energy of Formation ($\Delta \mathbf{G}_f$) of each species in aqueous medium could not be obtained with *FactSage*. *FactSage* provides the overall Free Energy of Formation of each species with water. Hence, the Standard Free Energy of Formation ($\Delta \mathbf{G}_f$) of each species was either:

- Obtained from literature.
- Calculated using A*b Initio* electronic structure results (*Gaussian-16)* as outlined by Ochterski, J W [2].

The *Gaussian-16* software does not offer $\Delta \mathbf{H}_f$ and $\Delta \mathbf{G}_f$ energies as a standard output property. A separate external $\Delta \mathbf{H}_f$ and $\Delta \mathbf{G}_f$ energies calculation was required. The calculation step was extracted from a publication by J. W. Ochterski [2] and the results presented in Table-**S7.**

*Table-**7.1**:* Calculated Gibbs Free Energies of Formation and Free Heat of Formation using values obtained with *Gaussian-16*

Species	ΔH_f (OK) (kcal/mol)	ΔH_f (298K) (kcal/mol)	ΔG_f (298K) (kcal/mol)
CℓO	29.77	29.715	22.07
$[C\ell O]^-$	-23.43	-23.46	-31.37
$[C\ell O]^+$	278.19	278.18	270.94
CℓOO	21.62	21.50	6.87
$[C\ell OO]^-$	-54.57	-54.75	-69.30
$[C\ell OO]^+$	300.13	299.79	284.57
CℓOCℓ	21.46	21.03	5.11
$[C\ell OC\ell]^-$	-34.99	-35.26	-50.19
$[C\ell OC\ell]^+$	269.53	269.03	253.32
CℓCℓO	35.05	34.64	19.18
$[C\ell C\ell O]^-$	-53.42	-54.10	-69.56
$[C\ell C\ell O]^+$	276.12	275.83	260.96
$C\ell C\ell O_2$	37.86	36.79	11.04
CℓOOO	68.41	67.8	43.48
$[C\ell OOO]^-$	-20.62	-21.94	-47.99
$C\ell(O)O_2$	69.75	69.46	46.56
$[C\ell(O)O_2]^-$	-20.62	-21.94	-47.99
$C\ell O_3$	49.16	47.79	21.47
$[C\ell O_3]^-$	-34.08	-35.31	-61.76
$[C\ell O_3]^+$	330.74	329.73	303.30
$C\ell O_4$	76.78	74.64	37.12
$[C\ell O_4]^-$	-40.15	-42.11	-79.79
CℓOCℓO	56.06	54.98	29.40
CℓOOCℓ	39.29	38.67	13.96
$C\ell OC\ell O_2$	50.56	48.83	12.93
$C\ell OC\ell O_3$	67.92	65.77	19.98
$C\ell O_2C\ell O_2$	73.08	69.78	21.80
$C\ell O_2$-O-$C\ell O_2$	84.34	81.21	24.39
$C\ell OOC\ell O_3$	75.18	72.17	15.45
$C\ell O_2$-O-$C\ell O_3$	89.75	85.25	16.03
$C\ell O_3$-O-$C\ell O_3$	93.30	89.64	13.61
$C\ell O_2$-O-O-$C\ell O_2$	107.20	104.17	37.96
$C\ell O_3$-O-O-$C\ell O_3$	124.17	118.45	28.50
$[C\ell O_3C\ell O_3]^{-2}$	110.20	105.74	36.14

Species	ΔH_f (OK) (kcal/mol)	ΔH_f (298K) (kcal/mol)	ΔG_f (298K) (kcal/mol)
OCℓO	24.50	23.89	7.45
$[OC\ell O]^-$	-15.96	-16.30	-32.48
$[OC\ell O]^+$	278.90	278.24	261.31
OCℓOO	51.67	51.63	30.17
$[OC\ell OO]^-$	-8.70	-9.87	-33.85
$OC\ell C\ell O_2$	147.45	146.67	113.47
$[C\ell OH_2]^+$	204.09	202.38	179.42
HOCℓ	-15.73	-16.44	-31.02
$[HOC\ell]^-$	54.74	54.25	38.96
$[HOC\ell]^+$	239.76	239.06	224.84
HOCℓO	14.44	13.01	-11.04
$[HOC\ell O]^-$	-55.76	-57.33	-80.78
$[HOC\ell O]^+$	240.42	238.93	215.1
$HOC\ell O_2$	13.26	11.17	-23.15
$HOC\ell O_3$	14.84	12.13	-32.56
$[HOC\ell O_3]^+$	327.65	325.73	283.97
HOOCℓ	4.06	2.60	-21.57
$[HOOC\ell]^-$	-9.90	-10.60	-32.12
$[HOOC\ell]^+$	254.85	253.29	229.36
HOOCℓO	29.56	27.78	-5.72
$HOOC\ell O_2$	40.10	37.26	-7.35
HOOOCℓ	29.47	27.44	-6.50
HOOOOCℓ	30.21	28.18	-14.83
HCℓO	34.60	33.89	19.39
$HC\ell O_2$	49.88	48.30	23.82
$HC\ell O_3$	48.51	46.07	11.05
H_2O	-49.76	-50.44	-64.83
CO_2	-410.17	-410.02	-426.77
C_2H_6	144.51	140.65	85.19
OH^-(g)			-33.15 [3]
H^+			-6.28 [4]
HCℓ			69.90 [5]
$[HOO]^-$			369.50 [6]
$C\ell^-$			-131.20 [3]

7.4 *GIBBS* Free Energy of Reactions

In an attempt to verify the major species in an aqueous medium with chlorine oxides achieved with *FactSage*, a possible reaction scheme is presented in Figure-7.1. The evaluation of $C\ell O_2$ behaviour in an aqueous medium was considered. The Standard Free Energy of Formation of the individual species (Table-7.1) was used to determine the overall reaction *GIBBS* Free Energy of Formation of the participating reactions.

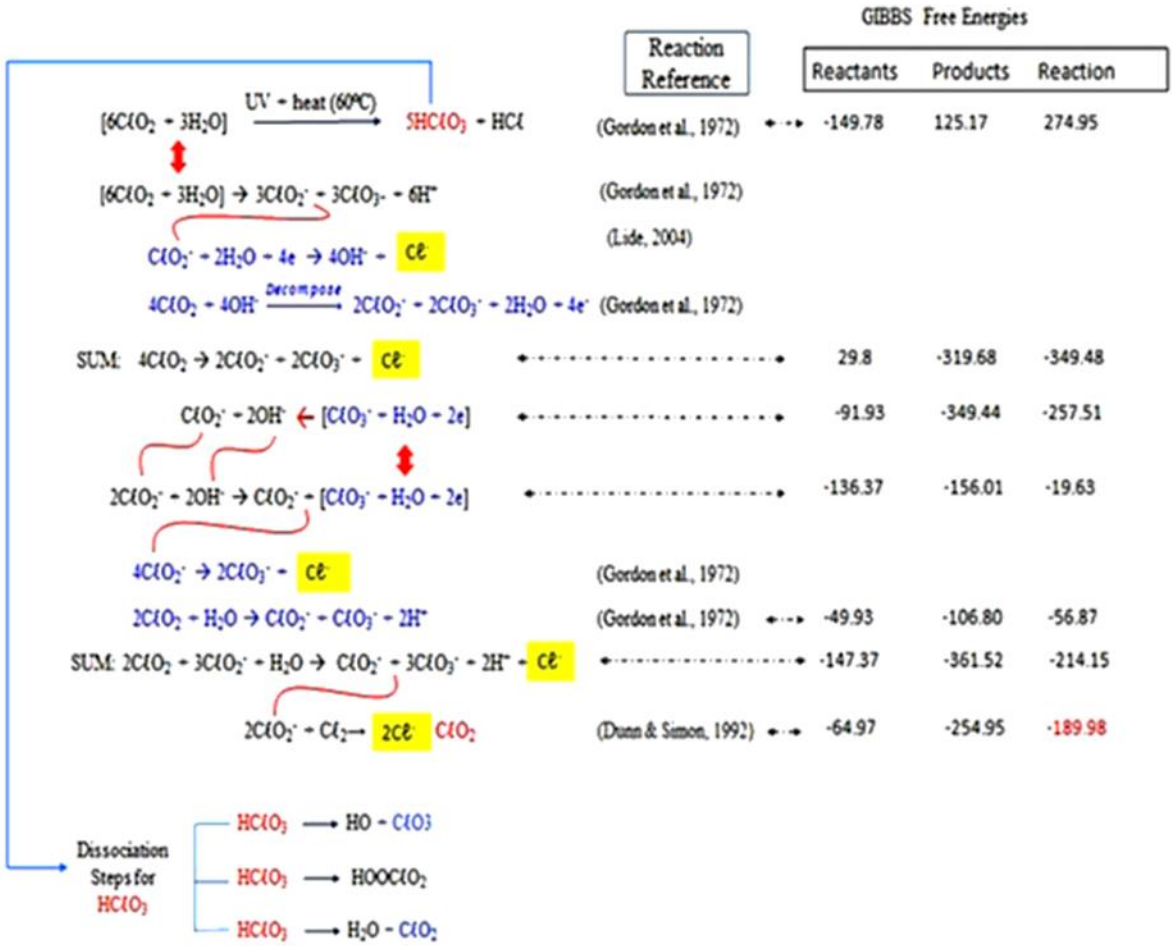

*Figure-**7.1**:* Sequence of the main reactions, some of their inter-dependencies and the distinct formation of $C\ell^-$, $[C\ell O_2]^-$ and $[C\ell O_3]^-$ in an aqueous medium
References [8,9,10] refer to the reaction sequences.

The reaction scheme considers the overall $C\ell O_2$ breakdown products released in an aqueous medium taking into consideration decomposition and dissociation reactions. Neutral and alkaline aqueous medium reaction were considered. The final reaction products of $C\ell^-$, $[C\ell O_2]^-$, $[C\ell O_3]^-$ verifies the major species identified by *FactSage* with the exception of O_2. The decomposition products of $C\ell O_2$ in sunlight is O_2 and $C\ell_2$ [7], however all major species identified are verified in the reaction scheme. The majority of reaction *GIBBS* Free Energies ($\triangle G_f$) reveal negative values, indicating that reactions are occurring spontaneously.

7.5 Conclusion

- Progressive partial regeneration of $C\ell O_2$ following consecutive reactions, with gradual depletion into other sub-species.
- The results obtained, identifies the following species: **O_2, $C\ell^-$, $[C\ell O_2]^-$, $[C\ell O_3]^-$** to be the main products in a large proportion of the reactions.
- This is further demonstrated by the thermochemical instability of some of the species (indicated by their high Heat of Formation values) in Chapter 6, Figure-**6.1** in forming excess amounts of O_2, $C\ell^-$, $C\ell_2$, $[C\ell O_2]^-$ and $[C\ell O_3]^-$ which in turn, could play a major role in pathogen control.
- It was observed (Appendix Table-**A7**) that all chlorine oxide species containing more than one chlorine atom (displaying lower Heats of Formation) resulted in the highest product components of: O_2 and $C\ell^-$ as basic precursors for further interactions.

7.6 References

[1] C. W. Bale, P. Chartrand, S. A. Degterov, G. Eriksson, K. Hack, R. B. Mahfoud, J. Melançon, A. D. Pelton and S. Petersen, “FactSage Thermochemical Software and Databases,” Computer Coupling of Phase Diagrams and Thermochemistry, vol. 26, no. 2, pp. 189-228, 2002.

[2] J. W. Ochterski, “Thermochemistry in Gaussian,” Gaussian Inc, 2 June 2000. [Online]. Available: www.gaussian.com. [Accessed 8 June 2019].

[3] M. W. Chase, Jr., “NIST-JANAF Thermochemical Tables,” American Chemical Society, American Institute of Physics for the National Institute of Standards and Technology, Washington, DC: New York, 1998.

[4] M. W. Palascak and G. C. Shields, “Accurate Experimental Values for the Free Energies of Hydration of H+, OH-, and H3O+,” Journal of Physical Chemistry A, vol. 108, pp. 3692-3694, 2004.

[5] J. W. Larson and T. B. McMahon, “Gas Phase Negative Ion Chemistry of Alkyl chloroformates,” Canadian Journal of Chemistry, vol. 62, p. 675, 1984.

[6] T. M. Ramond, S. J. Blanksby, S. Kato, V. M. Bierbaum, G. E. Davico, R. L. Schwartz and W. C. Lineberger, “Heat of Formation of the Hydroperoxyl Radical HOO via Negative Ion Studies,” Journal of Physical Chemistry A, vol. 106, no. 42, pp. 9641-9647, 2002.

[7] G. Gordon, "Is all Chlorine Dioxide Created Equal," Journal American Water Works Association, vol. 93, no. 4, p. 63–74, 2001.

[8] G.Gordon, R.G. Kieffer, D. H. Rosenblatt. The Chemistry Of Chlorine Dioxide. Progress in Inorganic Chemistry, John Wiley & Sons, Inc, 1972.

[9] Lide, D.R. CRC handbook of chemistry and physics, vol. 85, Florida, USA, CRC press, 2004.

[10] Dunn R.C. and Simon, J.D, “Excited-state photoreactions of chlorine dioxide in water.” Journal of the American Chemical Society, vol 114, no. 2, pp.4856-4860, 1992.

CHAPTER 8: CONCLUSION

8.1 Conclusion

This study was undertaken both as a theoretical and investigational computational approach. It exemplifies the core of this study in support of water purification treatment, applying $C\ell O_2$ as an oxidative agent.

The endeavour to create a *GIBBS* (GEMC) ensemble simulation environment (Chapter 5), has confirmed that acceptable thermochemical properties can be derived. This also offered optimum molecular geometries, in conjunction with subsequent minimization steps, applied during *Ab Initio* analysis – a joint approach. Not only can electronic properties be derived but Heat Capacity, Entropy and Free Energies as well. However, it is imperative for the GIBBS (GEMC) Canonical simulations to be supported by a proper set of force field parameters.

The ultimate objectives to identify the major species derived from $C\ell O_2$ through a computational approach have achieved all facets of:

a) optimum molecular geometries
b) deriving thermochemical properties
c) the ability to generate chemical reaction schemes.

The outcome of this work should lead to further studies in scaling these thermochemical observations into a finite element approach, to determine micro-scale physical interaction in quantifying macro-scale coagulation, in particular the interactions with fibrous material (NOM).

Considering the global water scarcity, this work will be useful, to understand the full benefits (health and economic) of $C\ell O_2$ in water purification processes, justifying its use in the water treatment industry.

8.2 Future work

A meso-scale investigation could utilize the results from this study, applied to various engineering initiatives to quantify the impact on inline treatment facilities.

a) Possible improvement in NOM removal upon the addition of $C\ell O_2$ as a pre-treatment agent was observed, which primed the investigation into the effects of $C\ell O_2$ species (as oxidant) have on aqueous NOM and coagulation [1], [2].
b) $C\ell O_2$ also appears to alter the chemical/physical state of dissolved and suspended solids, allowing for removal in a clarifier [1] [2]. These observations substantiate a probe into zeta-potential investigations of NOM particles once exposed to $C\ell O_2$.
c) A further study to identify the chemical species with the most appropriate ability to kill pathogens, is important and should be included in further studies. This implies an extensive quantum chemical resolution of the highest rate of charge transfer on an extreme model size,

between species and the environment. This can be accomplished through finite element analysis (an engineering feat), having the correct (meso-scale) charge dissipation of the large (molecular) model.

8.3 References

[1] E. M. Aieta and J. D. Berg, "A review of chlorine dioxide in drinking water treatment.," Journal of American Water Works Association, vol. 78, no. 6, pp. 62-72, 1986.

[2] P. Xie, Y. Chen, J. Ma, X. Zhang, J. Zou and Z. Wang, "A mini review of pre-oxidation to improve coagulation," Chemosphere, vol. 155, pp. 550-563, 2016.

APPENDIX

A4 - SUPPLEMENTARY DATA FOR CHAPTER 4

Tables-**A4-1** and **A4-2**: Calculation steps [7] to extract Heat of Formation, derived from *Gaussian*-16 applying **B3LYP** theory.

Table **A4-1:** Example of Heat of Formation calculation derived from molecular electronic energies, calculated with output from *Gaussian-16*

	OCℓO	O	Cℓ	H	Units
ε_0 (B3LYP)	-610.582863	-75.100483	-460.181573	-0.502428	Hartree
ε_{ZPE}	0.005783	0.000000	0.000000	0.000000	Hartree
E_tot	0.00894	0.001416	0.001416	0.001416	Hartree
H_corr	0.009884	0.002360	0.002360	0.002360	Hartree
G_corr	-0.019255	-0.013508	-0.013508	-0.010654	Hartree

Table-**A4-2**: Experimental enthalpies of formation of elements (kcal/mol) from JANAF tables [1]

Elements	ΔH_f(0K)	ΔH_f(298K)	ΔH_f(298K) - ΔH_f(0K)
H	51.63	52.64	1.01
O	58.99	60.03	1.04
Cℓ	28.59	29.69	1.10

a) First calculate ΔH_f (*M*, 0K) for each molecule: [2]

$$\Delta H_f\,(M, \mathbf{0K}) = \sum_{atoms} x\Delta H_f(X, 0K) - \sum D_0(M)$$

$$\Delta H_f\,(M, \mathbf{0K}) = \sum_{atoms} x\Delta H_f(X, 0K) - [\sum x\varepsilon_0(X) - \varepsilon_0(M) - \varepsilon_{ZPE}\,(M)]$$

$$= \sum_{atoms} x\Delta H_f(X, 0K) - [\mathbf{627.51} \sum x\varepsilon_0(X) - \varepsilon_0(M) - \varepsilon_{ZPE}\,(M)]$$

Where: *M* = Molecule

X = Elements which make up *M*

x = Number of atoms of *X* in *M*

$\sum D_0\,(M)$ = Atomization energy of the molecule

$\varepsilon_{ZPE}(M)$ = Zero Point energy of the species

ε_0(M) = Total energy of the species

H_corr = Thermal correction to Enthalpy

E_tot = Total electronic energy

G_corr = Correction to the Gibbs Free Energy

Multiply by 627.51 = Conversion (Hartree to kcal)

b) ΔH_f (M, 298K) for each molecule can be obtained as:

ΔH_f (M, **298K**) = $\Delta H_f(M, 0K) + [H°_M(298K) - H°_M(0K)]$

$- \sum_{atoms} x\,[H°x(298K) - H°x\,(0K)]$

c) Δ_f G°(M, 298K) is determined as:

$\Delta_f G°(298K) = \Delta H_f(298K) - 298.15[\sum S_{(X,\,298K)} - S_{(M,\,298K)}]$ [2]

$= \Delta H_f(298K) - 298.15[\sum S_{(X,\,298K)}$

– 627.51(H_corr**M** – G_corr**M**)/298.15] (Table-**A4.1**)

Elemental Entropies (cal/mol K):

$S_{(298K)}$ Cℓ = 39.481

$S_{(298K)}$ H = 27.418

$S_{(298K)}$ O = 38.494

$S_{(298K)}$ C = 37.787

d) *EXAMPLE* (OCℓO):

H_f (OCℓO, 0K) = (2*58.99 + 28.59) - ! Heats of Formation at 0K

627.51 * ! Conversion: Hartree to kcal/mol

[2(-75.1005) + (-460.1816) ! $\sum x\varepsilon_0(X)$

-(-610.583 + 0.005783)**]** ! $\varepsilon_0(M) - \varepsilon_{ZPE}(M)$ (Table-**A4.2**)

= 146.57 - **122.124**

= **24.45** kcal/mol

e) To calculate the ΔH_f (OCℓO, 298K):

ΔH_f (OCℓO, 298K) = **24.45** + 627.51 * [0.009884 - 0.005783] – (2*1.04 + 1.10)

= 24.45 + 2.57342 - 3.18

= **23.84** kcal/mol

f) ΔG_f (OCℓO, 298K) is determined as:

ΔG_f (OCℓO, 298K) = **23.84** - 298.15 [(2*38.494 + 39.481)/1000 ! Convert to kcal

– **627.51**(0.009884 – (-0.01926))/298.15] (Table-**A4.1**)

= **23.84** - 298.15 (0.116469 – 0.061338)

= **7.41** kcal/mol

A4.3 - Gaussian-16 Thermochemistry outputs

Electronic energies and derived molecular Heats of Formation of the sixty (60) chorine oxide species.

*Table **A-4.3**:* Gaussian DFT/B3LYP/cc-PV5Z output energies (Hartree) and associated Heats of Formation (kcal/mol)

Species	ε_0	ε_{ZPE}	E_tot	H_corr	G_corr	ΔH (OK)	ΔH (298K)	ΔG (298K)
O (cc-pv5z)	-75.045501	0	-0.00142	-0.00236	0.014952			
Cℓ (cc-pv5z)	-460.015052	0	-0.00142	-0.00236	0.015677			
H (cc-pv5z)	-0.50142	0	-0.00142	-0.00236	0.010654			
O (6-311++G(3df,2p)	-74.989847	0	0.001416	0.00236	-0.01351			
Cℓ (6-311++G(3df,2p)	-459.489755	0	0.001416	0.00236	-0.01392			
H (6-311++G(3df,2p)	-0.499995	0	0.001416	0.00236	-0.01568			
CℓO	-535.377	0.002787	0.005163	0.006107	-0.01876	29.77	29.715	22.07
$[CℓO]^-$	-535.461	0.001987	0.004407	0.005351	-0.01909	-23.43	-23.46	-31.37
$[CℓO]^+$	-534.98	0.001753	0.004201	0.005145	-0.02037	278.19	278.18	270.94
CℓOO	-610.586	0.004618	0.008553	0.009497	-0.02252	21.62	21.50	6.87
$[CℓOO]^-$	-610.707	0.004176	0.007997	0.008941	-0.02321	-54.57	-54.75	-69.30
$[CℓOO]^+$	-610.142	0.003875	0.00745	0.008394	-0.0227	300.13	299.79	284.57
CℓOCℓ	-995.618	0.003612	0.007145	0.00809	-0.02235	21.46	21.03	5.11
$[CℓOCℓ]^-$	-995.706	0.001233	0.005028	0.005973	-0.02604	-34.99	-35.26	-50.19
$[CℓOCℓ]^+$	-995.223	0.003982	0.007396	0.00834	-0.02244	269.53	269.03	253.32
$Cℓ_2O$	-995.597	0.00385	0.007412	0.008357	-0.02282	35.05	34.64	19.18

*Table **A-4.3*** continued

Species	ε_0	ε_{ZPE}	E_tot	H_corr	G_corr	ΔH (OK)	ΔH (298K)	ΔG (298K)
$[C\ell_2O]^{-}$*	-995.645	0.002096	0.005615	0.006559	-995.645	-53.42	-54.10	-69.56
$[C\ell_2O]^{+}$	-995.212	0.002828	0.006574	0.007518	-995.212	276.12	275.83	260.96
$C\ell C\ell O_2$	-1070.79	0.009595	0.013771	0.014715	-1070.79	37.86	36.79	11.04
$C\ell OOO$	-685.709	0.007877	0.012692	0.013636	-685.709	68.41	67.8	43.48
$[C\ell OOO]^{-}$	-685.851	0.007116	0.0108	0.011744	-685.851	-20.62	-21.94	-47.99
$C\ell(O)O_2$	-685.707	0.00776	0.01308	0.014024	-685.707	69.75	69.46	46.56
$[Cl(O)O_2]^{-}$	-685.851	0.007469	0.011147	0.012091	-685.851	-20.62	-21.94	-47.99
$C\ell O_3$	-685.743	0.010472	0.014074	0.015018	-685.743	49.16	47.79	21.47
$[C\ell O_3]^{-}$	-685.875	0.009585	0.013418	0.014362	-685.875	-34.08	-35.31	-61.76
$[C\ell O_3]^{+}$	-685.292	0.00839	0.012558	0.013502	-685.292	330.74	329.73	303.30
$C\ell O_4$*	-760.893	0.01041	0.014433	0.015377	-760.893	76.78	74.64	37.12
$[C\ell O_4]^{-}$	-761.083	0.014186	0.018493	0.019438	-761.083	-40.15	-42.11	-79.79
$C\ell OC\ell O$	-1070.76	0.00723	0.01139	0.012334	-1070.76	56.06	54.98	29.40
$C\ell OOC\ell$	-1070.79	0.006504	0.011388	0.012332	-1070.79	39.29	38.67	13.96
$C\ell OC\ell O_2$*	-1145.97	0.010652	0.015435	0.01638	-1145.97	50.56	48.83	12.93
$C\ell OC\ell O_3$	-1221.14	0.016573	0.022351	0.023295	-1221.14	67.92	65.77	19.98
$C\ell O_2C\ell O_2$	-1221.13	0.0143	0.018233	0.019177	-0.01505	73.08	69.78	21.80
$C\ell O_2$-O-$C\ell O_2$	-1296.31	0.018927	0.024792	0.025736	-0.01268	84.34	81.21	24.39
$C\ell O_2$-O-$C\ell O_3$	-1371.51	0.027295	0.032621	0.033565	-0.00339	89.75	85.25	16.03
$C\ell OOC\ell O_3$	-1296.33	0.01996	0.026008	0.026952	-0.01163	75.18	72.17	15.45

*Table **A-4.3*** continued

Species	ε_0	ε_{ZPE}	E_tot	H_corr	G_corr	ΔH (OK)	ΔH (298K)	ΔG (298K)
$C\ell O_3$-O-$C\ell O_3$	-1446.7	0.030374	0.038703	0.039647	-0.00473	93.30	89.64	13.61
$C\ell O_2$-O-O-$C\ell O_2$	-1371.47	0.023365	0.031038	0.031982	-0.00977	107.20	104.17	37.96
$C\ell O_3$-O-O-$C\ell O_3$	-1521.85	0.037317	0.044028	0.044972	0.004479	124.17	118.45	28.50
$[C\ell O_3\text{-}C\ell O_3]^{-2}$	-1371.47	0.028141	0.033538	0.034483	-0.00186	110.20	105.74	36.14
$OC\ell O$	-610.583	0.005783	0.00894	0.009884	-0.01926	24.50	23.89	7.45
$[OC\ell O]^-$	-610.645	0.003267	0.006849	0.007793	-0.02175	-15.96	-16.30	-32.48
$[OC\ell O]^+$	-610.178	0.006108	0.009185	0.010129	-0.01822	278.90	278.24	261.31
$OC\ell OO$	-685.733	0.004705	0.010421	0.011365	-0.02806	51.67	51.63	30.17
$[OC\ell OO]^-$	-685.829	0.00475	0.008655	0.009599	-0.02582	-8.70	-9.87	-33.85
$OC\ell C\ell O_2$*	-1145.81	0.005881	0.012201	0.013145	-0.02631	147.45	146.67	113.47
$[C\ell OH_2]^+$	-536.291	0.025091	0.028046	0.028991	0.002482	204.09	202.38	179.42
$HOC\ell$	-536.045	0.013162	0.016105	0.017049	-0.00978	-15.73	-16.44	-31.02
$[HOC\ell]^-$	-535.926	0.006934	0.010224	0.011168	-0.01455	54.74	54.25	38.96
$[HOC\ell]^+$	-535.637	0.012962	0.01592	0.016864	-0.01055	239.76	239.06	224.84
$HOC\ell O$	-611.193	0.015261	0.018722	0.019666	-0.01037	14.44	13.01	-11.04
$[HOC\ell O]^-$*	-611.066	0.011127	0.014348	0.015292	-0.01570	-55.76	-57.33	-80.78
$[HOC\ell O]^+$	-610.834	0.015946	0.019318	0.020262	-0.01012	240.42	238.93	215.1
$HOC\ell O_2$	-686.393	0.019286	0.023362	0.024307	-0.00765	13.26	11.17	-23.15
$HOC\ell O_3$	-761.593	0.027229	0.031957	0.032902	-0.00083	14.84	12.13	-32.56

*Table **A-4.3*** continued

Species	ε_0	ε_{ZPE}	E_tot	H_corr	G_corr	ΔH (OK)	ΔH (298K)	ΔG (298K)
$[HOC\ell O_3]^+$	-761.084	0.016512	0.022501	0.023446	-0.01494	327.65	325.73	283.97
HOOCℓ*	-611.212	0.017467	0.020866	0.02181	-0.00805	4.06	2.60	-21.57
$[HOOC\ell]^-$	-611.228	0.011698	0.016318	0.017262	-0.0168	-9.90	-10.60	-32.12
$[HOOC\ell]^+$	-610.812	0.016787	0.020038	0.020982	-0.00924	254.85	253.29	229.36
HOOCℓO*	-686.369	0.020306	0.024864	0.025809	-0.00746	29.56	27.78	-5.72
$HOOC\ell O_2$*	-761.551	0.024822	0.029341	0.030285	-0.00357	40.10	37.26	-7.35
HOOOCℓ	-686.37	0.021388	0.025538	0.026482	-0.00608	29.47	27.44	-6.50
HOOOOCℓ	-761.564	0.022424	0.028236	0.02918	-0.00723	30.21	28.18	-14.83
HCℓO	-535.961	0.009811	0.012762	0.013706	-0.01325	34.60	33.89	19.39
$HC\ell O_2$*	-611.137	0.015657	0.018874	0.019818	-0.00952	49.88	48.30	23.82
$HC\ell O_3$	-686.341	0.022859	0.026355	0.027299	-0.00356	48.51	46.07	11.05

Basis sets applied:

DFT B3LYP/(cc-PV5Z)
DFT/B3LYP 6-311++G/(3df,2p)
DFT/B3LYP/(aug-cc-pv5z)

The predominant basis set used was DFT/B3LYP (cc-PV5Z)
DFT/B3LYP 6-311G computations highlighted with *

A6 -SUPPLEMENTARY INFORMATION FOR CHAPTER 6

A6.1 ATOMIC PARTIAL CHARGES

Mulliken partial charges were obtained using *Gaussian-16* (DFT, B3LYP-cc-pV5Z), *MedeA*-3-31 and *MOPAC-2016*.

Bader charges were obtained using *MedeA-3-31/VASP*-5.4 software.

*Table-**A6**:* Net Atomic, Mulliken and Baden Partial Charges (ND Signifies: Not Determined)

	Atomic Partial Charges					
Species	Atom Label	Mulliken Charge *MOPAC-2016*	Mulliken Charge *Gaussian-16*: B3LYP cc-PV5Z	Net atomic Charge *MOPAC-2016*	Net Atomic Charge *Gaussian-16* B3LYP cc-PV5Z	Bader Charge Transfer *VASP-5.4*
CℓO	Cℓ	-0.39	0.08	-0.16	0.02	0.61
	O	-0.38	-0.08	-0.16	0.02	-0.6
$[C\ell O]^-$	Cℓ	-0.06	-0.83	-0.21	-0.53	0.02
	O	-0.06	-0.17	-0.79	-0.47	-1.02
$[C\ell O]^+$	Cℓ	-0.18	0.79	0.87	0.72	1.38
	O	-0.18	0.21	0.13	0.28	-0.38
OCℓO	Cℓ	-0.46	1.14	0.83	0.87	1.66
	O1	-0.42	-0.57	-0.41	-0.43	-0.81
	O2	-0.43	-0.57	-0.41	-0.43	-0.84
$[OC\ell O]^+$	Cℓ	-0.22	0.89	1.5	1.21	2.28
	O1	-0.21	0.05	-0.25	-0.1	-0.64
	O2	-0.22	0.05	-0.25	-0.1	-0.62
$[OC\ell O]^-$	Cℓ	-0.14	0.18	0.7	0.4	0.72
	O1	-0.09	-0.59	-0.85	-0.7	-0.86
	O2	-0.09	-0.59	-0.85	-0.7	-0.84
ClOO	Cl	-1.19	0.27	0.02	-0.07	1.66
	O1	-0.22	-0.3	-0.06	0.02	0.81
	O2	-0.1	0.03	0.04	0.05	-0.84
$[C\ell OO]^-$	Cℓ	-0.08	-0.26	-0.3	-0.86	-0.62
	O1	-0.13	-0.13	-0.09	0.41	-0.21
	O2	-0.13	-0.62	-0.62	-0.55	-0.17
$[C\ell OO]^+$	Cℓ	-0.23	0.49	0.6	0.23	0.58
	O1	-0.17	0.2	0.13	0.78	0.09
	O2	-0.24	0.31	0.27	-0.01	0.34
CℓOCℓ	Cℓ1	-0.08	0.11	0.06	-0.04	0.19
	Cℓ2	-0.13	0.11	0.06	-0.04	0.28
	O	-0.16	-0.23	-0.12	0.07	-0.48
$[C\ell OC\ell]^-$	Cℓ1	-0.18	-0.47	-0.39	-0.57	-0.6
	Cℓ2	-0.39	-0.47	-0.39	-0.57	0.34
	O	-0.25	-0.06	-0.23	0.14	-0.74

*Table-**A6*** continued

	Atomic Partial Charges					
Species	Atom label	Mulliken charge *MOPAC-2016*	Mulliken charge *Gaussian-16*: B3LYP cc-PV5Z	Net atomic charge *MOPAC-2016*	Net atomic charge *Gaussian-16* B3LYP cc-PV5Z	Bader charge transfer *VASP-5.4*
$[C\ell OC\ell]^+$	Cℓ1	-3.31	0.51	0.54	0.24	0.64
	Cℓ2	-2.00	0.51	0.54	0.24	0.71
	O	-0.14	-0.02	-0.09	0.52	-0.34
CℓCℓO	Cℓ1	-0.13	-0.21	-0.09	-0.24	-0.09
	Cℓ2	-0.18	0.42	0.57	0.50	0.83
	O	-0.12	-0.22	-0.48	-0.25	-0.74
$[C\ell C\ell O]^-$	Cℓ1	-0.33	-0.51	-0.53	-0.92	-0.6
	Cℓ2	-0.37	0.10	0.15	0.31	0.40
	O	-0.18	-0.59	-0.62	-0.40	-0.79
$[C\ell C\ell O]^+$	Cℓ1	-2.35	0.28	0.18	0.09	0.33
	Cℓ2	-0.43	0.72	0.75	0.86	1.30
	O	-0.15	-0.01	0.06	0.06	-0.62
CℓCℓ(O)O	Cℓ1	-0.09	-0.06	-0.42	-0.34	-0.20
	Cℓ2	-0.20	0.66	1.69	1.33	2.03
	O1	-0.19	-0.30	-0.63	-0.50	-0.90
	O2	-0.21	-0.30	-0.63	-0.50	-0.92
CℓOOCℓ	Cℓ1	-0.12	0.05	0.08	-0.15	0.25
	Cℓ2	-0.09	0.06	0.08	-0.15	0.26
	O1	-0.14	-0.03	-0.08	0.15	-0.26
	O2	-0.13	-0.08	-0.08	0.14	-0.26
CℓOCℓO	Cℓ1	-0.15	0.09	0.13	-0.02	0.17
	Cℓ2	-0.14	0.51	0.86	0.63	1.06
	O1	-0.17	-0.3	-0.39	-0.20	-0.62
	O2	-0.15	-0.3	-0.60	-0.41	-0.61
$C\ell O_3$	Cℓ	-0.17	0.52	2.77	1.88	1.87
	O1	-0.60	-0.26	-0.92	-0.63	-0.55
	O2	-0.22	0.00	-0.92	-0.63	-0.81
	O3	-0.60	-0.26	-0.92	-0.63	-0.51
$[C\ell O_3]^-$	Cℓ	-0.22	0.13	1.57	0.44	1.15
	O1	-0.15	-0.37	-0.86	-0.48	-0.66
	O2	-0.14	-0.38	-0.86	-0.48	-0.9
	O3	-0.15	-0.38	-0.86	0.48	-0.59
$[C\ell O_3]^+$	Cℓ	-0.25	0.78	1.68	0.15	3.01
	O1	-0.18	0.07	-0.23	0.21	-0.66
	O2	-0.13	0.08	-0.23	0.44	-0.68
	O3	-0.18	0.08	-0.23	0.21	-0.65

*Table-**A6*** continued

	Atomic Partial Charges					
Species	Atom Label	Mulliken Charge *MOPAC-2016*	Mulliken Charge *Gaussian-16*: B3LYP cc-PV5Z	Net Atomic Charge *MOPAC-2016*	Net Atomic Charge *Gaussian-16* B3LYP cc-PV5Z	Bader Charge Transfer *VASP-5.4*
CℓOOO	Cℓ	-0.51	0.11	0.01	0.09	0.54
	O1	-0.45	-0.09	-0.02	-0.43	-0.05
	O2	-0.16	0.07	0.00	0.33	0.00
	O3	-0.11	-0.10	0.02	0.01	-0.5
$[CℓOOO]^-$	Cℓ	0.06	-0.17	-0.20	-0.37	-0.53
	O1	-0.12	-0.41	-0.09	-0.39	-0.21
	O2	-0.16	-0.12	-0.10	0.44	0.09
	O3	-0.13	-0.31	-0.61	-0.67	-0.34
CℓO(O)O	Cℓ	-0.62	0.20	-0.07	0.34	0.12
	O1	-0.23	0.21	0.03	-0.17	0.09
	O2	-0.12	-0.20	0.03	-0.01	-0.10
	O3	-0.09	-0.20	0.02	-0.17	-0.11
$[CℓO(O)O]^-$	Cℓ	-0.07	-0.83	-0.45	0.16	-0.35
	O1	-0.17	0.33	0.64	-0.55	0.00
	O2	-0.18	-0.25	-0.59	-0.06	-0.31
	O3	-0.20	-0.25	-0.6	0.55	-0.33
OCℓOO	Cℓ	-0.17	0.08	0.33	-0.03	0.84
	O1	-0.10	-0.08	-0.15	0.02	-0.65
	O2	-0.19	0.00	-0.16	0.02	-0.13
	O3	-0.10	0.00	-0.02	-0.02	-0.06
$[OCℓOO]^-$	Cℓ	-0.14	0.33	0.51	-0.73	0.29
	O1	-0.08	-0.56	-0.79	0.05	-0.78
	O2	-0.13	-0.13	-0.11	0.19	-0.23
	O3	-0.10	-0.64	-0.61	-0.51	-0.25
$CℓO_4$	Cℓ	-0.16	1.08	2.98	1.18	3.45
	O1	-4.03	-0.27	-1.01	-0.14	-0.84
	O2	-0.27	-0.27	-0.66	-0.46	-0.84
	O3	-0.29	-0.27	-0.68	-0.14	-0.92
	O4	-0.28	-0.27	-0.65	-0.46	-0.84

*Table-**A6*** continued

	Atomic Partial Charges					
Species	Atom Label	Mulliken Charge *MOPAC-2016*	Mulliken Charge *Gaussian-16*: B3LYP cc-PV5Z	Net Atomic Charge *MOPAC-2016*	Net Atomic Charge *Gaussian-16* B3LYP cc-PV5Z	Bader Charge Transfer *VASP-5.4*
$[C\ell O_4]^-$	Cℓ	-0.19	0.96	2.77	1.63	3.29
	O1	-0.16	-0.46	-0.94	-0.8	-1.08
	O2	-0.11	-0.46	-0.94	-0.81	-1.07
	O3	-0.09	-0.46	-0.94	-0.21	-1.08
	O4	-0.12	-0.59	-0.94	-0.81	-1.06
Cℓ**O**CℓO_2	Cℓ1	-0.17	0.68	0.95	1.11	1.68
	Cℓ2	-0.13	0.21	0.17	-0.22	0.66
	O1	-0.15	-0.3	-0.45	-0.64	-0.85
	O2	-0.15	-0.29	-0.42	-0.34	-0.8
	O3	-0.12	-0.3	-0.25	0.09	-0.69
OCℓCℓO_2	Cℓ1	-0.17	0.53	0.88	1.17	1.59
	Cℓ2	-0.14	0.07	0.09	0.02	0.63
	O1	-0.21	-0.27	-0.3	-0.52	-0.78
	O2	-0.22	-0.28	-0.38	-0.54	-0.78
	O3	-0.2	0.05	-0.29	-0.12	-0.67
CℓO_2CℓO_2	Cℓ1	-0.21	0.33	1.01	1.05	1.68
	Cℓ2	-0.21	0.33	1.01	-0.53	1.62
	O1	-0.19	-0.16	-0.51	-0.53	-0.84
	O2	-0.21	-0.16	-0.51	-0.53	-0.82
	O3	-0.19	-0.16	-0.51	1.05	-0.8
	O4	-0.21	-0.16	-0.51	-0.53	-0.83
Cℓ**O**CℓO_3	Cℓ1	-0.2	0.52	2.33	2.09	3.19
	Cℓ2	-0.13	-0.26	0.31	0.05	0.33
	O1	-0.17	-0.26	-0.7	-0.57	-0.98
	O2	-0.1	-0.26	-0.69	-0.57	-1.01
	O3	-0.17	-0.26	-0.65	-0.61	-0.98
	O4	-0.15	0.52	-0.6	-0.39	-0.55

*Table-**A6*** continued

	Atomic Partial Charges					
Species	Atom Label	Mulliken Charge *MOPAC-2016*	Mulliken Charge *Gaussian-16*: B3LYP cc-PV5Z	Net Atomic Charge *MOPAC-2016*	Net Atomic Charge *Gaussian-16* B3LYP cc-PV5Z	Bader Charge Transfer *VASP-5.4*
Cℓ**OO**CℓO$_3$	Cℓ1	0.2	0.93	2.35	-0.52	2.89
	Cℓ2	-0.14	-0.0056	0.17	0.1	0.19
	O1	-0.15	-0.11	-0.51	2.29	-0.16
	O2	-0.13	-0.3	-0.68	0.01	-0.92
	O3	-0.13	-0.32	-0.66	-0.62	-0.91
	O4	-0.1	-0.25	-0.71	-0.64	-0.95
	O5	-0.16	0.06	0.04	-0.61	-0.13
CℓO$_2$-**O**-CℓO$_2$	Cℓ1	0.2	0.93	2.35	-0.52	2.89
	Cℓ2	-0.14	-0.01	0.17	0.1	0.19
	O1	-0.15	-0.11	-0.51	2.29	-0.16
	O2	-0.13	-0.3	-0.68	0.01	-0.92
	O3	-0.13	-0.32	-0.66	-0.62	-0.91
	O4	-0.1	-0.25	-0.71	-0.64	-0.95
	O5	-0.16	0.06	0.04	-0.61	-0.13
CℓO$_2$-**O**-CℓO$_3$	Cℓ1	-0.14	0.97	1.04	2.24	3.2
	Cℓ2	-0.12	0.78	0.72	1.71	2.21
	O1	-0.18	-0.28	-0.41	-1.15	-0.65
	O2	-0.12	-0.25	-0.21	-0.55	-0.88
	O3	-0.14	-0.26	-0.23	-0.49	-0.86
	O4	-0.13	-0.35	-0.29	-0.6	-1.02
	O5	-0.11	-0.29	-0.3	-0.6	-1
	O6	-0.09	-0.31	-0.33	0.55	-1
CℓO$_2$-**O**-**O**-CℓO$_2$	Cℓ1	-0.22	0.278	1.89	1.02	0.8
	Cℓ2	-0.22	0.278	1.88	1.02	0.8
	O1	-0.15	-0.195	-0.51	-0.42	-0.05
	O2	-0.15	-0.212	-0.51	-0.44	-0.06
	O3	-0.2	0.13	-0.7	-0.16	-0.07
	O4	-0.18	0.13	-0.67	-0.16	-0.68
	O5	-0.18	-0.212	-0.67	-0.42	-0.68
	O6	-0.2	-0.195	-0.71	-0.44	-0.05

*Table-**A6*** continued

	Atomic Partial Charges					
Species	Atom Label	Mulliken Charge *MOPAC-2016*	Mulliken Charge *Gaussian-16*: B3LYP cc-PV5Z	Net Atomic Charge *MOPAC-2016*	Net Atomic Charge *Gaussian-16* B3LYP cc-PV5Z	Bader Charge Transfer *VASP-5.4*
$C\ell O_3$-**O**-$C\ell O_3$	Cℓ1	-0.2	0.99	2.32	2.19	3.21
	Cℓ2	-0.2	0.99	2.32	2.19	3.22
	O1	-0.19	-0.28	-0.61	-0.56	-0.96
	O2	-0.17	-0.28	-0.58	-0.61	-0.97
	O3	-0.19	-0.3	-0.62	-0.56	-0.96
	O4	-0.11	-0.26	-1.03	-0.93	-0.58
	O5	-0.18	-0.3	-0.61	-0.56	-0.98
	O6	-0.12	-0.28	-0.58	-0.61	-1
	O7	-0.17	-0.28	-0.61	-0.56	-0.97
$C\ell O_3$-**O**-**O**-$C\ell O_3$	Cℓ1	-0.20	1.022	2.23	2.47	1.87
	Cℓ2	-0.20	1.022	2.22	2.47	1.85
	O1	-0.18	-0.139	-0.34	-0.47	-0.09
	O2	-0.17	-0.139	-0.32	-0.47	-0.04
	O5	-0.15	-0.297	-0.65	-0.64	-0.89
	O6	-0.17	-0.289	-0.57	-0.69	-0.84
	O7	-0.19	-0.296	-0.65	-0.67	-0.11
	O8	-0.18	-0.289	-0.60	-0.69	-0.85
	O9	-0.09	-0.296	-0.67	-0.67	-0.03
	O10	-0.18	-0.297	-0.65	-0.64	-0.86
$[C\ell OH_2]^+$	Cℓ	-0.15	0.3	0.41	0.66	0.52
	O	-0.09	-0.16	-0.22	-0.5	-1.1
	H1	0	0.43	0.41	0.42	0.81
	H2	0	0.43	0.41	0.42	0.79
HOCℓ	Cℓ	-0.12	0.04	0.1	0.03	0.24
	O	-0.14	-0.37	-0.41	-0.28	-0.9
	H	ND	0.33	0.31	0.29	0.66
$[HOC\ell]^-$	Cℓ	-0.35	-0.27	-0.64	-0.95	-0.53
	O	-0.22	0.211	-0.42	-0.5	-1.06
	H	ND	-0.941	0.056	0.444	0.59

*Table-**A6*** continued

	Atomic Partial Charges					
Species	Atom Label	Mulliken Charge *MOPAC-2016*	Mulliken Charge *Gaussian-16*: B3LYP cc-PV5Z	Net Atomic Charge *MOPAC-2016*	Net Atomic Charge *Gaussian-16* B3LYP cc-PV5Z	Bader Charge Transfer *VASP-5.4*
$[HOC\ell]^+$	Cℓ	-0.62	0.63	0.62	0.49	0.93
	O	-0.17	-0.02	0.02	0.09	-0.68
	H	ND	0.4	0.35	0.42	0.76
HOCℓO	Cℓ	-0.14	0.34	0.83	0.64	1.1
	O1	-0.12	-0.26	-0.6	-0.38	-0.89
	O2	-0.12	-0.33	-0.56	-0.52	-1
	H	ND	0.24	0.33	0.25	0.69
[HOCℓO]-	Cℓ	-0.31	-0.34	-0.47	-0.18	-1.11
	O1	-0.17	-0.25	-0.36	-0.11	-0.86
	O2	-0.2	-0.38	-0.3	-0.68	0.41
	H	ND	-0.03	0.13	0.03	0.56
$[HOC\ell O]^+$	Cℓ	-0.39	0.84	0.65	0.24	1.77
	O1	-0.17	-0.02	0.17	0.34	-0.75
	O2	-0.48	-0.17	-0.14	0.01	-0.75
	H	ND	0.36	0.32	0.41	0.75
HOOCℓ	Cℓ	-0.11	0.04	-0.06	-0.18	0.3
	O1	-0.14	-0.24	-0.18	-0.29	-0.62
	O2	-0.13	-0.1	0.02	0.23	-0.37
	H	ND	0.31	0.22	0.24	0.68
$[HOOC\ell]^+$	Cℓ	-0.27	0.31	0.59	0.31	0.73
	O1	-0.72	0.11	-0.04	-0.33	-0.38
	O2	-0.25	0.24	0.17	0.48	-0.09
	H	ND	0.34	0.28	0.55	0.75
HOOOCℓ	Cℓ	-0.13	0.1	0.01	0.38	0.12
	O1	-0.16	-0.27	-0.04	-0.07	-0.16
	O2	-0.15	-0.07	-0.01	0.27	0
	O3	-0.15	-0.09	-0.17	-0.01	-0.61
	H	ND	0.34	0.21	0.43	0.65

*Table-**A6*** continued

	Atomic Partial Charges					
Species	Atom Label	Mulliken Charge *MOPAC-2016*	Mulliken Charge *Gaussian-16*: B3LYP cc-PV5Z	Net Atomic Charge *MOPAC-2016*	Net Atomic Charge *Gaussian-16* B3LYP cc-PV5Z	Bader Charge Transfer *VASP-5.4*
HOOCℓO	Cℓ	-0.11	0.52	0.48	0.68	0.82
	O1	-0.11	-0.32	-0.20	-0.32	-0.48
	O2	-0.13	-0.22	-0.13	-0.28	-0.22
	O3	-0.14	-0.33	-0.39	-0.39	-0.78
	H	ND	0.34	0.25	0.31	0.66
HOCℓ(O)O	Cℓ	-0.17	0.67	0.94	1.17	1.39
	O1	-0.13	-0.37	-0.3	0.24	-0.71
	O2	-0.13	-0.28	-0.44	-0.49	-0.86
	O3	-0.14	-0.33	-0.46	-0.40	-0.50
	H	ND	0.31	0.26	-0.53	0.68
$HOC\ell O_3$	Cℓ	-0.22	0.5	1.88	2.27	3.6
	O1	-0.12	-0.26	-0.45	-0.71	-1.12
	O2	-0.14	-0.17	-0.58	-0.63	-1.06
	O3	-0.12	-0.19	-0.59	-0.66	-1.14
	O4	-0.15	-0.17	0.55	-0.6	-0.96
	H	ND	0.3	0.29	0.32	0.69
$[HOC\ell O_3]^+$	Cℓ	-0.14	1.01	3.11	1.88	3.62
	O1	-0.32	-0.18	-0.86	-0.30	-0.92
	O2	-0.28	-0.08	-0.54	-0.31	-0.84
	O3	-0.17	-0.09	-0.54	-0.34	-0.91
	O4	-0.32	-0.08	-0.54	-0.31	-0.68
	H	ND	0.41	0.35	0.37	0.74
HOOCℓ(O)O	Cℓ	-0.2	0.72	1.83	1.18	1.96
	O1	-0.13	-0.28	-0.26	-0.32	-0.53
	O2	-0.14	-0.11	-0.51	-0.10	-0.29
	O3	-0.2	-0.34	-0.68	-0.46	-0.91
	O4	-0.18	-0.32	-0.71	-0.54	-0.91
	H	ND	0.32	0.33	0.24	0.67

*Table-**A6*** continued

	Atomic Partial Charges					
Species	Atom Label	Mulliken Charge *MOPAC-2016*	Mulliken Charge *Gaussian-16*: B3LYP cc-PV5Z	Net Atomic Charge *MOPAC-2016*	Net Atomic Charge *Gaussian-16* B3LYP cc-PV5Z	Bader Charge Transfer *VASP-5.4*
HOOOOCℓ	Cℓ	-0.12	0.24	0.02	0.3	0.33
	O1	-0.14	-0.54	-0.18	-0.06	-0.63
	O2	-0.14	-0.022	0.02	0.01	0.05
	O3	-0.16	-0.021	-0.03	-0.24	0
	O4	-0.17	-0.25	-0.04	-0.42	-0.38
	H	ND	0.59	0.22	0.42	0.64
HCℓO	Cℓ	0.455	0.41	0.32	0.24	0.23
	O	-0.5	-0.47	-0.46	-0.35	-0.89
	H	0.045	0.06	0.14	0.11	0.67
$HC\ell O_2$	Cℓ	-0.23	0.32	1.1	0.617	-0.77
	O1	-0.16	-0.46	-0.43	-0.331	0.98
	O2	-0.23	-0.46	-0.43	-0.331	-0.88
	H	ND	0.14	-0.24	0.045	0.67
$HC\ell O_3$	Cℓ	0.948	0.94	1.87	1.93	2.18
	O1	-0.11	-0.33	-0.58	-0.62	-0.89
	O2	-0.1	-0.33	-0.58	-0.62	-1.01
	O3	-0.09	-0.33	-0.58	-0.62	-0.96
	H	ND	0.06	-0.14	-0.06	0.68

A7 - SUPPLEMENTARY INFORMATION FOR CHAPTER 7

Major product species extracted from the reaction with H_2O

*Table-**A7:*** Major species products -- Exposed to Water

H_2O + Reactant (1:1)	Water	Reactant	O_2	Cℓ[-]	$CℓOH_2$[+]	H_2O
CℓO	1	1	0.32	0.32	0.32	0.031214
CℓOO	1	1	0.48	0.24	0.24	0.031222
CℓOCℓ	1	1	0.20	0.40	0.40	0.000013
CℓCℓO	1	1	0.20	0.40	0.40	0.000013
$CℓCℓO_2$	1	1	0.33	0.33	0.33	0.000012
CℓOOO	1	1	0.58	0.19	0.19	0.031225
$Cℓ(O)O_2$	1	1	0.58	0.19	0.19	0.030783
$CℓO_3$	1	1	0.58	0.19	0.19	0.031225
$CℓO_4$	1	1	0.65	0.16	0.16	0.031226
CℓOCℓO	1	1	0.33	0.33	0.33	0.000012
CℓOOCℓ	1	1	0.33	0.33	0.33	0.000012
$CℓOCℓO_2$	1	1	0.43	0.29	0.29	0.000012
$CℓOCℓO_3$	1	1	0.50	0.25	0.25	0.000012
$CℓO_2CℓO_2$	1	1	0.50	0.25	0.25	0.000012
$CℓO_2$-O-$CℓO_2$	1	1	0.56	0.22	0.22	0.000012
$CℓOOCℓO_3$	1	1	0.56	0.22	0.22	0.000012
$CℓO_2$-O-$CℓO_3$	1	1	0.60	0.20	0.20	0.000012
$CℓO_3$-O-$CℓO_3$	1	1	0.64	0.18	0.18	0.000012
$CℓO_2$-O-O-$CℓO_2$	1	1	0.60	0.20	0.20	0.000012
$CℓO_3$-O-O-$CℓO_3$	1	1	0.65	0.16	0.16	0.030785
OCℓO	1	1	0.48	0.24	0.24	0.030781
OCℓOO	1	1	0.58	0.19	0.19	0.030783
$OCℓCℓO_2$	1	1	0.43	0.29	0.29	0.000012
HOCℓ	1	1	0.39	0.39	0.19	0.030761
HOCℓO	1	1	0.42	0.28	0.28	0.030777
$HOCℓO_2$	1	1	0.54	0.22	0.22	0.030782
$HOCℓO_3$	1	1	0.62	0.18	0.18	0.030784
HOOCℓ	1	1	0.42	0.28	0.28	0.030777
HOOCℓO	1	1	0.54	0.22	0.22	0.030782
$HOOCℓO_2$	1	1	0.62	0.18	0.18	0.030784
HOOOCℓ	1	1	0.54	0.22	0.22	0.030782
HOOOOCℓ	1	1	0.62	0.18	0.18	0.030784
HCℓO	1	1	0.19	0.39	0.39	0.030761
$HCℓO_2$	1	1	0.24	0.28	0.28	0.030777
$HCℓO_3$	1	1	0.54	0.22	0.22	0.030782

Appendix References

[1] M. W. Chase, Jr., "NIST-JANAF Thermochemical Tables," American Chemical Society, American Institute of Physics for the National Institute of Standards and Technology, Washington, DC: New York, 1998.

[2] J. W. Ochterski, "Thermochemistry in Gaussian," Gaussian Inc, 2 June 2000. [Online]. Available: www.gaussian.com. [Accessed 8 June 2019].